

CRYSTALLOGRAPHIC STUDY  
OF  
ALKALI METAL DICHROMATES

CRYSTALLOGRAPHIC STUDY  
OF  
ALKALI METAL DICHROMATES

by

NICOLAS CHRESTOU PANAGIOTOPOULOS, B.Sc.

A Thesis

Submitted to the School of Graduate Studies

in Partial Fulfilment of the Requirements

for the Degree

Doctor of Philosophy

McMaster University

May 1972

DOCTOR OF PHILOSOPHY (1972)  
(Physics)

McMASTER UNIVERSITY  
Hamilton, Canada

TITLE: Crystallographic Study of Alkali Metal  
Dichromates

AUTHOR: Nicolas Chrestou Panagiotopoulos, B.Sc.  
(University of Athens, Greece)

SUPERVISOR: Dr. I. D. Brown

NUMBER OF PAGES: xi ,121

SCOPE AND CONTENTS:

The alkali metal dichromates show extensive polymorphism. The crystal structures of the polymorphs  $\alpha$ - $\text{Na}_2\text{Cr}_2\text{O}_7$ ,  $\beta$ - $\text{Na}_2\text{Cr}_2\text{O}_7$ ,  $\beta 1$ - $\text{Rb}_2\text{Cr}_2\text{O}_7$  and  $P2_1/c$   $\text{NaRbCr}_2\text{O}_7$  have been determined with x-ray methods. Crystal data were determined for  $\beta 2$ - $\text{Rb}_2\text{Cr}_2\text{O}_7$ ,  $P\bar{1}$   $\text{Cs}_2\text{Cr}_2\text{O}_7$  and the  $P2_1/c$   $\text{NaCsCr}_2\text{O}_7$ .

The dichromate ions found in this work have been compared with the dichromate ions found in other crystal structure determinations. The anions are described in terms of the bridging oxygen angles  $b$  and the torsion angles  $\alpha_1$  and  $\alpha_2$ . Many of the dichromate ions are close to having  $C_{2v}$  symmetry with values for  $\alpha_1$  and  $\alpha_2$  close to zero and bridging angles of around  $124^\circ$ . But there is a number of dichromates with  $\alpha_1 = -\alpha_2$  and  $0^\circ < |\alpha| < 60^\circ$  for which the bridging angle varies between  $131^\circ$  to  $141^\circ$ .

The structures determined in this work are discussed as part of a unified description of thortveitite like and dichromate

like structures in terms of layers of  $Y_2O_7$  anions. In terms of this description and Brown and Calvo's classification a structure is proposed for the  $\beta 2Rb_2Cr_2O_7$ , while for the structure of  $NaCsCr_2O_7$  it is suggested that it is isostructural to that of  $P2_1/c NaRbCr_2O_7$ . The phase transition of  $\alpha-Na_2Cr_2O_7$  to  $\beta-Na_2Cr_2O_7$  is considered and it is suggested that a twisting thermal mode plays an important role in this as well as in other transitions.

## ACKNOWLEDGEMENTS

I would like to express my gratitude to the following persons.

Dr. I. D. Brown for his encouragement, advice and criticism so kindly offered during his supervision of this research.

Dr. C. Calvo for many helpful suggestions and discussions.

To the other members of the crystallography group and especially Dr. H. D. Grundy, Dr. N. Krishnamachari and Dr. J. J. Park for helpful discussions.

## TABLE OF CONTENTS

<u>CHAPTER</u>	<u>Page</u>	
1	INTRODUCTION: SURVEY OF THE POLYMORPHISM OF ALKALI METAL DICHROMATES	1
2	METHODS OF CRYSTAL STRUCTURE ANALYSIS	7
3	EXPERIMENTAL PROCEDURES AND CRYSTAL STRUCTURE DETERMINATION	15
	3.1.0 $\alpha$ and $\beta$ $\text{Na}_2\text{Cr}_2\text{O}_7$ . Introduction and Preliminary Survey	15
	3.1.1 a $\beta$ - $\text{Na}_2\text{Cr}_2\text{O}_7$ . Experimental Procedure	17
	3.1.1 b Structure Determination	19
	3.1.2 a $\alpha$ - $\text{Na}_2\text{Cr}_2\text{O}_7$ . Experimental Procedure	22
	3.1.2 b Structure Determination	28
	3.1.2 c Possible Disorder in $\alpha$ - $\text{Na}_2\text{Cr}_2\text{O}_7$	29
	3.2.0 $\text{Rb}_2\text{Cr}_2\text{O}_7$ Introduction	40
	3.2.1 a $\beta 1$ (VIII) $\text{P}\bar{1}$ $\text{Rb}_2\text{Cr}_2\text{O}_7$ . Experimental Procedure	41
	3.2.1 b Structure Determination	43
	3.2.2 $\beta 2$ $\text{P}\bar{1}$ $\text{Rb}_2\text{Cr}_2\text{O}_7$ Experimental Procedure	45
	3.3 $\text{Cs}_2\text{Cr}_2\text{O}_7$ . Experimental Procedure	52
	3.4.0 $\text{NaRbCr}_2\text{O}_7$ and $\text{NaCsCr}_2\text{O}_7$ . Introduction	57
	3.4.1 a $\text{NaRbCr}_2\text{O}_7$ Sample Preparation	57
	3.4.1 b $\text{NaRbCr}_2\text{O}_7$ Preliminary Investigation and Determination of the Structure with Precession Photographs	58

TABLE OF CONTENTS (continued)

<u>CHAPTER</u>		<u>PAGE</u>
	3.4.1 c Crystal Data and Intensities	
	Measured on the Diffractometer	61
	3.4.1 d Refinement with the Diffractometer	
	Measurements	64
	3.4.2 NaCsCr <sub>2</sub> O <sub>7</sub> Experimental Procedure	68
4	THE DICHROMATE ION	69
	4.1 The Geometry of the Dichromate Ion	69
	4.2 Analysis of the Temperature Factors	72
	4.3 Discussion on the Conformation of the	
	Dichromate Ion	91
	4.4 The $\alpha$ to $\beta$ Phase Transition in Na <sub>2</sub> Cr <sub>2</sub> O <sub>7</sub>	96
5	LAYERS IN THORTVEITITE AND DICHROMATE LIKE	
	STRUCTURES	98
	5.1 Introduction. Description of the Layers	98
	5.2 The Structure and Packing of Typical	
	Layers	105
	5.3 Special Cases of Layers in Small Cation	
	Structures	108
	5.4 Special Cases of Layers in Medium and	
	Large Cation Structures	109
	5.4.1 Ag <sub>2</sub> Cr <sub>2</sub> O <sub>7</sub>	109
	5.4.2 $\beta$ -Na <sub>2</sub> Cr <sub>2</sub> O <sub>7</sub>	109
	5.4.3 P2 <sub>1/n</sub> and $\beta 1$ P $\bar{1}$ Rb <sub>2</sub> Cr <sub>2</sub> O <sub>7</sub>	109

TABLE OF CONTENTS (continued)

<u>CHAPTER</u>		<u>Page</u>
5.4.4	$\beta 1(V) \text{ P}\bar{1} \text{ K}_2\text{Cr}_2\text{O}_7$	110
5.4.5	$\text{P}2_1/c \text{ NaRbCr}_2\text{O}_7$	111
5.4.6	$\alpha\text{-Ca}_2\text{P}_2\text{O}_7$	111
5.6	The Structure of $\beta 2 \text{ Rb}_2\text{Cr}_2\text{O}_7$	114
6	SUMMARY	116
	BIBLIOGRAPHY	119



## LIST OF FIGURES

<u>FIGURE NO.</u>		<u>Page</u>
1.1	Phase transformations in alkali metal dichrometers	3
3.1	$\text{Na}_2\text{Cr}_2\text{O}_7$ $\beta$ disordered structure and $\alpha$ ordered structure	32
3.2	$\text{Cs}_2\text{Cr}_2\text{O}_7$ <i>h0l</i> Weissenberg photograph	53
3.3	$\text{Cs}_2\text{Cr}_2\text{O}_7$ <i>hk0</i> precession photograph	54
3.4	$\text{Cs}_2\text{Cr}_2\text{O}_7$ <i>0kl</i> precession photograph	55
4.1	Special symmetric conformations of $\text{Y}_2\text{O}_7$ ions	70
4.2	The dichromate ions found in this work	71
4.3	Conformations of the dichromate ion	93
5.1	Layers in $\beta 1\text{-Rb}_2\text{Cr}_2\text{O}_7$ , $\text{NaRbCr}_2\text{O}_7$ and $\text{Sc}_2\text{Si}_2\text{O}_7$	100
5.2	Layers of $\alpha\text{-Mg}_2\text{P}_2\text{O}_7$ , $\alpha\text{-Na}_2\text{Cr}_2\text{O}_7$ and $\text{X-Rb}_2\text{Cr}_2\text{O}_7$	101
5.3	Packing of the layers in $\alpha\text{-Mg}_2\text{P}_2\text{O}_7$ , $\alpha\text{-Na}_2\text{Cr}_2\text{O}_7$ and $\text{X-Rb}_2\text{Cr}_2\text{O}_7$	102
5.4	Layers of $\text{Ag}_2\text{Cr}_2\text{O}_7$ and $\beta\text{-Na}_2\text{Cr}_2\text{O}_7$	103
5.5	Layers of $\text{VII-Rb}_2\text{Cr}_2\text{O}_7$ and $\beta 1\text{-Rb}_2\text{Cr}_2\text{O}_7$	104
5.6	The $\text{NaRbCr}_2\text{O}_7$ layer	112
5.7	Layer of $\alpha\text{-Ca}_2\text{P}_2\text{O}_7$	113

LIST OF TABLES

<u>TABLE NO.</u>		<u>Page</u>
1.1	Cell constants and space groups	2
3.1	Crystal data for $\alpha$ and $\beta$ $\text{Na}_2\text{Cr}_2\text{O}_7$	16
3.2	$\beta$ - $\text{Na}_2\text{Cr}_2\text{O}_7$ Angular settings for 15 reflections	18
3.3	$\beta$ - $\text{Na}_2\text{Cr}_2\text{O}_7$ Atomic positional and thermal coordinates	23
3.4	Observed and calculated structure factors for $\beta$ - $\text{Na}_2\text{Cr}_2\text{O}_7$	25
3.5	$\alpha$ - $\text{Na}_2\text{Cr}_2\text{O}_7$ Atomic positional and thermal coordinates	30
3.6	$\alpha$ - $\text{Na}_2\text{Cr}_2\text{O}_7$ observed and calculated structure factors	31
3.7	Disorder separations in $\alpha$ and $\beta$ disordered structures	35
3.8	Geometry of the dichromate ion in $\alpha$ and $\beta$ ordered structure	36
3.9	Principal axes of thermal ellipsoids in $\beta$ - $\text{Na}_2\text{Cr}_2\text{O}_7$ and in $\alpha$ and $\beta$ ordered structures	37
3.10	Crystal data for $\beta 1$ and $\beta 2$ $\text{Rb}_2\text{Cr}_2\text{O}_7$	42
3.11	$\beta 1$ $\text{P}\bar{1}$ $\text{Rb}_2\text{Cr}_2\text{O}_7$ atomic positional and thermal coordinates	46

LIST OF TABLES (continued)

<u>TABLE NO.</u>		<u>Page</u>
3.12	$\beta 1$ $\text{Rb}_2\text{Cr}_2\text{O}_7$ Observed and calculated structure factors	47
3.13	$\text{Cs}_2\text{Cr}_2\text{O}_7$ Crystal data	56
3.14	Crystal data for $\text{NaRbCr}_2\text{O}_7$ and $\text{NaCsCr}_2\text{O}_7$	59
3.15	$\text{NaRbCr}_2\text{O}_7$ Crystal shape	62
3.16	$\text{NaRbCr}_2\text{O}_7$ Angular settings for 14 reflections	63
3.17	$P2_1/c$ $\text{NaRbCr}_2\text{O}_7$ Atomic positional and thermal coordinates	65
3.18	$\text{NaRbCr}_2\text{O}_7$ Observed and calculated structure factors	66
4.1	$\beta$ - $\text{Na}_2\text{Cr}_2\text{O}_7$ Principal axes of anisotropic temperature factors	74
4.2	$\alpha$ - $\text{Na}_2\text{Cr}_2\text{O}_7$ Principal axes of anisotropic temperature factors	77
4.3	$\beta 1$ - $\text{Rb}_2\text{Cr}_2\text{O}_7$ Principal axes of anisotropic temperature factors	79
4.4	$P2_1/c$ $\text{NaRbCr}_2\text{O}_7$ Principal axes of aniso- tropic temperature factors	81
4.5	Raman spectra of $\beta 1$ $\text{K}_2\text{Cr}_2\text{O}_7$	84
4.6	Estimates of libration and torsion amplitudes	86
4.7	$\beta$ - $\text{Na}_2\text{Cr}_2\text{O}_7$ Interatomic Distances	87

## LIST OF TABLES (continued)

<u>TABLE NO.</u>		<u>Page</u>
4.8	$\alpha$ -Na <sub>2</sub> Cr <sub>2</sub> O <sub>7</sub> Interatomic Distances	88
4.9	$\beta$ 1-Rb <sub>2</sub> Cr <sub>2</sub> O <sub>7</sub> Interatomic Distances	89
4.10	NaRbCr <sub>2</sub> O <sub>7</sub> Interatomic Distances	90
4.11	Geometry of the dichromate ion	92

## CHAPTER 1

### INTRODUCTION: SURVEY OF THE POLYMORPHISM OF ALKALI METAL DICHROMATES

The alkali metal dichromates show extensive polymorphism. Though all of them melt at around 400° they show two or three phase transitions between room temperature and the melting point. A knowledge of the structure of the various polymorphs is necessary in order to understand the nature of the phase transitions between them. When this work started only two structures had been reported, those of  $(\text{NH}_4)_2\text{Cr}_2\text{O}_7$  (1) and triclinic  $\text{K}_2\text{Cr}_2\text{O}_7$  (2).

We have summarized in table 1.1 the cell constants and space groups of phases for which they are known, and in figure 1.1 the phase transitions of the various compounds.

$\text{K}_2\text{Cr}_2\text{O}_7$  and  $\text{Rb}_2\text{Cr}_2\text{O}_7$  have more than one phase stable at room temperature. We will distinguish these by calling them as the  $\beta_1, \beta_2, \dots$  phase while we will use the letters  $\alpha, c$  and  $d$  for the higher temperature phases. Alternatively we will take advantage of the classification scheme of dichromate like structures proposed by Brown and Calvo (3) and call the phases as I, II, ... the number

Table 1.1 Cell constants and space groups of the dichromates

Compound	Phase	Type of Structure	Space Group	a(Å)	b(Å)	c(Å)	$\alpha(^{\circ})$	$\beta(^{\circ})$	$\gamma(^{\circ})$	V(Å <sup>3</sup> )	Reference
Na <sub>2</sub> Cr <sub>2</sub> O <sub>7</sub>	$\alpha$	I	A $\bar{1}$	7.82	10.36	9.54	89.5	110.1	113.4	659	This Work
	$\beta$	I	P $\bar{1}$	7.70	10.38	9.40	89.41	109.57	114.26	639	This Work
K <sub>2</sub> Cr <sub>2</sub> O <sub>7</sub>	$\beta$ 1	V	P $\bar{1}$	13.37	7.38	7.44	90.75	96.21	97.96	722	(2)
	$\alpha$	VII(†)	P2 <sub>1</sub> /n	13.45	7.52	7.55		91.68		763	(6)
		X(†)	C2/c	13.06	7.37	7.43		91.85		715	(6)
Rb <sub>2</sub> Cr <sub>2</sub> O <sub>7</sub>	$\beta$ 1	VIII	P $\bar{1}$	13.55	7.64	7.74	93.64	98.52	88.80	790	This Work
	$\beta$ 2	I(†)	P $\bar{1}$	7.60	7.39	7.85	90.2	70.0	70.5	387	This Work
		VII	P2 <sub>1</sub> /n	13.71	7.60	7.70		93.35		802	(11)
		X	C2/c	13.33	7.55	7.73		92.04		778	(10)
Cs <sub>2</sub> Cr <sub>2</sub> O <sub>7</sub>	$\beta$		P $\bar{1}$	7.8	7.9	8.5	110.5	98.3	95.7	482	This Work
(NH <sub>4</sub> ) <sub>2</sub> Cr <sub>2</sub> O <sub>7</sub>	$\alpha$	X	C2/c	13.26	7.54	7.74		93.2		776	(1)
NaRbCr <sub>2</sub> O <sub>7</sub>			P2 <sub>1</sub> /c	12.95	11.13	10.04		93.42		1444	This Work
NaCsCr <sub>2</sub> O <sub>7</sub>			P2 <sub>1</sub> /c	12.98	11.58	10.10		93.8		1514	This Work

† Probable structural type



indicating the structural group to which they belong.

Our present knowledge of the polymorphism is summarized below.

### Na<sub>2</sub>Cr<sub>2</sub>O<sub>7</sub>

Vesnín and Khripin (4) have studied the phase transformations of the anhydrous Na<sub>2</sub>Cr<sub>2</sub>O<sub>7</sub> with differential thermal analysis, measurements of refractive indices and x-ray powder patterns and have identified four phases between room temperature and the melting point. The phase transitions are reversible transformations and occur at 240, 295 and 330°C. Following Samuseva et al. (5) who examined the crystals using DTA we designate the phases above and below 240°C as  $\alpha$  and  $\beta$ . In the present work we determined the structure of the  $\alpha$  and  $\beta$  phase. The results are given in Chapter 3.1. Nothing is known about the structures of the other phases.

### K<sub>2</sub>Cr<sub>2</sub>O<sub>7</sub>

K<sub>2</sub>Cr<sub>2</sub>O<sub>7</sub> exists in two forms at room temperatures, a triclinic phase  $\beta$ 1(V) and a metastable monoclinic phase (X), space group C2/c. Klement and Schwab (6) report that the single crystals of the  $\beta$ 1 transform irreversibly but without destruction of the crystal at 270° to a monoclinic form  $\alpha$ (VII), space group P2<sub>1</sub>/n. On cooling a reversible transition occurs around 250°C but there is a dispute as to whether the structure formed below this transition ( $\beta$ 2) is the original triclinic phase (4,6,7). According to Vesnín and Khripin (4) there are two more reversible phase transitions at 345°C



and 380°C. The only phase whose structure has been determined so far is the triclinic phase (2).

### Rb<sub>2</sub>Cr<sub>2</sub>O<sub>7</sub>

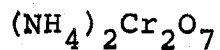
Rubidium dichromate grown from aqueous solution at room temperatures forms three phases, one triclinic  $\beta 1$  (VIII) and two monoclinic, VII, space group  $P2_1/n$  and X, space group  $C2/c$  (6,8). We have determined the structure of  $\beta 1$  (9). Löfgren and Walterson (10) have determined the structure of X and Löfgren (11) the structure of VII.

On heating crystals of the triclinic phase two transformations take place, an irreversible transition at 318° and a reversible one at 337°. On cooling a reversible endothermic effect is observed at 260° (4). The phase formed before this transition is designated  $\beta 2$ .

We grew crystals of  $\beta 2$ -Rb<sub>2</sub>Cr<sub>2</sub>O<sub>7</sub> from the melt and found that they are twinned belonging to the triclinic class. An account of them is given in Chapter 3.2.2.

### Cs<sub>2</sub>Cr<sub>2</sub>O<sub>7</sub>

For the Cs<sub>2</sub>Cr<sub>2</sub>O<sub>7</sub> two reversible phase transitions have been reported at 347°, Samuseva (5) and at 362°, Vesnin (6). We looked at crystals grown from aqueous solutions and we found that they are triclinic but disordered and twinned. These results are discussed in Chapter 3.3.



Jaffray (12,13) reports two phase transitions at  $-2^\circ\text{C}$  and  $-150^\circ\text{C}$  for the  $(\text{NH}_4)_2\text{Cr}_2\text{O}_7$  but the phases are unidentified. The room temperature structure belongs to the space group  $\text{C2/c}$  and has been shown by Byström and Wilhelmi (1) to be of type X.

### Binary Systems

Binary systems of the alkali dichromates have been studied by Lehrman (14)  $\text{K}_2\text{Cr}_2\text{O}_7\text{-Na}_2\text{Cr}_2\text{O}_7$ ; and Samuseva (15)  $\text{K}_2\text{Cr}_2\text{O}_7\text{-Rb}_2\text{Cr}_2\text{O}_7$ ,  $\text{K}_2\text{Cr}_2\text{O}_7\text{-Cs}_2\text{Cr}_2\text{O}_7$ ,  $\text{Rb}_2\text{Cr}_2\text{O}_7\text{-Cs}_2\text{Cr}_2\text{O}_7$ . All these have been found to form a continuous series of solid solutions, except for the systems of  $\text{Na}_2\text{Cr}_2\text{O}_7\text{-Rb}_2\text{Cr}_2\text{O}_7$  and  $\text{Na}_2\text{Cr}_2\text{O}_7\text{-Cs}_2\text{Cr}_2\text{O}_7$  where congruently melting compounds in the molar ratio 1:1 have been found (5). We studied single crystals of both of these compounds and determined the structure of  $\text{NaRbCr}_2\text{O}_7$ . This work is reported in Chapter 3.4.

Lately Hazell (16) reported the structure of  $\text{Ag}_2\text{Cr}_2\text{O}_7$  which is triclinic at room temperature with structure I.

The structure of hydrated sodium dichromate  $\text{Na}_2\text{Cr}_2\text{O}_7 \cdot 2\text{H}_2\text{O}$  has been determined recently by Kharitonov et al. (17) and Datt et al. (18) have given the results of a preliminary investigation of  $\text{Li}_2\text{Cr}_2\text{O}_7 \cdot 2\text{H}_2\text{O}$ . These structures and that of  $(\text{NH}_4)_2\text{Cr}_2\text{O}_7$  are not very accurate and will not be discussed further in this thesis.

## CHAPTER 2

### METHODS OF CRYSTAL STRUCTURE ANALYSIS

The purpose of this section is to define some of the nomenclature of the crystal structure determination methods used in this thesis.

Crystals are known to be homogeneous, symmetric and generally anisotropic solids. These properties are consequences of the periodic nature of the crystal, that is the electron density is a triply periodic function such that:

$$\rho(\underline{r}) = \rho(\underline{r} + \underline{r}_\ell) \quad [1]$$

$$\underline{r}_\ell = u\underline{a} + v\underline{b} + w\underline{c} \quad [2]$$

where  $u, v, w$  are integers and  $\underline{a}, \underline{b}, \underline{c}$  are three non coplanar vectors usually selected so that they are the three smallest non coplanar translations in the crystal. They are called the lattice constants or lattice parameters. The set of points defined by equation [2] is called a lattice and the set of  $\underline{r}_\ell$  are called the lattice vectors.

In diffraction of x-rays by an arbitrary object the radiation interacts with the electrons. If  $\underline{k}_0$  is the wave vector of the incident radiation and  $\underline{k}$  that of the scattered radiation the phase difference between the two waves scattered by two points separated by  $\underline{r}$  is  $2\pi(\underline{k}_0 - \underline{k})\underline{r}$ . Thus

the resultant amplitude of the scattered radiation summed over the whole object is

$$F(\underline{r}^*) = \int \rho(\underline{r}) \exp(2\pi i \underline{r}^* \cdot \underline{r}) dv \quad [3]$$

where

$$\underline{r}^* = \underline{k}_0 - \underline{k}. \quad [4]$$

If the scatterer is an ideal crystal, e.g. has perfect periodicity then from [1] and [3]

$$\begin{aligned} F(\underline{r}^*) &= \sum_{uvw} \int_{\text{unit cell}} \rho(\underline{r}) \exp(2\pi i \underline{r}^* \cdot (\underline{r} + \underline{r}_\ell)) dv \\ &= \int \rho(\underline{r}) \exp(2\pi i \underline{r}^* \cdot \underline{r}) dv \sum_{uvw} \exp(2\pi i \underline{r}^* \cdot \underline{r}_\ell) \end{aligned}$$

and the amplitude has discrete values only at points

$$\underline{r}^* = \underline{h} = h\underline{a}^* + k\underline{b}^* + l\underline{c}^* \quad [5]$$

where  $h, k, l$  are integers, everywhere else the amplitude is zero. The three non coplanar vectors  $\underline{a}^*, \underline{b}^*, \underline{c}^*$  (reciprocal lattice constants) satisfy the relations

$$\begin{aligned} \underline{a} \cdot \underline{a}^* &= 1, \quad \underline{b} \cdot \underline{b}^* = 1, \quad \underline{c} \cdot \underline{c}^* = 1 \\ \underline{a} \cdot \underline{b}^* &= 0, \quad \underline{a} \cdot \underline{c}^* = 0 \quad \text{etc.} \end{aligned} \quad [6]$$

So from [5]:

$$\underline{h} \cdot \underline{a} = k, \quad \underline{h} \cdot \underline{b} = l, \quad \underline{h} \cdot \underline{c} = m \quad [7]$$

which are called the Laue equations and from equation [4]

$$|\underline{h}| = |\underline{k}_0 - \underline{k}| = 2 \sin \theta / \lambda \quad [8]$$

which is the Bragg's law.

The intensity is given by  $I(\underline{h}) = F(\underline{h})F^*(\underline{h})$ . The intensity measured experimentally depends on the atoms present in the unit cell, their position and a number of additional factors

$$I(\underline{h}) = CLp A_{\underline{h}} |F(\underline{h})|^2 .$$

C is a constant which depends on the volume and density of the crystal irradiated and the intensity of the incident beam. L represents the dependence of the intensity on the diffraction geometry and it is called the Lorentz factor. p is equal to  $(1+\cos^2 2\theta)/2$  and arises from the unpolarized nature of the x-ray beam and the manner in which its reflection efficiency varies with reflection angle.

When x-rays pass through the crystal their intensity is attenuated by absorption. This effect is represented by the factor  $A_{\underline{h}}$  which is called the transmission coefficient

$$A_{\underline{h}} = \frac{1}{v} \int_v \exp(-\mu(p+q)dv)$$

where v is the volume of the crystal,  $\mu$  is the linear absorption coefficient and p and q are the path lengths of the radiation before and after scattering.

The Fourier transform of the electron density of a single atom is denoted by  $f(\underline{h})$  and is called the atomic scattering factor. For a crystal with N atoms per unit cell equation [3] becomes

$$F(\underline{h}) = V \sum_{i=1}^N f_i(\underline{h}) \exp(2\pi i \underline{h} \cdot \underline{r}_i). \quad [9]$$

$F(\underline{h})$  is called the Structure Factor.

But the atoms in a crystal undergo thermal motion which reduces the amplitude of the structure factor  $F$ . This effect could be taken into account as Debye has shown (19) by multiplying  $f_i(\underline{h})$  by  $\exp(-2\pi^2 \sum_{j,k} U(i)_{jk} h_j h_k)$ . Where the matrix  $U(i)_{jk}$  represents the thermal motion of the  $i$  atom and is called the anisotropic temperature factor.

Since the structure factor  $F$  is the Fourier transform of the electron density the electron density is the inverse Fourier transform of the structure factor and

$$\rho(\underline{r}) = \frac{1}{V} \sum_{\underline{h}} F(\underline{h}) \exp(-2\pi i \underline{h} \cdot \underline{r}). \quad [10]$$

From a diffraction experiment which measures the intensity we can deduce  $FF^*$  but the information about the phase of  $F$ , in general a complex quantity, is not measurable. The problem of crystal structure determination is to find the phase of each of the structure factors. The methods which have been applied in this thesis for the solution of this problem are Patterson method and one of the direct methods.

The intensity is the Fourier transform of the convolution (or correlation) of the electron density with itself. From [3]

$$\begin{aligned} F(\underline{r}^*)F^*(\underline{r}^*) &= \int \rho(\underline{r}) \exp(2\pi i \underline{r}^* \cdot \underline{r}) dV_{\underline{r}} \int \rho(\underline{r}') \exp(-2\pi i \underline{r}^* \cdot \underline{r}') dV_{\underline{r}'} \\ &= \int \rho(\underline{r}) \rho(\underline{r}+\underline{u}) \exp(-2\pi i \underline{r}^* \cdot \underline{u}) dV_{\underline{r}} dV_{\underline{u}} \end{aligned}$$

where  $\underline{u} = \underline{r}' - \underline{r}$ . The inverse Fourier transform of the intensity is called in crystallography the Patterson function:

$$P(\underline{r}) = \frac{1}{V} \sum_{\underline{h}} FF^* \exp(-2\pi i \underline{h} \cdot \underline{r}) \quad [11]$$

It contains the image of the electron density convoluted with itself and it is a vector map whose peaks are weighted according to the number of electrons of the correlated atoms. The problem is to deduce the positions of the atoms from it.  $P(\underline{r})$  is usually poorly resolved and the complexity of its interpretation becomes more involved with an increase in the number of atoms to be determined. If heavy and light atoms are present in the structure the heavy atoms dominate the Patterson function and their positions can be determined.

These positions determine the probable sign of a number of structure factors. Then the positions of the light atoms can be found from a difference synthesis  $\Delta\rho$  which is equal to the difference between  $\rho_0$ , which is an "ideal" electron density corresponding to the  $F_0$ 's (observed structure factors) and the "proposed" electron density  $\rho_c$  which corresponds to the  $F_c$ 's (calculated structure factors).

$$\Delta\rho(\underline{r}) = \sum_{\underline{h}} (|F_0(\underline{h})| - |F_c(\underline{h})|) e^{i\alpha_c} e^{-2\pi i \underline{h} \cdot \underline{r}} \quad [12]$$

$\alpha_c$  is the phase of  $F_c$ .  $\Delta\rho(\underline{r})$  has peaks which should correspond to the positions of the light atoms.

There is a variety of methods, the direct methods (20), in which the determination of the phases of the  $F$ 's is attempted

by considering solely the structure factor amplitudes. These methods are based on the fundamental principle that the electron density has to be everywhere non-negative.

The method employed here (Chapter 3.4.1) applies in centrosymmetric structures where the phases are  $0^\circ$  or  $180^\circ$ . For this the normalized structure factors  $E_{\underline{h}}$ , defined by  $E_{\underline{h}}^2 = |F_{\underline{h}}|^2 / \sum_{i=1}^N f_i^2$  is introduced. In 1952 Sayre showed that for any equal-atom structure

$$F_{\underline{h}} = \phi_{\underline{h}} \sum F_{\underline{h}'} F_{\underline{h}-\underline{h}'}$$

where  $\phi_{\underline{h}}$  is a scaling term. If the structure factors involved are sufficiently large then this equation shows that  $F_{\underline{h}} F_{\underline{h}'} F_{\underline{h}+\underline{h}'}$  is positive. Even if the structure factors are not large enough there may be a strong probability that the following relationship is true

$$s(\underline{h})s(\underline{h}')s(\underline{h}+\underline{h}') \sim 1 \quad [13]$$

where  $s(\underline{h})$  means the sign of  $F_{\underline{h}}$  and  $\sim$  means is probably equal to. The probability that [13] is true is

$$P = \frac{1}{2} + \frac{1}{2} \tanh\left\{\frac{1}{N} |E_{\underline{h}} E_{\underline{h}'} E_{\underline{h}+\underline{h}'}|\right\}. \quad [14]$$

In general an algorithm is set up by assigning symbolic phases to reflections with sufficiently large values of  $|E|$  ( $\geq 1.5$  usually) (21). All the symbolic phases are not independent and their number is reduced to a minimum with the help of the relationships [13] (which are called "sigma two relationships") and relationships derived by forming



products between the relationships [13] which have a common factor. The probability for these relationships of being correct has to be high ( $P > 0.97$ ) if the method is to work. Then the origin is specified by assigning actual phases ( $0^\circ$  or  $180^\circ$ ) to a properly chosen set of symbolic phases. The remaining symbolic phases are then found from the relationships derived above. Sometimes no additional symbols need be specified. This is more likely to happen in space groups of higher symmetry and when heavy atoms are present.

With the signs of a few hundred reflections determined it is useful to compute a Fourier map with the E structure factors as coefficients (E map). This will give peaks at the positions of the atoms if the solution is correct.

Once the positions of the atoms are known either from Patterson or direct methods they can be further refined either with difference Fourier synthesis or by least squares.

In the difference Fourier synthesis the atoms are moved from areas where the synthesis is negative towards areas where it is positive.

In least squares small shifts of the atoms are calculated so as to minimize the numerator of the quantity.

$$R_2 = \left[ \frac{\sum_{\underline{h}} w(\underline{h}) (|F_o(\underline{h})| - |F_c(\underline{h})|)^2}{\sum_{\underline{h}} w(\underline{h}) |F_o(\underline{h})|^2} \right]^{1/2}$$

called the weighted R factor. The weight  $w$  is to be taken as  $w(\underline{h}) = 1/\sigma(\underline{h})$  where  $\sigma(\underline{h})$  is the standard error of the corresponding observation. Usually it is not feasible in routine structure determinations involving large numbers of reflections to obtain reliable estimates of  $\sigma$ . Cruickshank et al. (22) suggest that  $w(\underline{h}) = (a + b|F_o(\underline{h})| + c|F_o(\underline{h})|^2)^{-1}$ . It is then possible to account for systematic unknown errors if  $w(\underline{h}) \cdot (|F_o(\underline{h})| - |F_c(\underline{h})|)^2$  is not a function of  $|F_o(\underline{h})|$ .

In the past, before the advent of the use of computers, it was more convenient to use

$$R_1 = \frac{\sum_{\underline{h}} (|F_o(\underline{h})| - |F_c(\underline{h})|)}{\sum_{\underline{h}} F_o(\underline{h})}$$

which is called the unweighted R factor or agreement index.

## CHAPTER 3

### EXPERIMENTAL PROCEDURES AND CRYSTAL STRUCTURE DETERMINATION

#### 3.1.0 $\alpha$ and $\beta$ $\text{Na}_2\text{Cr}_2\text{O}_7$ . Introduction and Preliminary Survey

Vesnina and Khripin (4) have examined the phase transitions in  $\text{Na}_2\text{Cr}_2\text{O}_7$  using DTA and refractive index and have identified four phases between room temperature and the melting point with transitions at  $240^\circ$ ,  $270^\circ$  and  $330^\circ$ . The phases above and below the  $240^\circ\text{C}$  transition we will designate, following Samusev, Palataev and Plyshev (5), as  $\alpha$  and  $\beta$  respectively.

As is shown in the following paragraphs the crystals of  $\beta\text{-Na}_2\text{Cr}_2\text{O}_7$  are triclinic, space group  $\text{P}\bar{1}$ , with four molecules per unit cell and with the lattice parameters at room temperature given in Table 3.1. From single crystal photographs it is apparent that reflections with  $k+l$  odd are in general considerably weaker than those with  $k+l$  even and, on heating, the odd reflections become even weaker, disappearing at around  $240^\circ\text{C}$ . The  $k+l$  even reflections change only slightly during this process. Above  $240^\circ\text{C}$  the crystal, now  $\alpha\text{-Na}_2\text{Cr}_2\text{O}_7$ , is still single with a very similar unit cell to  $\beta\text{-Na}_2\text{Cr}_2\text{O}_7$  but with space group  $\text{A}\bar{1}$ .

Table 3.1 Crystal data for  $\alpha$  and  $\beta$   $\text{Na}_2\text{Cr}_2\text{O}_7$ . Standard errors in the last figures quoted are given in parentheses

Compound	$\beta\text{-Na}_2\text{Cr}_2\text{O}_7$	$\alpha\text{-Na}_2\text{Cr}_2\text{O}_7$
Space group	$P\bar{1}$	$A\bar{1}$
a ( $\text{\AA}$ )	7.702(10)	7.82(3)
b ( $\text{\AA}$ )	10.380(10)	10.36(3)
c ( $\text{\AA}$ )	9.402(10)	9.54(3)
$\alpha$	89.41 (10)°	89.5 (3)°
$\beta$	109.57 (10)°	110.1 (3)°
$\gamma$	114.26 (10)°	113.4 (3)°
V ( $\text{\AA}^3$ )	639	659
Z	4	4
$D_m$	2.73 (1)	
$D_x$	2.72	2.64
$\mu(\text{MoK}\alpha)$	3.67 $\text{mm}^{-1}$	3.56 $\text{mm}^{-1}$

### 3.1.1a $\beta$ -Na<sub>2</sub>Cr<sub>2</sub>O<sub>7</sub>. Experimental Procedure

#### Sample preparation and crystal data

Crystals of sodium dichromate were grown from melt in an open furnace. The hydrated Na<sub>2</sub>Cr<sub>2</sub>O<sub>7</sub>·2H<sub>2</sub>O (Shawinigan Reagent, grade 99.5) was heated up to 180°C and kept at this temperature for 24 hours as the crystals lose the water of hydration at 130°C. The anhydrous sample was then heated 20 degrees above the melting point (360°C) and kept at this temperature for a few hours. The sample then was cooled gradually and at around 200°C it was transferred to a dry box containing a dry nitrogen atmosphere.

Powder photographs of the sample sealed in capillary tubes are the same as the powder pattern given for Na<sub>2</sub>Cr<sub>2</sub>O<sub>7</sub> in ASTM x-ray powder data file (23).

The crystals were selected and sealed in thin walled quartz capillary tubes inside the dry box in nitrogen atmosphere. From x-ray precession photographs it was found that the crystals of the room temperature phase belong to the triclinic class. From these precession photographs preliminary cell constants were measured which were used throughout the analysis. In order to determine accurate bond lengths, accurate cell constants were determined from a least squares refinement of the angular settings of 15 reflections, Table 3.2, of a crystal mounted on a Syntex diffractometer. They are given in Table 3.1. The density of 2.73 gm/cm<sup>3</sup> was measured by

Table 3.2  $\beta$ -Na<sub>2</sub>Cr<sub>2</sub>O<sub>7</sub> Angular settings for 15 reflections.

$hkl^*$	$2\theta$	$\omega$	$\phi$	$\chi$
200	8.69	.01	84.79	48.37
312	17.78	359.93	144.59	76.95
1 $\bar{1}$ 4	19.53	.04	292.77	65.32
2 $\bar{1}$ 3	18.06	359.97	328.44	73.54
4 $\bar{1}$ 1	20.75	360.00	48.83	53.70
50 $\bar{1}$	21.72	.01	78.57	36.46
112	12.97	359.99	219.47	55.27
1 $\bar{3}$ 0	19.31	.07	26.52	8.54
2 $\bar{4}$ 2	21.32	.11	347.89	.25
1 $\bar{1}$ 2	13.17	.09	241.62	18.41
31 $\bar{2}$	13.48	.08	109.46	11.60
611	26.73	359.98	86.17	63.82
130	16.94	.08	190.69	12.88
1 $\bar{3}$ 0	19.27	.13	26.61	8.43
224	26.14	.02	207.34	56.88

\*The indices are given in the cell  $a = 10.067$ ,  $b = 7.702$   
 $c = 9.401$ ,  $\alpha = 109.575$ ,  $\beta = 104.225$ ,  $\gamma = 70.040$ .

flotation in an equidensity mixture of  $\text{CH}_3\text{I}$  and  $\text{CHBr}_3$  and corresponds to four  $\text{Na}_2\text{Cr}_2\text{O}_7$  units per unit cell.

#### Intensity measurements

Intensities were measured with two crystals mounted on precession cameras with  $\text{MoK}\alpha$  radiation. The first crystal of dimensions  $0.23 \times 0.32 \times 0.14$  mm was mounted along its  $[011]^*$  reciprocal axis and was used to record the layers with  $h = 0, 1, 2$  and layers with  $k = \ell - h - n$  where  $n = 0, 1, 2$  and 3. The second crystal,  $0.31 \times 0.35 \times 0.22$  mm, mounted along the  $[111]^*$  axis was used to record the layers  $h, \bar{h}, \ell; h, k, k; h, k, -(k+2h)$ .

The intensities measured with Joyce-Loebl microdensitometer were corrected for Lorentz and polarization effect but not for absorption which is effectively uniform over each precession photograph with the crystal settings used.

In all 1181 unique observed reflections were measured. Another 557 unobserved reflections were included in the final set of data plus 64 reflections which were considered as unreliable either because they were too strong to be measured or because they were behind the backstop.

#### 3.1.1b Structure Determination

The  $N(\bar{z})$  statistical test of Howells, Phillips and Rogers (20) was applied to the intensity measurements of the  $(\bar{1}10)$  and  $(010)$  projections and showed centrosymmetric in-

intensity distribution for the (010) and a hypercentric intensity distribution for ( $\bar{1}10$ ) so the space group  $P\bar{1}$  was assumed. The hypercentric distribution suggests noncrystallographic centers of symmetry such as would occur if two parallel noncentrosymmetric motifs are related by a noncrystallographic translation consistent with the supposition of a superstructure.

The structure was initially determined in the space group  $A\bar{1}$ . The ( $\bar{1}10$ ) and (010) Patterson projections calculated with the  $k+l$  even intensities gave positions for the chromium atoms which corresponded to the higher symmetry  $A\bar{1}$ . The Cr-Cr intramolecular vectors were identified in the peaks around the origin of these projections and a model was constructed for the Cr atom positions. Least squares refinement of the scale factors gave an agreement index  $R_1 = 0.55$ . It was assumed at this stage that the dichromate ion had a confirmation similar to that found in  $P\bar{1} Rb_2Cr_2O_7$ . With the positions of the Cr atoms roughly known all that was needed for the determination of the oxygen positions was the determination of an azimuthal angle around each Cr-Cr axis to give the orientation of the  $Cr_2O_7$  ion. This was found by considering the packing of the ions and the resultant model gave  $R = 0.40$  for the  $h+k$  even reflections. Difference synthesis maps for the (010) and ( $\bar{1}10$ ) projections gave the positions of the Na atoms. This model was then refined by least squares in the space group  $A\bar{1}$  using



all the  $k+l$  even reflections to give  $R_1 = 0.08$ . Deviations of the chromium atoms from these mean positions were postulated in the  $P\bar{1}$  space group using the Patterson function calculated with only the  $k+l$  odd reflections (24). In going from space group  $A\bar{1}$  to  $P\bar{1}$ , one of the two sets of centers of symmetry is lost. Since it is not obvious which set is lost, two possible models for the superstructure must be tested.

In addition, since the two  $CrO_4$  tetrahedra in a single  $Cr_2O_7$  group can be shifted from their  $A\bar{1}$  positions in the same or in opposite directions, a total of four possible models have to be tested. Only one refined satisfactorily, giving  $R_2 = 0.12$  for the  $k+l$  odd reflections.

At this stage anisotropic temperature factors were introduced, and the structure was refined further by full matrix least squares. Reflections were weighted by the function  $(3.649 - 0.083|F_o| + 0.0034|F_o|^2)^{-1}$  (22) except that zero weight was given to unobserved reflections for which  $|F_c| < |F_{min}|$  and other reflections for which measurements of  $F_o$  were judged to be particularly unreliable. Scattering factors for  $Na^+$ ,  $Cr^{++}$  and  $O^-$  (0 for the bridging oxygen atoms) were taken from International Tables for X-ray Crystallography (25) and the final weighted agreement index,  $R_2$  was 0.089 and unweighted agreement index  $R_1$  was 0.078. For the  $k+l$  odd reflections  $R_2$  was 0.109 and  $R_1$  was 0.104. In the final round of refinement 751 observed  $k+l$  odd reflections were used. In addition the 24 of the 201 unobserved

$k+l$  odd reflections for which  $|F_c| > |F_{\min}|$  were also included. Final parameter shifts were of the order of  $0.1\sigma$ , none being larger than  $0.5\sigma$ . The final atomic positions and temperature factors are given in Table 3.3 and the structure factors in Table 3.4.

### 3.1.2a $\alpha$ - $\text{Na}_2\text{Cr}_2\text{O}_7$ . Experimental Procedure

#### Specimen heating

Air at constant pressure was passed through a tubular electric furnace and was directed from above onto the crystal. The temperature was controlled by adjusting the electric current in the furnace with a potentiometer. No special attempt was made to stabilize the temperature. A Chromel Alumel thermocouple set close above the crystal was used to record the temperature on a chart recorder. The temperature fluctuation never exceeded  $\pm 2.5^\circ\text{C}$  during a 60 hour exposure.

#### Crystal data

The single crystal of  $\beta$ - $\text{Na}_2\text{Cr}_2\text{O}_7$  used for this work was sealed in a thin walled quartz capillary tube in nitrogen atmosphere.

The cell constants were measured from three precession photographs of the  $(110)$ ,  $(\bar{1}01)$  and  $(21\bar{1})$  projections. The crystal was mounted along the  $[1\bar{1}1]^*$  reciprocal axis. For each projection the same reciprocal plane of the room and the high temperature phase was photographed on the same film. The cell constants of the  $\alpha$  phase, given in Table 3.1, were

Table 3.3  $\beta$ -Na<sub>2</sub>Cr<sub>2</sub>O<sub>7</sub> Atomic positional and thermal coordinates

	x	y	z	u <sub>11</sub>	u <sub>22</sub>	u <sub>33</sub>	u <sub>12</sub>	u <sub>13</sub>	u <sub>23</sub>
Cr1	-0.1939(3)	0.0119(2)	0.1509(2)	215(15)	229(9)	225(9)	96(11)	51(9)	9(7)
Cr2	0.2488(3)	0.0803(2)	0.4091(2)	252(15)	249(9)	195(8)	135(11)	71(9)	30(7)
O11	-0.3849(15)	0.0258(1)	0.1747(9)	195(62)	459(53)	309(41)	167(54)	124(40)	98(37)
O12	-0.2380(16)	-0.1542(10)	0.1238(10)	342(72)	299(43)	345(43)	141(51)	126(43)	-9(35)
O13	-0.1368(16)	0.0913(10)	0.0150(9)	273(67)	328(45)	335(43)	41(51)	128(44)	102(35)
O21	0.3598(16)	0.1634(10)	0.5812(9)	335(71)	341(47)	283(39)	161(52)	50(42)	29(35)
O22	0.3937(18)	0.1479(12)	0.3109(10)	469(86)	635(68)	304(44)	306(69)	199(46)	176(43)
O23	0.1992(20)	-0.0871(10)	0.4072(10)	803(104)	285(46)	388(47)	321(62)	114(55)	117(38)
B12	0.0188(16)	0.0999(10)	0.3237(9)	313(69)	364(49)	261(39)	124(52)	-57(42)	-89(34)
Cr3	-0.1751(3)	0.5287(2)	0.6285(2)	220(15)	210(9)	193(8)	96(10)	56(8)	17(6)
Cr4	0.2332(3)	0.5588(2)	0.9095(2)	213(15)	240(9)	176(8)	107(11)	58(8)	31(7)
O31	-0.3367(19)	0.5531(11)	0.6831(11)	524(90)	458(58)	545(58)	342(67)	336(56)	131(47)
O32	-0.2299(17)	0.3606(9)	0.6031(10)	403(81)	265(44)	419(48)	94(55)	131(49)	-43(37)
O33	-0.1591(17)	0.5969(11)	0.4759(9)	430(77)	501(54)	231(38)	261(58)	91(43)	129(37)
O41	0.3167(17)	0.6520(11)	1.0729(9)	351(73)	460(54)	236(37)	186(57)	78(41)	-8(36)
O42	0.4257(17)	0.5752(12)	0.8634(10)	345(74)	546(64)	344(47)	141(63)	170(46)	-43(43)
O43	0.1086(18)	0.3916(11)	0.9152(11)	418(83)	367(53)	538(57)	180(61)	101(55)	170(45)
B34	0.0762(15)	0.6217(9)	0.7693(9)	241(63)	256(40)	305(40)	72(46)	-47(41)	30(32)
Na1	0.3744(10)	0.3511(6)	0.7359(5)	562(48)	336(26)	281(23)	251(31)	77(26)	43(20)
Na2	-0.2391(11)	0.2267(6)	0.3930(6)	458(53)	400(28)	323(24)	106(35)	173(28)	32(21)
Na3	0.2941(11)	0.8263(6)	1.2146(6)	669(53)	480(33)	319(25)	380(38)	201(28)	85(23)
Na4	-0.2334(9)	0.7414(5)	0.8979(5)	326(43)	338(26)	320(23)	141(31)	135(24)	61(20)

cont'd...

Table 3.3 (cont'd)

Standard errors in the last figures quoted as given by the final round of least squares analysis are shown in parantheses. The temperature factors were calculated using the expression

$$\exp[-2\pi^2 \cdot 10^{-4} (u_{11} h^2 a^{*2} + u_{22} k^2 b^{*2} + u_{33} l^2 c^{*2} + 2u_{12} hk a^*b^* + 2u_{13} hl a^*c^* + 2u_{23} kl b^*c^*)]$$

Table 3.4 Observed and calculated structure factors for  
 $\beta\text{-Na}_2\text{Cr}_2\text{O}_7$

Unobserved reflections are marked with an asterisk. U indicates an unreliable measurement which was given zero weight during refinements. Unobserved reflections for which  $F_c < F_o$  are not included.



measured from these films relative to the known cell constants of the  $\beta$  phase. The difference, in spacing and in the angles between rows of reflections of the room and the high temperature phase, was used to calculate the cell constants from the accurately known  $\beta$  cell constants.

#### Intensity measurements

Intensities were measured from integrated precession photographs taken, with  $\text{MoK}\alpha$  radiation, from a single crystal mounted along the  $[\bar{1}\bar{1}1]^*$  reciprocal axis on a precession camera. The crystal had an irregular shape which would be approximated with a spheroid of 0.29 mm height, along  $[\bar{1}\bar{1}1]^*$ , and a base with 0.19 mm length parallel to the  $(0\bar{1}\bar{1})^*$  reciprocal plane and 0.15 mm length normal to it. Integrated intensity photographs were taken of the layers  $h, -h, l; h, -(h+1), l; h, -(h+2), l; h, k, -k; h, k, -(k+2); h, k, h; h, k, h+1$  at an estimated temperature of  $260 (\pm 10)^\circ\text{C}$ . The intensities were measured with a Joyce-Loebel microdensitometer and were corrected for Lorentz and polarization effects.

In all 820 reflections were measured. After averaging of the common reflections (see in the next paragraph) a set of 512 observed reflections and 202 unobserved reflections was obtained. Absorption correction was not considered necessary.

### 3.1.2b Structure Determination

The atomic coordinates obtained during the refinement of the structure of the  $\beta$  phase in space group  $A\bar{1}$  were used as the initial coordinates of the  $\alpha$  phase structure. This model was refined with isotropic temperature factors, individual scale factors for each layer and unit weights. After three cycles the agreement factor was  $R_1 = 0.09$ . At this stage the common reflections were averaged. Further refinement was attempted with a Cruickshank weighting scheme and one overall scale but failed to give any significant improvement. The value of the weighted agreement index  $R_2$  was 0.11 and  $R_1$  0.09.

When anisotropic temperature factors for the chromium and sodium atoms were introduced and refined the weighted and unweighted agreement indices dropped to 0.088 and 0.071 respectively.

Finally anisotropic temperature factors were introduced for all atoms and the model refined further. With 100 parameters the agreement indices dropped to  $R_2 = 0.054$  and  $R_1 = 0.043$ . In the final cycle of the refinement 18 unobserved reflections, with calculated structure factors lower than the observed, were included. The reflections were weighted with the function  $w = (3.17 - 0.111|F_o| + 0.0025|F_o|^2)^{-1}$ . The scattering factors used for the  $Na^+$ ,  $Cr^{++}$ ,  $O^-$  and  $O$  for the bridging oxygen atoms were those given in the



International Tables (25).

The final atomic positions and temperature factors are given in Table 3.5 and the observed and final calculated structure factors in Table 3.6.

### 3.1.2c Possible Disorder in $\alpha$ - $\text{Na}_2\text{Cr}_2\text{O}_7$

Although the geometry of the dichromate ion in the  $\alpha$ - $\text{Na}_2\text{Cr}_2\text{O}_7$  shows bond lengths and angles close to the ones found in the other dichromates the temperature factors of the atoms of the anion are of the order of magnitude of the maximum values found in the other dichromates. Particularly the atoms 022, 023 and B12 have exceptionally large temperature factors. There are two alternative interpretations of these temperature factors, either they represent real thermal effects or the structure is disordered.

In the rest of this section we will examine the possibility of disorder in the  $\alpha$  phase. This will be done in terms of certain artificial models:

- 1) The ordered model refined with structure factors measured above the phase transition ( $\alpha$  ordered structure) or refined with  $k+l$  even structure factors measured at room temperature ( $\beta$  ordered structure).
- 2) The disordered model, Figure 3.1a, which is generated from the  $\beta$ - $\text{Na}_2\text{Cr}_2\text{O}_7$  structure by a superposition of the  $\beta$  structure and the  $\beta$  structure translated by  $(\underline{b}+\underline{c})/2$ ,

Table 3.5  $\alpha$ -Na<sub>2</sub>Cr<sub>2</sub>O<sub>7</sub>. Atomic positional and thermal coordinates

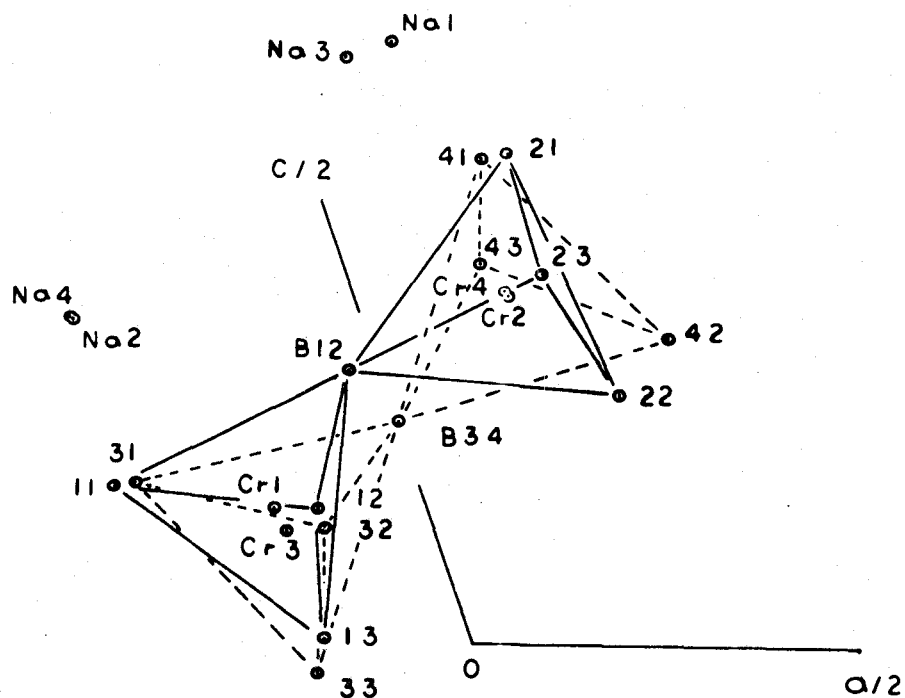
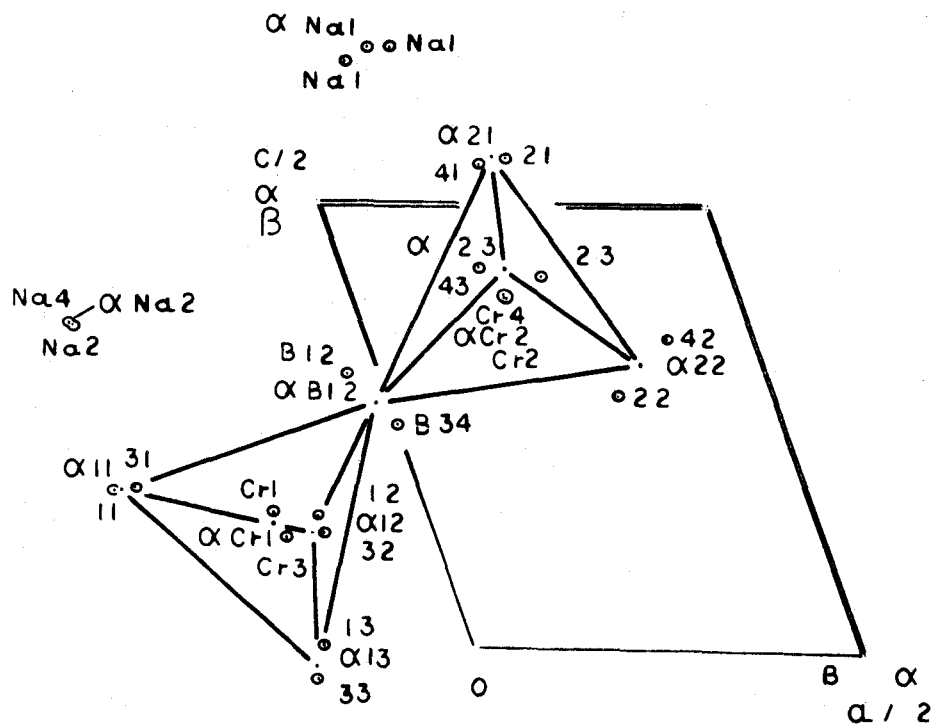
	x	y	z	u <sub>11</sub>	u <sub>22</sub>	u <sub>33</sub>	u <sub>12</sub>	u <sub>13</sub>	u <sub>23</sub>
Cr1	-0.1842(2)	0.0204(2)	0.1397(2)	362(8)	420(12)	390(8)	164(7)	92(6)	25(7)
Cr2	0.2391(2)	0.0680(2)	0.4086(2)	427(9)	438(13)	336(7)	206(8)	74(7)	21(8)
O11	-0.3569(12)	0.0439(9)	0.1782(8)	649(45)	747(72)	693(45)	366(44)	340(43)	106(47)
O12	-0.2347(11)	-0.1456(9)	0.1159(9)	619(46)	589(61)	759(49)	208(41)	250(41)	-39(43)
O13	-0.1536(12)	0.0891(10)	-0.0088(8)	784(52)	867(73)	565(42)	310(48)	385(44)	269(46)
O21	0.3338(11)	0.1541(9)	0.5757(7)	691(47)	783(69)	466(37)	336(45)	134(38)	-3(43)
O22	0.4107(14)	0.1128(15)	0.3367(10)	633(55)	1820(137)	852(60)	98(69)	425(56)	-310(76)
O23	0.1523(18)	-0.0981(12)	0.4107(11)	1693(99)	641(74)	826(59)	769(72)	-22(65)	22(65)
B12	0.0504(11)	0.1137(9)	0.2914(9)	667(46)	450(52)	896(55)	238(39)	-210(41)	33(45)
Na1	0.3377(8)	0.3429(6)	0.7265(5)	1021(36)	798(44)	586(25)	540(31)	275(27)	168(28)
Na2	-0.2351(7)	0.2382(6)	0.3934(5)	690(27)	697(37)	608(25)	93(24)	302(24)	95(23)

Standard errors in the last figures quoted as given by the final round of least squares analysis are shown in parentheses. The temperature factors were calculated using the expression given in Table 3.3.

Table 3.6  $\alpha\text{-Na}_2\text{Cr}_2\text{O}_7$ . Observed and calculated structure factors.

Unobserved reflections are marked with an asterisk. U indicates unreliable measurement which was given zero weight during refinements.

h	k	l	FO	FC
0	0	0	1000	1000
0	0	1	1000	1000
0	0	2	1000	1000
0	0	3	1000	1000
0	0	4	1000	1000
0	0	5	1000	1000
0	0	6	1000	1000
0	0	7	1000	1000
0	0	8	1000	1000
0	0	9	1000	1000
0	0	10	1000	1000
0	0	11	1000	1000
0	0	12	1000	1000
0	0	13	1000	1000
0	0	14	1000	1000
0	0	15	1000	1000
0	0	16	1000	1000
0	0	17	1000	1000
0	0	18	1000	1000
0	0	19	1000	1000
0	0	20	1000	1000
0	0	21	1000	1000
0	0	22	1000	1000
0	0	23	1000	1000
0	0	24	1000	1000
0	0	25	1000	1000
0	0	26	1000	1000
0	0	27	1000	1000
0	0	28	1000	1000
0	0	29	1000	1000
0	0	30	1000	1000
0	0	31	1000	1000
0	0	32	1000	1000
0	0	33	1000	1000
0	0	34	1000	1000
0	0	35	1000	1000
0	0	36	1000	1000
0	0	37	1000	1000
0	0	38	1000	1000
0	0	39	1000	1000
0	0	40	1000	1000
0	0	41	1000	1000
0	0	42	1000	1000
0	0	43	1000	1000
0	0	44	1000	1000
0	0	45	1000	1000
0	0	46	1000	1000
0	0	47	1000	1000
0	0	48	1000	1000
0	0	49	1000	1000
0	0	50	1000	1000
0	0	51	1000	1000
0	0	52	1000	1000
0	0	53	1000	1000
0	0	54	1000	1000
0	0	55	1000	1000
0	0	56	1000	1000
0	0	57	1000	1000
0	0	58	1000	1000
0	0	59	1000	1000
0	0	60	1000	1000
0	0	61	1000	1000
0	0	62	1000	1000
0	0	63	1000	1000
0	0	64	1000	1000
0	0	65	1000	1000
0	0	66	1000	1000
0	0	67	1000	1000
0	0	68	1000	1000
0	0	69	1000	1000
0	0	70	1000	1000
0	0	71	1000	1000
0	0	72	1000	1000
0	0	73	1000	1000
0	0	74	1000	1000
0	0	75	1000	1000
0	0	76	1000	1000
0	0	77	1000	1000
0	0	78	1000	1000
0	0	79	1000	1000
0	0	80	1000	1000
0	0	81	1000	1000
0	0	82	1000	1000
0	0	83	1000	1000
0	0	84	1000	1000
0	0	85	1000	1000
0	0	86	1000	1000
0	0	87	1000	1000
0	0	88	1000	1000
0	0	89	1000	1000
0	0	90	1000	1000
0	0	91	1000	1000
0	0	92	1000	1000
0	0	93	1000	1000
0	0	94	1000	1000
0	0	95	1000	1000
0	0	96	1000	1000
0	0	97	1000	1000
0	0	98	1000	1000
0	0	99	1000	1000
0	0	100	1000	1000

Table 3.1  $\text{Na}_2\text{Cr}_2\text{O}_7$   $\beta$  disordered structure and  $\alpha$  ordered structure.a)  $\text{Na}_2\text{Cr}_2\text{O}_7$   $\beta$  disordered structure (orthogonal projection).b)  $\text{Na}_2\text{Cr}_2\text{O}_7$ . Superposition of the orthogonal projections of the  $\alpha$  ordered structure and the  $\beta$  disordered structure.

the A centering symmetry operation. In this model atoms which in the  $\beta$ - $\text{Na}_2\text{Cr}_2\text{O}_7$  were related by the A pseudo-centering are in the  $\beta$  disordered model very close to each other. The distance between them will be called the "disorder separation". This model corresponds to a disorder structure, space group  $A\bar{1}$ , in which each dichromate ion has two possible conformations similar to the ones found in  $\beta$ - $\text{Na}_2\text{Cr}_2\text{O}_7$ , each possible conformation occurring with equal probability. This model can be refined using the structure factors measured above the phase transition ( $\alpha$ -disordered structure) or using the  $k+l$  even structure factors measured at room temperature ( $\beta$ -disordered structure).

All these structures with the exception of the  $\beta$  disordered structure have been refined.

From the experimental evidence of only small changes in the intensities of even reflections and small changes in volume, we expect that the structure of the  $\alpha$  phase will differ very little either from the  $\beta$  ordered structure if the  $\alpha$  structure is ordered or from the  $\beta$  disordered structure if the  $\alpha$  structure is disordered.

The  $\alpha$  disordered structure with isotropic temperature factors, 89 variables, gave final agreement indices  $R_1 = 0.051$  and  $R_2 = 0.063$ . In this structure it is not possible to identify two dichromate ions with interatomic

distances and angles close to those found in other dichromate structures. Bond lengths for the terminal oxygen atoms deviate up to  $0.1 \text{ \AA}$  from the usual values of  $1.60$  to  $1.63 \text{ \AA}$ . The disorder separations in this structure, Table 3.7, when compared with those of the  $\beta$  disordered structure show no difference except for the Cr1, 032 and B12 for which the separation has decreased and the Na<sub>2</sub> for which it has increased. This indicates that if the  $\alpha$  structure is disordered the Cr<sub>2</sub>O<sub>7</sub> ions are closer to their mean positions than they are in the  $\beta$  phase.

The  $\beta$  ordered structure with anisotropic temperature factors, 100 variables, gave an agreement index  $R_1 = 0.081$ , using unit weights. The geometry for the dichromate ion is similar to that found in the  $\alpha$  ordered model, Table 3.8, but the Cr-O bond lengths are rather short, especially the Cr2-B12 distance of  $1.71 \text{ \AA}$ . In Table 3.9 we compare the temperature factors of the  $\alpha$  and  $\beta$  ordered structures with those found in  $\beta\text{-Na}_2\text{Cr}_2\text{O}_7$ . The temperature factors of the  $\alpha$  ordered structure have been corrected to room temperature by reducing them by the empirical factor of 0.3. The temperature factors which are starred (\*) are for those atoms which show significant deviations from room temperature values. The atoms marked in Table 3.9 with a dagger (+) show significant deviations only in the  $\beta$  ordered structure. For these atoms the true disorder separation should be zero in the

Table 3.7 Disorder separations in  $\alpha$  and  $\beta$  disordered structures

	Disorder separation in $\text{\AA}$	
	$\beta$ disordered structure	$\alpha$ disordered structure
Cr1-Cr3	0.31 $\text{\AA}$	0.19 $\text{\AA}$
Cr2-Cr4	0.21	0.25
011-031	0.35	0.28
012-032	0.26	0.27
013-033	0.37	0.34
021-041	0.28	0.30
022-042	0.97	0.71
023-043	0.67	0.65
B12-B34	0.76	0.58
Na1-Na3	0.53	0.40
Na2-Na4	0.14	0.40

Table 3.8 Geometry of the dichromate ion in  $\alpha$  and  $\beta$  ordered structure

	Distances in Å angles in degrees	
	$\alpha$ sodium ordered structure	$\beta$ sodium ordered structure
Distances and Angles		
Cr1-011	1.620 Å	1.598 Å
-012	1.604	1.607
-013	1.627	1.586
B12	1.785	1.779
O11-Cr1-012	110.6°	110.1°
013	112.3	112.1
B12	108.7	109.2
012 013	109.6	110.4
B12	110.3	109.4
013 B12	105.2	105.4
Cr2-021	1.604 Å	1.595 Å
022	1.618	1.554
023	1.583	1.590
B12	1.750	1.712
O21-Cr1-022	109.2°	109.7°
023	111.2	111.7
B12	110.4	110.6
022 023	109.1	108.3
B12	106.7	107.1
023 B12	110.0	109.3
Cr1-B12-Cr2	135.1°	136.6°
Cr1-Cr2	3.27 Å	3.24 Å



Table 3.9 Principal axes of thermal ellipsoids in  $\beta$ -Na<sub>2</sub>Cr<sub>2</sub>O<sub>7</sub> and in  $\alpha$  and  $\beta$  ordered structures

Atom	Cr1			Cr2			O11			O12			O13			O21		
	$\beta$ 1	16	15	14	17	14	14	22	17	12	20	18	16	22	18	14	20	18
$\beta$ 2	16	14	14	16	15	13	26	21	14	22	21	15	23	20	14	22	19	15
$\beta$ ord.str.	23*	16	15 <sup>†</sup>	20*	16	14 <sup>†</sup>	26	20	16	25*	19	17 <sup>†</sup>	26*	23*	18*	26*	21	17 <sup>†</sup>
$\alpha$ ord. str.	17	16	15	18	16	14	22	21	17	23	20	18	24	22	15	23	21	17

Atom	O22			O23			B12			Na1			Na2		
	$\beta$ 1	26	20	16	30	20	13	24	20	12	25	17	16	24	19
$\beta$ 2	26	19	16	26	20	17	23	16	13	26	18	17	18	18	17
$\beta$ ord. str.	62*	21	13*	45*	22	15	52*	17	14	40*	19	17	22	20	18
$\alpha$ ord. str.	39*	21	17	37*	22	15	32*	17	15	26	20	18	25	20	17

The axes are given in  $10^{-2}$  Å. The  $\alpha$  and  $\beta$  ordered structure axes have been corrected to room temperature.

\* Atoms which show significant deviations from room temperature values.

† Atoms which show significant deviations only in the  $\beta$  ordered structure.

$\beta$ 2 Signifies that the temperature factor belongs to the atom related by a pseudotranslation with the one named in the table.

disordered  $\alpha$  structure and for all practical purposes they can be considered ordered<sup>†</sup>. In almost all cases the major axis in the  $\beta$  ordered refinement is larger, as one expects from the disorder separation in this model, but the temperature factors for the  $\alpha$  ordered structure are normal except for the 022, 023 and B12 atoms which show significantly large deviations both in  $\alpha$  and  $\beta$  ordered structures. The major axes in the  $\alpha$  phase are all the same size as in the  $\beta$  phase (except for the three anomalous ones) and almost all are smaller than temperature factors of the  $\beta$  ordered structure.

Hamilton's statistical test (26) applied to the  $\alpha$  ordered structure ( $R_1 = 0.043$ ,  $R_2 = 0.054$ , 100 variables) and the  $\alpha$  disordered structure ( $R_1 = 0.051$ ,  $R_2 = 0.063$ , 89 variables) shows that the  $\alpha$  disordered structure must be rejected at the 0.005 significance level.

The geometry of the dichromate ion in the  $\alpha$  ordered structure has bond lengths and angles very similar to those found in the other dichromates while the geometry of the anions of the  $\alpha$  disordered structure is much less reasonable.

---

<sup>†</sup>The disorder separation calculated for these atoms,  $\alpha$  ordered structure, arises because the  $\alpha$  disordered structure has been calculated with isotropic temperature factors. The real anisotropy of the temperature factors is fitted by separating the atoms by about 0.2 Å.

As was mentioned in section 3.1.0 the intensities of the reflections of a single crystal of  $\text{Na}_2\text{Cr}_2\text{O}_7$  have been observed as a function of temperature from a series of precession photographs. Reflections with  $k+l = \text{odd}$  become weaker as the temperature is raised, becoming zero above the transition temperature while reflections with  $k+l$  even change only slightly. No diffuse scattering was observed around the positions of the  $k+l$  odd reflections either below or above the transition and their shape remained sharp up to the transition, further indicating that the phase transition does not involve disorder.

From the discussion above the only feature which suggests that the  $\alpha$  phase is disordered is the anomalously large temperature factors of the atoms 022, 023 and B12. On the other hand, the statistical test, the molecular geometry, the general reduction of the disorder separations or anisotropic temperature factors and the absence of any diffuse reflections in the x-ray photographs all suggest that the structure is ordered.

If this is the case, the atoms 022, 023 and B12 must have large real thermal motions and this effect will be discussed in Chapter 4.

### 3.2.0 Rb<sub>2</sub>Cr<sub>2</sub>O<sub>7</sub>.Introduction

Rb<sub>2</sub>Cr<sub>2</sub>O<sub>7</sub> is polymorphic. At room temperatures it has been observed in four forms two monoclinic VII P2<sub>1/n</sub> and X C2/c and two triclinic β1(VIII)P $\bar{1}$  and β2P $\bar{1}$ . The VII, X and β1 are grown from aqueous solutions (8), the β2P $\bar{1}$  is obtained by cooling from a high polymorph. The VII (P2<sub>1/n</sub>) phase is metastable (27,28,29) however its stability differs only slightly from that of αP $\bar{1}$  and the two forms may exist in contact for a long period (29). β1P $\bar{1}$  Rb<sub>2</sub>Cr<sub>2</sub>O<sub>7</sub> undergoes an irreversible transition to an unknown structure at 318°C. This transition takes place slowly and with a well-defined boundary (6), on further heating a reversible transition occurs at 337°C. On cooling the 318° effect disappears and is replaced by a reversible phase transition at 260°C to a new triclinic phase, the β2 P $\bar{1}$  Rb<sub>2</sub>Cr<sub>2</sub>O<sub>7</sub>.

A knowledge of the structure of the various polymorphous is necessary in order to understand the nature of phase transitions between them. We have determined the structure of β1(VIII) P $\bar{1}$  Rb<sub>2</sub>Cr<sub>2</sub>O<sub>7</sub> (see also (9)). During the course of our work we learned of the work of P. Löfgren and K. Waltersson (10) and P. Löfgren (11) who have determined the C2/c and P2<sub>1/n</sub> structures. We have also briefly examined the β2 P $\bar{1}$  phase.

### 3.2.1a $\beta 1$ (VIII) $P\bar{1}$ $Rb_2Cr_2O_7$ . Experimental Procedure

#### Sample preparation and crystal data

An ion exchange column was prepared in the Rb salt form through treatment with RbI. The column was then treated with  $Na_2Cr_2O_7$ . Crystals were obtained by slow evaporation of the solution at 42°C.

Originally the crystals studied from this sample were monoclinic space group  $P2_1/n$ . After six months only triclinic ( $\beta 1$ ) could be found.

Preliminary studies of the triclinic single crystals using precession and Weissenberg photographs showed that the cell constants agreed with those given by Klement and Schwab (6). Accurate cell constants were measured from Weissenberg photographs calibrated with rutile ( $a = 4.59369$ ,  $c = 2,95814 \text{ \AA}$  (30) by mounting first the rutile crystal and then the  $Rb_2Cr_2O_7$  on the same camera and recording their diffraction patterns on the same film. The density of 3.12  $gr. cm^{-3}$  given in (31) corresponds to four  $Rb_2Cr_2O_7$  units per unit cell. The crystal data are listed in Table 3.10.

#### Intensity measurements

Intensities were measured on a Joyce-Loebel microdensitometer from integrated Weissenberg photographs of the layers with  $k = 0, 1, 2, 3, 4$  taken with  $CuK\alpha$  radiation using a crystal of dimensions  $0.06 \times 0.20 \times 0.06$  mm with the long edge along the  $b$  and integrated precession photographs

Table 3.10 Crystal data for  $\beta 1$  and  $\beta 2$   $\text{Rb}_2\text{Cr}_2\text{O}_7$ . Standard errors in the last figures quoted are given in parentheses.

Compound	$\beta 1$ $\text{Rb}_2\text{Cr}_2\text{O}_7$	$\beta 2$ $\text{Rb}_2\text{Cr}_2\text{O}_7$
System	Triclinic	Triclinic
Space group	$\text{P}\bar{1}$	$\text{P}\bar{1}$
a (Å)	13.554 (1)	7.60 (3)
b (Å)	7.640 (3)	7.39 (3)
c (Å)	7.735 (2)	7.85 (3)
$\alpha$	93.64 (20)°	90.2 (4)°
$\beta$	98.52 (1)°	70.0 (4)°
$\gamma$	88.80 (4)°	70.5 (4)°
$V(\text{Å}^3)$	790	387
Z	4	2
$D_m$	3.12	
$D_x$	3.25	
$\mu(\text{MoK}\alpha)$	15.78 $\text{mm}^{-1}$	
$\mu(\text{CuK}\alpha)$	40.44 $\text{mm}^{-1}$	

of the layers with  $l = 0, 1, 2$  and  $h = 0, 1, 2$  taken with MoK $\alpha$  radiation using a second crystal with dimensions  $0.09 \times 0.30 \times 0.09$  mm with the long edge along the  $b$ .

The intensities were corrected for Lorentz and polarization effects but not for absorption. A standard error ( $\sigma$ ) was estimated for each intensity measurement for use in weighting the observed structure factors during the least-squares refinement. Each unobserved reflection was assigned the value of the local minimum observed intensity. In all 3221 measurements were made of 2881 independent reflections, of which 1618 were observed and 1263 unobserved.

### 3.2.1b Structure Determination

It was assumed that the structure of triclinic Rb<sub>2</sub>Cr<sub>2</sub>O<sub>7</sub> would be related to that of triclinic K<sub>2</sub>Cr<sub>2</sub>O<sub>7</sub> (2) since it had a similar unit cell and therefore it was assumed that the space group was also  $P\bar{1}$ . The structure was solved from the (010) and the (001) Patterson projections. In the (001) projection the Rb-Rb and Rb-Cr peaks were concentrated in a few regions in the map giving big peaks with the individual Rb-Rb or Rb-Cr vectors completely unresolved. Nevertheless this helped to give a rough estimate of the Rb  $x, y$  coordinates, which were refined by difference Fourier synthesis. Positions for the Cr atoms were determined from the difference synthesis and with successive difference synthe-

ses the x and y coordinates of the oxygen atoms were found. The z coordinates were determined from the (010) Patterson projection for the Rb and Cr atoms and from the (010) difference synthesis for the oxygen atoms.

This model was refined with isotropic temperature factors with a full matrix least-squares program to an agreement index of  $R_2 = 0.08$ . At this stage anisotropic temperature factors were introduced and the model was refined further. Throughout the refinement a scale factor for each of the 11 independently measured layers was used. The scattering factors used for  $\text{Rb}^+$ ,  $\text{Cr}^{++}$ , O (bridging oxygen) and  $\text{O}^-$  (terminal oxygen atoms) were those given in the International Tables (25) corrected for dispersion using the mean value of the real parts of the corrections for  $\text{CuK}\alpha$  and  $\text{MoK}\alpha$  radiations (25). In the refinement the weight used was  $1/\sigma^2$ . Comparison between  $F_o$  and  $F_c$  for the largest values of  $F_o$  at small  $2\theta$ , showed that systematically  $F_o$  was less than  $F_c$  indicating secondary extinction. The effect was appreciable for the 400 and 102 reflections only and their weight was set to zero. The weight was set to zero also for all unobserved reflections with  $F_c < F_o$  and for 43 other reflections judged a priori to be unreliable. The final weighted agreement index  $R_2$  was 0.058 and the unweighted agreement index  $R_1$  0.063. The mean value of  $w(|F_o| - |F_c|)^2$  plotted as a function of  $F_o$  showed no systematic variation which would indicate that the



weighting scheme was inadequate.

The final atomic coordinates and temperature factors are given in Table 3.11. The observed and final calculated structure factors are given in Table 3.12.

### 3.2.2 $\beta 2 \bar{P}1 \text{ Rb}_2\text{Cr}_2\text{O}_7$ . Experimental Procedure

#### Sample preparation and crystal data

Crystals of  $\text{Rb}_2\text{Cr}_2\text{O}_7$  in powder form were heated above the melting point ( $390^\circ\text{C}$ ) and then they were gradually cooled. Crystals from the sample were mounted on a precession camera. The x-ray photographs showed that the crystals were twinned and belonged to the triclinic crystal class. The existence of centers of symmetry in  $\beta 1 \text{ Rb}_2\text{Cr}_2\text{O}_7$  and in  $\beta 1 \text{ K}_2\text{Cr}_2\text{O}_7$  to whose structures the  $\beta 2 \text{ Rb}_2\text{Cr}_2\text{O}_7$  probably is similar suggest as  $\bar{P}1$  the most probable space group of the  $\beta 2 \text{ Rb}_2\text{Cr}_2\text{O}_7$ . The cell constants measured from uncalibrated precession photographs are given in Table 3.10.

The volume of  $387 \text{ \AA}^3$  corresponds to two units of  $\text{Rb}_2\text{Cr}_2\text{O}_7$  per unit cell.

It was found that the twins were related by a mirror plane parallel to the a,b axis (twinning plane).

The structure of the phase is discussed in Chapter 5.6.

Table 3.11  $\beta_1 \text{P}\bar{1}$   $\text{Rb}_2\text{Cr}_2\text{O}_7$  atomic positional and thermal coordinates.\*

Atom	$\underline{x}$	$\underline{y}$	$\underline{z}$	Temperature factor components					
				$\beta_{11}$	$\beta_{22}$	$\beta_{33}$	$\beta_{12}$	$\beta_{13}$	$\beta_{23}$
Rb1	0.13528	0.11118	0.87628	37	91	106	-12	20	-18
Rb2	-0.15303	0.22589	0.62431	32	122	73	-8	6	16
Rb3	0.34205	0.55555	0.80287	24	102	88	-2	8	12
Rb4	0.62878	0.78601	0.70265	37	131	86	-7	14	6
$\sigma(\text{Rb})$	0.00011	0.00019	0.00016	1	4	3	2	1	3
Cr1	0.1107	0.2853	0.3915	24	73	73	-16	4	-7
Cr2	-0.0853	0.3531	0.1361	26	71	79	-2	13	7
Cr3	0.3883	0.0613	0.7559	28	93	84	-8	13	1
Cr4	0.5826	0.3022	0.7157	26	85	78	-12	13	-0
$\sigma(\text{Cr})$	0.0002	0.0003	0.0003	2	6	4	3	2	4
B12	0.0238	0.4283	0.2734	50	59	105	0	10	-10
O11	0.1994	0.4025	0.4953	23	117	193	9	-13	-67
O12	0.1543	0.1463	0.2571	46	168	93	28	11	-27
O13	0.0546	0.1833	0.5225	40	267	122	2	25	49
O21	-0.1478	0.5180	0.0506	21	73	192	15	15	54
O22	-0.1528	0.2493	0.2534	44	91	80	-20	13	-2
O23	-0.0546	0.2166	-0.0158	46	128	80	23	14	-13
B34	0.4712	0.1857	0.6530	37	111	127	-41	15	32
O31	0.2966	0.0102	0.6072	35	135	142	-5	16	24
O32	0.3496	0.1818	0.9121	29	151	97	8	21	-22
O33	0.4430	-0.1138	0.8289	48	140	156	-7	-14	4
O41	0.6197	0.3717	0.5466	69	115	103	1	55	31
O42	0.6678	0.1800	0.8150	34	129	191	16	27	39
O43	0.5604	0.4666	0.8438	48	118	104	6	34	-17
$\sigma(\text{O})$	0.0007	0.0013	0.0012	8	26	20	11	10	17

\*The standard errors are those indicated by the least-squares refinement. The temperature factors appear in the structure factor calculation as  $\exp(-10^{-4}(\beta_{11}h^2 + \beta_{22}k^2 + \beta_{33}l^2 + 2\beta_{12}hk + 2\beta_{13}hl + 2\beta_{23}kl))$ .

Table 3.12  $\beta\text{-Rb}_2\text{Cr}_2\text{O}_7$ . Observed and calculated structure factors

Unobserved reflections are marked with an asterisk. U indicates an unreliable measurement and X indicates a reflection believed to show extinction effects. S is the estimated standard error of FO.

FO	FC	S
111	111	1.1
112	112	1.1
113	113	1.1
114	114	1.1
115	115	1.1
116	116	1.1
117	117	1.1
118	118	1.1
119	119	1.1
120	120	1.1
121	121	1.1
122	122	1.1
123	123	1.1
124	124	1.1
125	125	1.1
126	126	1.1
127	127	1.1
128	128	1.1
129	129	1.1
130	130	1.1
131	131	1.1
132	132	1.1
133	133	1.1
134	134	1.1
135	135	1.1
136	136	1.1
137	137	1.1
138	138	1.1
139	139	1.1
140	140	1.1
141	141	1.1
142	142	1.1
143	143	1.1
144	144	1.1
145	145	1.1
146	146	1.1
147	147	1.1
148	148	1.1
149	149	1.1
150	150	1.1
151	151	1.1
152	152	1.1
153	153	1.1
154	154	1.1
155	155	1.1
156	156	1.1
157	157	1.1
158	158	1.1
159	159	1.1
160	160	1.1
161	161	1.1
162	162	1.1
163	163	1.1
164	164	1.1
165	165	1.1
166	166	1.1
167	167	1.1
168	168	1.1
169	169	1.1
170	170	1.1
171	171	1.1
172	172	1.1
173	173	1.1
174	174	1.1
175	175	1.1
176	176	1.1
177	177	1.1
178	178	1.1
179	179	1.1
180	180	1.1
181	181	1.1
182	182	1.1
183	183	1.1
184	184	1.1
185	185	1.1
186	186	1.1
187	187	1.1
188	188	1.1
189	189	1.1
190	190	1.1
191	191	1.1
192	192	1.1
193	193	1.1
194	194	1.1
195	195	1.1
196	196	1.1
197	197	1.1
198	198	1.1
199	199	1.1
200	200	1.1
201	201	1.1
202	202	1.1
203	203	1.1
204	204	1.1
205	205	1.1
206	206	1.1
207	207	1.1
208	208	1.1
209	209	1.1
210	210	1.1
211	211	1.1
212	212	1.1
213	213	1.1
214	214	1.1
215	215	1.1
216	216	1.1
217	217	1.1
218	218	1.1
219	219	1.1
220	220	1.1
221	221	1.1
222	222	1.1
223	223	1.1
224	224	1.1
225	225	1.1
226	226	1.1
227	227	1.1
228	228	1.1
229	229	1.1
230	230	1.1
231	231	1.1
232	232	1.1
233	233	1.1
234	234	1.1
235	235	1.1
236	236	1.1
237	237	1.1
238	238	1.1
239	239	1.1
240	240	1.1
241	241	1.1
242	242	1.1
243	243	1.1
244	244	1.1
245	245	1.1
246	246	1.1
247	247	1.1
248	248	1.1
249	249	1.1
250	250	1.1
251	251	1.1
252	252	1.1
253	253	1.1
254	254	1.1
255	255	1.1
256	256	1.1
257	257	1.1
258	258	1.1
259	259	1.1
260	260	1.1
261	261	1.1
262	262	1.1
263	263	1.1
264	264	1.1
265	265	1.1
266	266	1.1
267	267	1.1
268	268	1.1
269	269	1.1
270	270	1.1
271	271	1.1
272	272	1.1
273	273	1.1
274	274	1.1
275	275	1.1
276	276	1.1
277	277	1.1
278	278	1.1
279	279	1.1
280	280	1.1
281	281	1.1
282	282	1.1
283	283	1.1
284	284	1.1
285	285	1.1
286	286	1.1
287	287	1.1
288	288	1.1
289	289	1.1
290	290	1.1
291	291	1.1
292	292	1.1
293	293	1.1
294	294	1.1
295	295	1.1
296	296	1.1
297	297	1.1
298	298	1.1
299	299	1.1
300	300	1.1
301	301	1.1
302	302	1.1
303	303	1.1
304	304	1.1
305	305	1.1
306	306	1.1
307	307	1.1
308	308	1.1
309	309	1.1
310	310	1.1
311	311	1.1
312	312	1.1
313	313	1.1
314	314	1.1
315	315	1.1
316	316	1.1
317	317	1.1
318	318	1.1
319	319	1.1
320	320	1.1
321	321	1.1
322	322	1.1
323	323	1.1
324	324	1.1
325	325	1.1
326	326	1.1
327	327	1.1
328	328	1.1
329	329	1.1
330	330	1.1
331	331	1.1
332	332	1.1
333	333	1.1
334	334	1.1
335	335	1.1
336	336	1.1
337	337	1.1
338	338	1.1
339	339	1.1
340	340	1.1
341	341	1.1
342	342	1.1
343	343	1.1
344	344	1.1
345	345	1.1
346	346	1.1
347	347	1.1
348	348	1.1
349	349	1.1
350	350	1.1
351	351	1.1
352	352	1.1
353	353	1.1
354	354	1.1
355	355	1.1
356	356	1.1
357	357	1.1
358	358	1.1
359	359	1.1
360	360	1.1
361	361	1.1
362	362	1.1
363	363	1.1
364	364	1.1
365	365	1.1
366	366	1.1
367	367	1.1
368	368	1.1
369	369	1.1
370	370	1.1
371	371	1.1
372	372	1.1
373	373	1.1
374	374	1.1
375	375	1.1
376	376	1.1
377	377	1.1
378	378	1.1
379	379	1.1
380	380	1.1
381	381	1.1
382	382	1.1
383	383	1.1
384	384	1.1
385	385	1.1
386	386	1.1
387	387	1.1
388	388	1.1
389	389	1.1
390	390	1.1
391	391	1.1
392	392	1.1
393	393	1.1
394	394	1.1
395	395	1.1
396	396	1.1
397	397	1.1
398	398	1.1
399	399	1.1
400	400	1.1
401	401	1.1
402	402	1.1
403	403	1.1
404	404	1.1
405	405	1.1
406	406	1.1
407	407	1.1
408	408	1.1
409	409	1.1
410	410	1.1
411	411	1.1
412	412	1.1
413	413	1.1
414	414	1.1
415	415	1.1
416	416	1.1
417	417	1.1
418	418	1.1
419	419	1.1
420	420	1.1
421	421	1.1
422	422	1.1
423	423	1.1
424	424	1.1
425	425	1.1
426	426	1.1
427	427	1.1
428	428	1.1
429	429	1.1
430	430	1.1
431	431	1.1
432	432	1.1
433	433	1.1
434	434	1.1
435	435	1.1
436	436	1.1
437	437	1.1
438	438	1.1
439	439	1.1
440	440	1.1
441	441	1.1
442	442	1.1
443	443	1.1
444	444	1.1
445	445	1.1
446	446	1.1
447	447	1.1
448	448	1.1
449	449	1.1
450	450	1.1
451	451	1.1
452	452	1.1
453	453	1.1
454	454	1.1
455	455	1.1
456	456	1.1
457	457	1.1
458	458	1.1
459	459	1.1
460	460	1.1
461	461	1.1
462	462	1.1
463	463	1.1
464	464	1.1
465	465	1.1
466	466	1.1
467	467	

Table 3.12  $\beta 1\text{-Rb}_2\text{Cr}_2\text{O}_7$  (continued)

FO	FC	S
1	1	1
2	2	2
3	3	3
4	4	4
5	5	5
6	6	6
7	7	7
8	8	8
9	9	9
10	10	10
11	11	11
12	12	12
13	13	13
14	14	14
15	15	15
16	16	16
17	17	17
18	18	18
19	19	19
20	20	20
21	21	21
22	22	22
23	23	23
24	24	24
25	25	25
26	26	26
27	27	27
28	28	28
29	29	29
30	30	30
31	31	31
32	32	32
33	33	33
34	34	34
35	35	35
36	36	36
37	37	37
38	38	38
39	39	39
40	40	40
41	41	41
42	42	42
43	43	43
44	44	44
45	45	45
46	46	46
47	47	47
48	48	48
49	49	49
50	50	50
51	51	51
52	52	52
53	53	53
54	54	54
55	55	55
56	56	56
57	57	57
58	58	58
59	59	59
60	60	60
61	61	61
62	62	62
63	63	63
64	64	64
65	65	65
66	66	66
67	67	67
68	68	68
69	69	69
70	70	70
71	71	71
72	72	72
73	73	73
74	74	74
75	75	75
76	76	76
77	77	77
78	78	78
79	79	79
80	80	80
81	81	81
82	82	82
83	83	83
84	84	84
85	85	85
86	86	86
87	87	87
88	88	88
89	89	89
90	90	90
91	91	91
92	92	92
93	93	93
94	94	94
95	95	95
96	96	96
97	97	97
98	98	98
99	99	99
100	100	100





Table 3.12  $^{81}\text{-Rb}_2\text{Cr}_2\text{O}_7$  (continued)

FO	FC	S
1	1	1
2	2	2
3	3	3
4	4	4
5	5	5
6	6	6
7	7	7
8	8	8
9	9	9
10	10	10
11	11	11
12	12	12
13	13	13
14	14	14
15	15	15
16	16	16
17	17	17
18	18	18
19	19	19
20	20	20
21	21	21
22	22	22
23	23	23
24	24	24
25	25	25
26	26	26
27	27	27
28	28	28
29	29	29
30	30	30
31	31	31
32	32	32
33	33	33
34	34	34
35	35	35
36	36	36
37	37	37
38	38	38
39	39	39
40	40	40
41	41	41
42	42	42
43	43	43
44	44	44
45	45	45
46	46	46
47	47	47
48	48	48
49	49	49
50	50	50
51	51	51
52	52	52
53	53	53
54	54	54
55	55	55
56	56	56
57	57	57
58	58	58
59	59	59
60	60	60
61	61	61
62	62	62
63	63	63
64	64	64
65	65	65
66	66	66
67	67	67
68	68	68
69	69	69
70	70	70
71	71	71
72	72	72
73	73	73
74	74	74
75	75	75
76	76	76
77	77	77
78	78	78
79	79	79
80	80	80
81	81	81
82	82	82
83	83	83
84	84	84
85	85	85
86	86	86
87	87	87
88	88	88
89	89	89
90	90	90
91	91	91
92	92	92
93	93	93
94	94	94
95	95	95
96	96	96
97	97	97
98	98	98
99	99	99
100	100	100

### 3.3 Cs<sub>2</sub>Cr<sub>2</sub>O<sub>7</sub>. Experimental Procedure

#### Crystal data

Crystals of Cs<sub>2</sub>Cr<sub>2</sub>O<sub>7</sub> were grown from aqueous solutions prepared from Cs<sub>2</sub>Cr<sub>2</sub>O<sub>7</sub> Alfa Inorganics, Reagent, 99.9%. The crystals obtained were needle like thin (~ 0.02 mm) plates of orange colour. The crystals examined with a polarizing microscope showed very sharp extinction. Preliminary studies with Weissenberg and precession cameras showed that the crystals were triclinic and twinned. Diffuse streaks indicated that the crystals were disordered as well. The photograph given in Figure 3.2 was obtained with a Weissenberg camera. The crystal was mounted with its needle axis lying approximately along the spindle axis of the camera. The photographs, Figures 3.3 and 3.4, were obtained with a precession camera from the same crystal. Because the 3.3 and 3.4 photographs show diffuse streaks it was not possible to determine the position of these planes accurately enough. The cell constants given in Table 3.13 should only be regarded as approximate.



Figure 3.2  $\text{Cs}_2\text{Cr}_2\text{O}_7$  *h0l* Weissenberg photograph. Cu  
unfiltered radiation

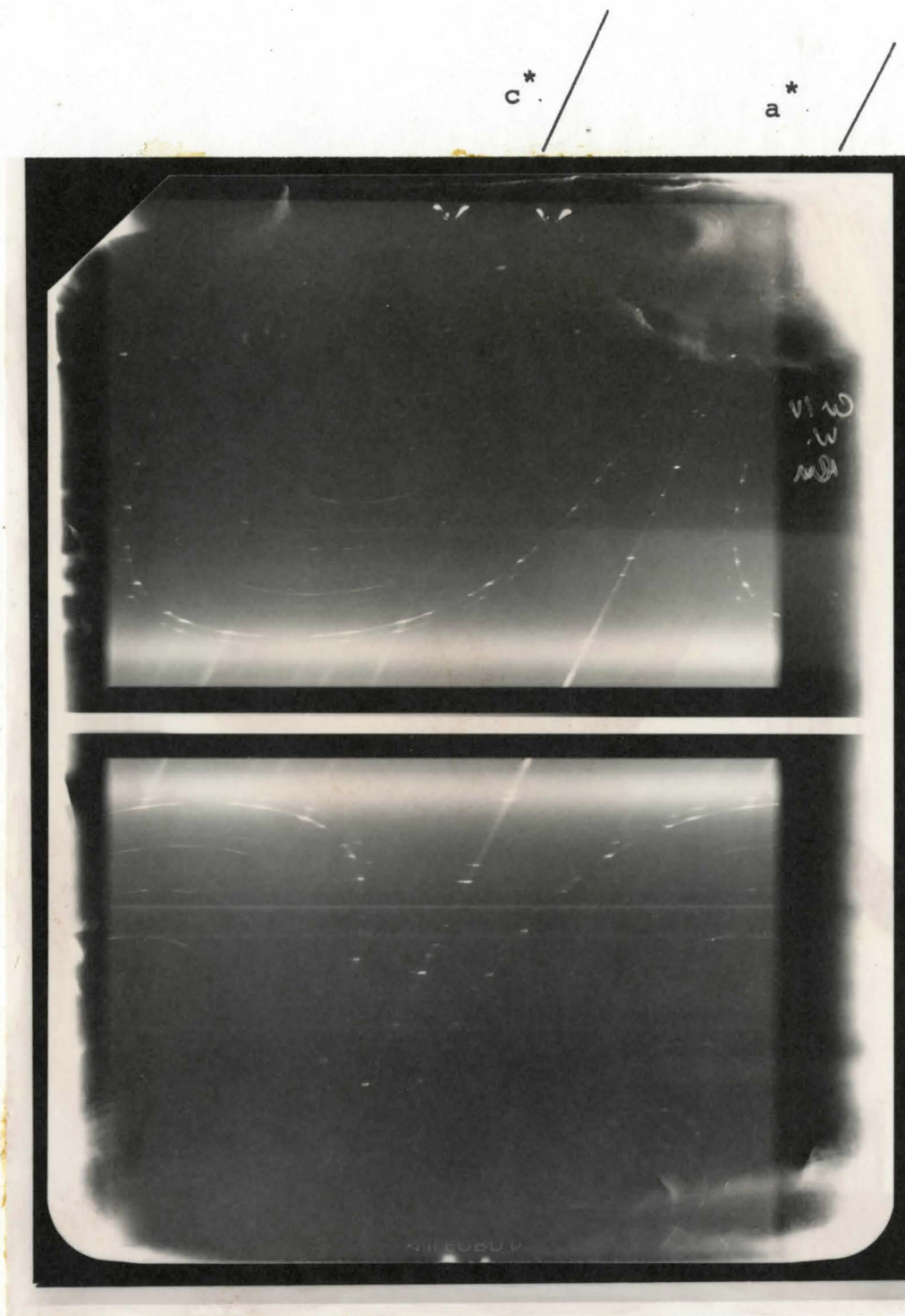


Figure 3.3  $\text{Cs}_2\text{Cr}_2\text{O}_7$   $hk0$  precession photograph.  
(Mo radiation, spindle axis  $18^\circ 15'$ )

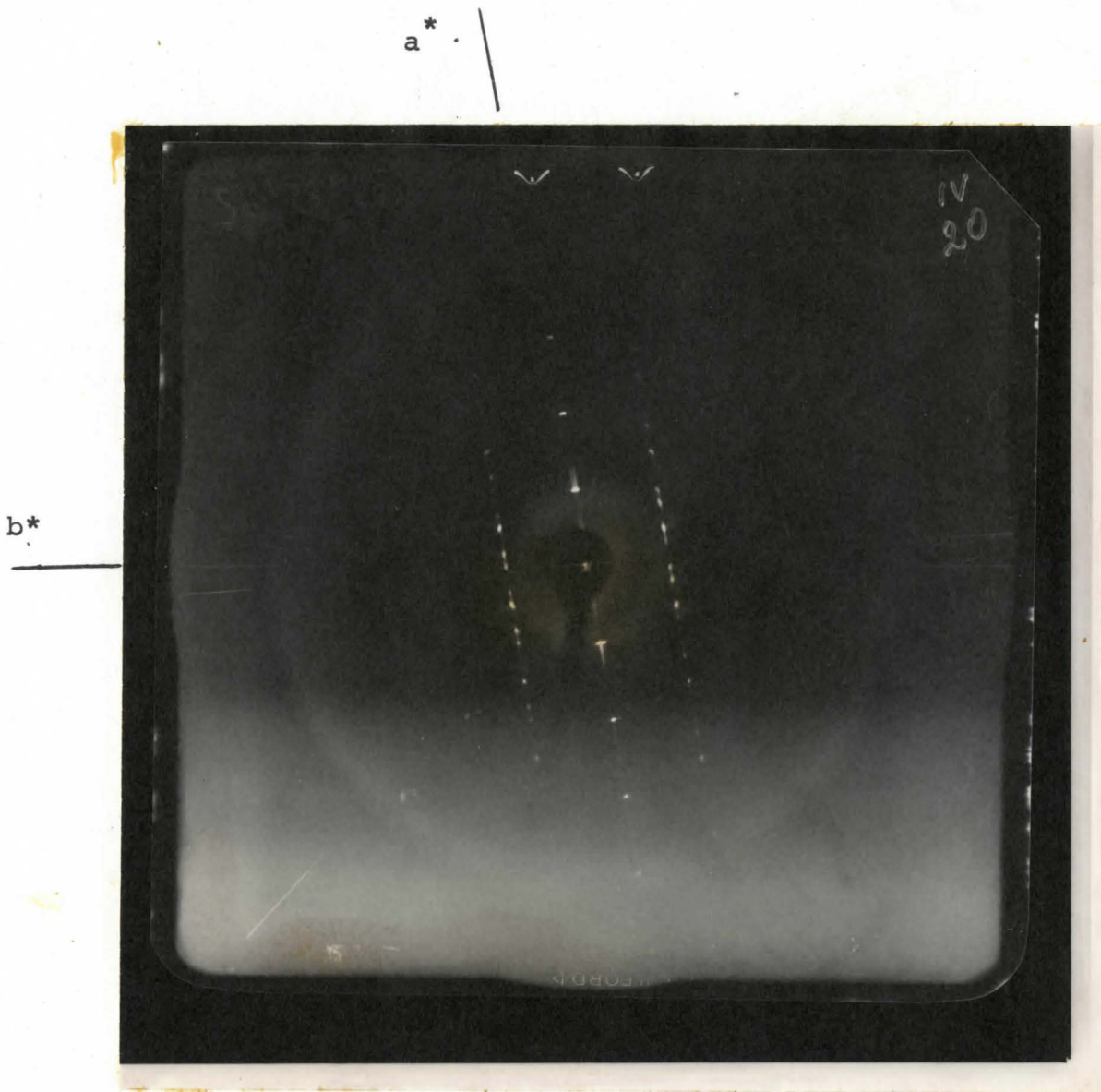


Figure 3.4  $\text{Cs}_2\text{Cr}_2\text{O}_7$   $0kl$  precession photograph.  
(Mo radiation, spindle axis  $99^\circ 35'$ )

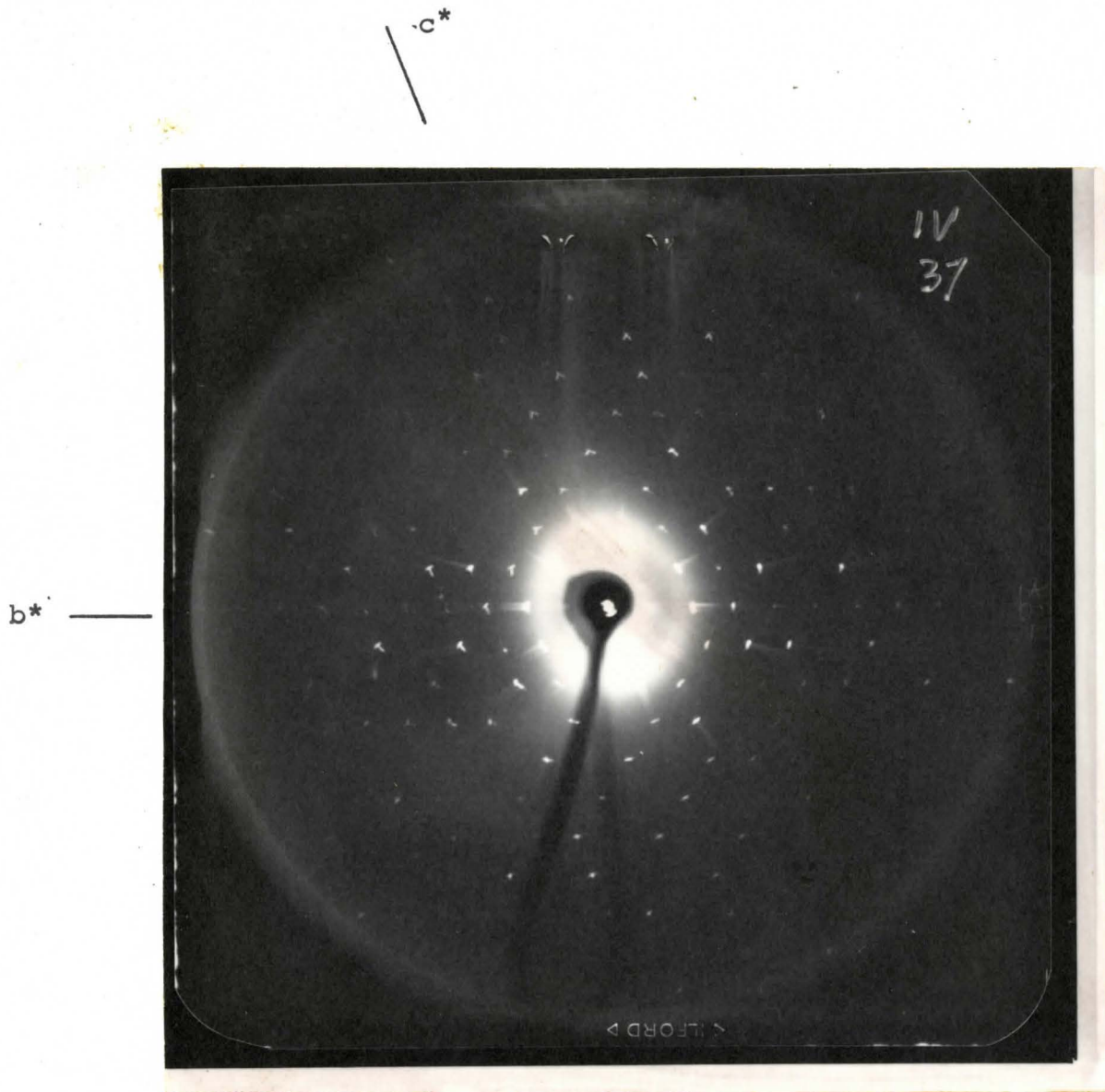


Table 3.13  $\text{Cs}_2\text{Cr}_2\text{O}_7$ . Crystal data\*

Compound	$\text{Cs}_2\text{Cr}_2\text{O}_7$
Space group	$P\bar{1}$
a (Å)	7.8
b (Å)	7.9
c (Å)	8.5
$\alpha$	$110.5^\circ$
$\beta$	$98.3^\circ$
$\gamma$	$95.7^\circ$
V (Å <sup>3</sup> )	482
Z	2

\*These cell constant should be regarded as approximate. See text.

### 3.4.0 NaRbCr<sub>2</sub>O<sub>7</sub> and NaCsCr<sub>2</sub>O<sub>7</sub>. Introduction

The only congruently melting compounds found so far in the binary systems of alkali metal dichromates are NaRbCr<sub>2</sub>O<sub>7</sub> and NaCsCr<sub>2</sub>O<sub>7</sub>, Samuseva, Poletaev and Plyushev (5).

We undertook the determination of the NaRbCr<sub>2</sub>O<sub>7</sub> structure since the presence of Cs in NaCsCr<sub>2</sub>O<sub>7</sub> would have resulted in a less accurate determination of the Cr<sub>2</sub>O<sub>7</sub> ion.

#### 3.4.1a NaRbCr<sub>2</sub>O<sub>7</sub>. Sample Preparation

A mixture of powdered anhydrous Na<sub>2</sub>Cr<sub>2</sub>O<sub>7</sub> prepared from Na<sub>2</sub>Cr<sub>2</sub>O<sub>7</sub>·2H<sub>2</sub>O (Shawinigan, Reagent 99.5%) and powdered Rb<sub>2</sub>Cr<sub>2</sub>O<sub>7</sub> (Alfa Inorganics) in molecular ratio 1:1 was heated 20° above the melting point (362°) and kept at this temperature for a few hours, then it was cooled gradually and at around 200°C was transferred to a dry box with nitrogen atmosphere.

The crystals selected from the sample were hygroscopic and were sealed in thin walled quartz capillary tubes in a dry nitrogen atmosphere. Under examination with a polarizing microscope the crystals showed poor extinction so the final selection of good crystals was made with a precession camera.

3.4.1b NaRbCr<sub>2</sub>O<sub>7</sub> Preliminary Investigation and Determination of the Structure with Precession Photographs

Preliminary studies of single crystals using a precession camera showed that the crystals were monoclinic with approximate cell constants close to those given in Table 3.14. The  $h0\ell$ ,  $h\ell\ell$ , and  $hk0$  layer photographs showed systematic absences for  $h0\ell$  reflection with  $\ell$  odd and for  $0k0$  reflections with  $k$  odd. These systematic absences identify the space group uniquely as  $P2_1/c$ . The volume of the unit cell corresponds to 8 NaRbCr<sub>2</sub>O<sub>7</sub> units per unit cell. The structure was solved and refined initially from photographic measurements but was later refined using diffractometer measured intensities.

Intensities were measured from integrated precession photographs of the layers  $hk0$ ,  $hkl$ ,  $h0\ell$ ,  $h\ell\ell$ . The crystal was mounted on the precession camera with its  $a^*$  axis along the spindle axis. MoK $\alpha$  radiation was used. The intensities were corrected for Lorentz and polarization effects and were scaled with a least squares program written by Dr. J. S. Stephens. Averaging the common reflections gave 600 unique observed reflections.

A three dimensional Patterson function calculated with these reflections showed a well defined peak, which was attributed to a Rb-Rb vector, in the  $z = \frac{1}{2}$  Harker section.

From this Rb coordinates were chosen and these gave a

Table 3.14 Crystal data for  $\text{NaRbCr}_2\text{O}_7$  and  $\text{NaCsCr}_2\text{O}_7$ . Standard errors in the last figures quoted are given in parentheses

Compound	$\text{NaRbCr}_2\text{O}_7^*$	$\text{NaCsCr}_2\text{O}_7^\dagger$
Space group	$P2_1/c$	$P2_1/c$
a (Å)	12.947 (15)	12.98 (2)
b (Å)	11.133 (11)	11.58 (2)
c (Å)	10.037 (18)	10.10 (2)
$\beta$	93.42 (8)	93.8 (2)
V (Å <sup>3</sup> )	1444	1514
Z	8	8
$D_x$	2.98	
$\mu$ (MoK $\alpha$ )	10.25 mm <sup>-1</sup>	

\*measured on diffractometer

†measured from film, may be systematically too small by one standard deviation.

satisfactory agreement between observed and calculated structure factors ( $R_1 = 55\%$ ).

Concurrently a solution was attempted with sign determining relationships (Chapter 2). The x-ray 67 programs were used for this. There were 215 reflections with normalized structure factors  $E \geq 1.2$  but only 110 reflections with  $E \geq 1.5$ . The largest  $E$  value was 3.13. The sigma two relationships were calculated for the set of reflections with  $E \geq 1.2$  and a solution of the phase problem was attempted with 80 of the highest  $E$  values in the fundamental set.

After two cycles the signs of 190 reflections with  $E \geq 1.2$  were determined. An  $E$  map of the  $h0l$  projection was calculated and showed Rb peaks at the same positions as were determined from the Patterson synthesis.

Additional strong peaks separated by about  $2 \overset{\circ}{\text{Å}}$  in projection were suspected of being Cr atoms. A three dimensional  $E$  map showed that such an interpretation was consistent with the  $3 \overset{\circ}{\text{Å}}$  intramolecular Cr-Cr distance found in the  $\text{Cr}_2\text{O}_7$  ion in other structures. A least squares refinement of these positions gave a satisfactory agreement index of 0.42.

The remaining Na and O atoms were determined from successive 3-dimensional difference synthesis. The model, refined with a full matrix least squares program and with isotropic temperature factors and unit weights, gave  $R_1 = 0.10$ .



### 3.4.1c Crystal Data and Intensities Measured on the Diffractometer

A single crystal sealed in a thin walled quartz capillary tube was selected for cell constant and intensity measurements with the Syntex diffractometer. The crystal had an irregular shape which was approximated by 12 bounded planes. The Miller indices of the bounded planes and their distance from the center of the crystal are given in Table 3.15. The approximate volume of the crystal was  $6 \times 10^{-3}$  mm<sup>3</sup>. The crystal was mounted on the diffractometer with the [563]\* reciprocal axis close to the  $\phi$  axis. Accurate cell constants measured from the angular settings of 14 low angle reflections, Table 3.16, MoK $\alpha$  radiation ( $\lambda = 0.71069 \text{ \AA}$ ) are given in Table 3.14.

The intensities were measured with MoK $\alpha$  in the range  $5 < 2\theta < 55^\circ$  and a limited number up to  $2\theta = 65^\circ$  for the quadrant of the reciprocal space with  $l$  and  $k \geq 0$ . In all 3200 unique reflections were measured. The intensities were corrected for absorption with the ABSORP program (32). This program calculates the transmission coefficient  $A_h$  for each reflection with a numerical integration from the shape of the crystal defined as in Table 3.15, the linear absorption coefficient and the orientation of the crystal in the Eulerian cradle. The transmission coefficient calculated for the reflections

Table 3.15 NaRbCr<sub>2</sub>O<sub>7</sub>. Crystal Shape

Crystal faces	$d(10^{-1} \text{ mm})^\dagger$
(1 4 5)	0.80
( $\bar{9}$ $\bar{8}$ 10)	0.97
(0 $\bar{1}$ 5)	0.80
( $\bar{1}$ $\bar{4}$ $\bar{5}$ )	1.29
(3 $\bar{2}$ 1)	0.80
( $\bar{6}$ 1 0)	0.97
( $\bar{5}$ $\bar{6}$ 3)	1.29
(5 6 $\bar{3}$ )	1.29
(0 0 $\bar{7}$ )	0.97
( $\bar{1}$ 0 $\bar{1}$ )	0.97
(1 0 1)	0.97
( $\bar{3}$ 3 2)	0.97

<sup>†</sup>Distances of the crystal faces from the center of the crystal.

Tabl3 3.16 NaRbCr<sub>2</sub>O<sub>7</sub>. Angular settings for 14 reflections

$h$	$k$	$l$	$2\theta$	$\omega$	$\phi$	$\chi$
$\bar{2}$	$\bar{3}$	1	13.22	359.93	90.69	85.70
$\bar{1}$	$\bar{3}$	1	12.08	359.96	167.54	72.48
$\bar{2}$	$\bar{3}$	0	12.69	359.96	101.72	66.57
$\bar{3}$	$\bar{1}$	1	10.73	.00	2.31	59.32
0	$\bar{2}$	2	10.98	.07	235.88	51.91
$\bar{3}$	0	2	12.12	.06	332.50	41.33
1	$\bar{2}$	2	11.53	.10	228.41	37.36
$\bar{3}$	1	2	12.67	.19	334.80	24.31
$\bar{4}$	1	1	13.53	.14	359.55	23.29
$\bar{3}$	$\bar{1}$	$\bar{2}$	13.39	.07	69.96	20.47
3	$\bar{3}$	1	15.21	.11	197.55	19.18
3	$\bar{1}$	2	13.39	.08	229.31	4.13
$\bar{3}$	$\bar{3}$	$\bar{1}$	15.26	.06	83.91	50.69
1	$\bar{3}$	2	14.15	.09	213.27	43.80

varied between 0.22 and 0.28. Because of the complicated shape of the crystal a very accurate identification of the Miller indices was not possible, so the bounding planes defined in Table 3.15 are only approximate. As a result the applied absorption correction was also only approximate.

After the absorption correction intensities less than three times the standard deviation calculated from counting statistics were characterized as unobserved. The number of observed reflections thus left was 1406. The intensities were then corrected for Lorentz and polarization effects.

#### 3.4.1d Refinement with the Diffractometer Measurements

The model refined with the measurement from the precession photographs was further refined with the diffractometer measurements and with anisotropic temperature factors to a final agreement indices  $R_1 = 0.046$ ,  $R_2 = 0.058$ . A Cruickshank weighting scheme was used with  $w = (17.10 w = (17.710 - 0.3817|F_o| + 0.0042|F_o|^2)^{-1}$ . The scattering curves of  $Rb^+$ ,  $Cr^{++}$ ,  $O^-$ , O (for the bridging oxygen) and  $Na^+$  (25) were used. The  $Rb^+$  and  $Cr^{++}$  curves were corrected for the real and imaginary parts of dispersion for  $MoK\alpha$  radiation. The final atomic and thermal coordinates are given in Table 3.17. The values of  $F_o$  and  $F_c$  are given in Table 3.18

Table 3.17  $P2_1/c$  NaRbCr<sub>2</sub>O<sub>7</sub>. Atomic positional and thermal coordinates

	x	y	z	u <sub>11</sub>	u <sub>22</sub>	u <sub>33</sub>	u <sub>12</sub>	u <sub>13</sub>	u <sub>23</sub>
Cr1	0.1579(1)	0.1037(2)	0.3862(2)	215(9)	199(11)	197(10)	-34(9)	10(7)	-18(8)
Cr2	-0.0032(1)	-0.0952(2)	0.2545(2)	146(8)	280(11)	209(9)	-15(9)	-19(7)	-9(9)
O11	0.1294(8)	0.2195(9)	0.4705(10)	446(57)	340(58)	393(58)	5(48)	48(45)	-133(49)
O12	0.2025(7)	0.1393(10)	0.2450(9)	379(53)	573(68)	202(47)	-102(51)	29(40)	72(49)
O13	0.2424(8)	0.0265(9)	0.4705(10)	420(57)	398(64)	375(53)	58(50)	-49(43)	244(50)
O21	-0.1275(7)	-0.0812(9)	0.2396(10)	203(42)	398(58)	402(56)	-73(44)	17(37)	2(50)
O22	0.0314(8)	-0.2247(9)	0.3155(10)	435(57)	401(60)	360(55)	151(51)	3(44)	91(48)
O23	0.0441(7)	-0.0781(9)	0.1099(9)	332(52)	356(58)	329(55)	-60(46)	58(42)	14(48)
B12	0.0432(8)	0.0178(11)	0.3644(9)	353(54)	762(82)	267(49)	-288(58)	72(41)	-223(56)
Cr3	0.4398(1)	0.2710(2)	0.4696(2)	182(9)	243(11)	200(10)	-1(9)	-34(7)	14(9)
Cr4	0.6642(1)	0.3644(2)	0.6089(2)	192(9)	246(11)	284(11)	-36(9)	-28(8)	-12(9)
O31	0.3332(7)	0.3204(10)	0.5189(11)	331(52)	537(70)	545(66)	-7(50)	135(48)	67(59)
O32	0.4592(8)	0.1341(9)	0.5228(10)	531(62)	210(50)	348(55)	-122(49)	-134(46)	31(46)
O33	0.4354(8)	0.2717(11)	0.3069(9)	567(65)	628(76)	186(46)	86(59)	-17(43)	77(50)
O41	0.6671(9)	0.4575(10)	0.7315(11)	686(73)	334(61)	456(63)	-31(57)	-90(54)	-185(54)
O42	0.7408(8)	0.4056(11)	0.4972(11)	508(65)	524(74)	452(69)	56(58)	230(53)	3(58)
O43	0.6960(8)	0.2321(9)	0.6596(12)	424(55)	307(56)	617(72)	-15(49)	28(50)	201(57)
B34	0.5364(8)	0.3666(10)	0.5368(12)	361(56)	304(59)	798(85)	-19(49)	-321(55)	56(60)
Na1	0.1521(4)	0.0765(5)	0.0161(5)	345(27)	264(29)	291(27)	18(24)	-64(21)	33(24)
Na2	0.2817(4)	0.3440(5)	0.1800(5)	343(27)	308(30)	344(29)	98(24)	12(22)	7(25)
Rb1	0.1483(1)	0.6833(1)	0.0862(1)	369(7)	274(7)	338(7)	12(6)	24(5)	-36(6)
Rb2	0.4171(1)	-0.0087(1)	0.2603(1)	329(6)	275(7)	338(7)	36(6)	14(5)	3(6)

Standard errors in the last figures quoted as given by final round of least squares analysis are shown in parentheses. The temperature factors were calculated using the expression given in Table 3.3.



Table 3.18 NaRbCr<sub>2</sub>O<sub>7</sub> (continued)

The figure displays an X-ray diffraction pattern for NaRbCr<sub>2</sub>O<sub>7</sub>. The vertical axis represents intensity, and the horizontal axis represents the diffraction angle 2θ. The plot is divided into several regions marked with letters: X, K, L, S, Y, Z, and a scale bar at the top. Numerous peaks are labeled with Miller indices (hkl) and their corresponding d-spacings (d) in Å. The patterns are arranged in a grid-like fashion, showing multiple sets of diffraction peaks for different reflections.

Miller Index (hkl)	d-spacing (Å)
001	2.00
100	1.50
110	1.11
111	0.84
200	0.75
210	0.60
211	0.54
300	0.50
310	0.40
311	0.38
400	0.37
410	0.33
411	0.32
500	0.30
510	0.28
511	0.27
600	0.26
610	0.25
611	0.24

### 3.4.2 NaCsCr<sub>2</sub>O<sub>7</sub>. Experimental Procedure

Crystals of NaCsCr<sub>2</sub>O<sub>7</sub> were obtained by slow cooling of the congruently melting (362°C) 1:1 mixture of anhydrous sodium and cesium dichromate. The powdered Na<sub>2</sub>Cr<sub>2</sub>O<sub>7</sub> was prepared from Na<sub>2</sub>Cr<sub>2</sub>O<sub>7</sub> · 2H<sub>2</sub>O Shawinigan, Reagent, 99.5% and the powdered cesium dichromate was obtained from Alfa Inorganic, 99.9%.

Single crystal precession photographs of the *hk0*, *h0l*, *h1l*, and *hkl* layer were taken and showed systematic absences of *l* odd for the *h0l* reflections and *k* odd for the *0k0* reflections in a monoclinic unit cell. The space group is thus uniquely determined as P2<sub>1</sub>/c. The cell constants measured from uncalibrated photographs are given in Table 3.14. Since the cell constants of NaRbCr<sub>2</sub>O<sub>7</sub> measured in the same way were systematically smaller than those measured with the Syntex diffractometer, the values of NaCsCr<sub>2</sub>O<sub>7</sub> cell constants given in Table 3.14 might also be systematically smaller by about one standard deviation. The volume of 1514 Å<sup>3</sup> corresponds to eight NaCsCr<sub>2</sub>O<sub>7</sub> units per unit cell.

The similarity of the unit cells and the intensities of the *h0l*, *hk0*; *h1l* layers of NaCsCr<sub>2</sub>O<sub>7</sub> with those of NaRbCr<sub>2</sub>O<sub>7</sub> indicates that these two compounds are probably isostructural.



## CHAPTER 4

### THE DICHROMATE ION

#### 4.1 The Geometry of the Dichromate Ion

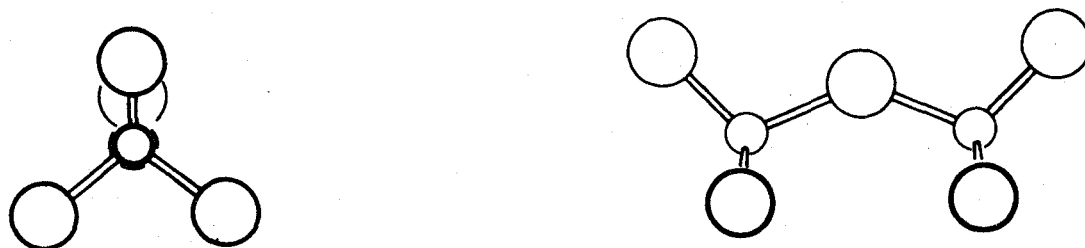
The dichromate anion  $\text{Cr}_2\text{O}_7^{2-}$  consists of two  $\text{CrO}_4$  tetrahedra sharing one oxygen atom. We will call the shared oxygen the bridging oxygen atom and the other oxygens as the terminal ones.

In all dichromate ions whose structures have so far been determined the bridging oxygen angle (Cr-B (bridging oxygen)-Cr) varies between 121 to 141 degrees, while the O-Cr-O angles are very close to the tetrahedral angle which is  $109.5^\circ$ . The Cr-O terminal distances are all equal ( $1.62 \text{ \AA}$ ) but the Cr-B distances are somewhat larger ( $1.79 \text{ \AA}$ ).

For a  $\text{Y}_2\text{O}_7$  molecule with the above geometry and with a bridging angle different from  $180^\circ$  there are three special symmetric conformations. Two eclipsed conformations have symmetry  $C_{2v}(\text{mm})$  and one staggered conformation has symmetry  $C_s(\text{m})$ , (Figure 4.1 a,b,c). We shall call the staggered conformation C and the two eclipsed conformations A or B depending on whether the bridging oxygen lies inside or outside respectively of the quadrilateral defined by

Figure 4.1 Special symmetric conformations of  $Y_2O_7$  ions.

a) Conformation A ( $C_{2v}$ ). From  $SrCr_2O_7$ .



b) Conformation B ( $C_{2v}$ ). From  $SrCr_2O_7$ .

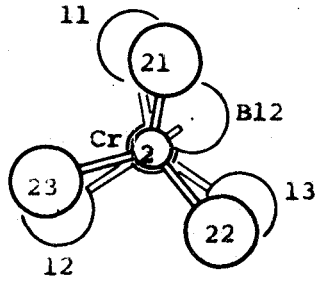


c) Conformation C ( $C_s$ ). From  $\alpha-Mg_2P_2O_7$ .

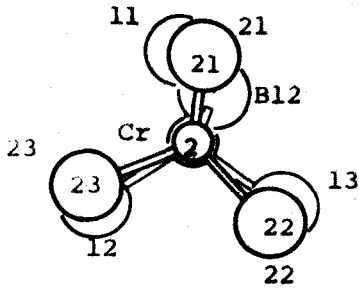


Figure 4.2 The dichromate ions found in this work. 71  
 (Viewed along the Cr-Cr axis)

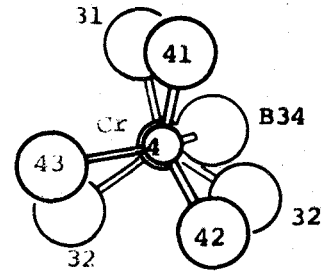
a)  $\alpha\text{-Na}_2\text{Cr}_2\text{O}_7$



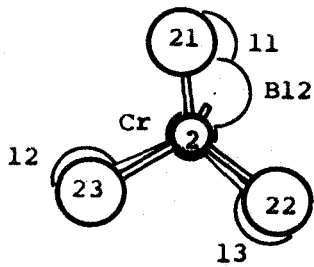
b)  $\beta\text{-Na}_2\text{Cr}_2\text{O}_7$



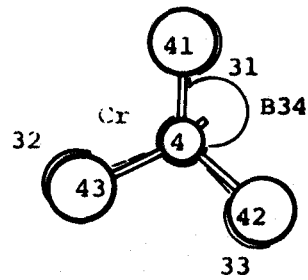
c)  $\beta\text{-Na}_2\text{Cr}_2\text{O}_7$



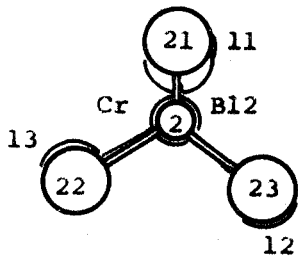
d)  $\text{NaRbCr}_2\text{O}_7$



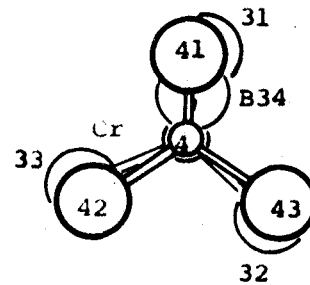
e)  $\text{NaRbCr}_2\text{O}_7$



f)  $\beta 1\text{-Rb}_2\text{Cr}_2\text{O}_7$



g)  $\beta 1\text{-Rb}_2\text{Cr}_2\text{O}_7$



the two Cr and the two oxygen atoms lying on the plane of symmetry.

Both the A and B conformations have been found in  $\text{SrCr}_2\text{O}_7$  (8) but the staggered conformation has not yet been found in the dichromates, although it is frequently found in other groups such as  $\text{P}_2\text{O}_7^{4-}$ .

The  $\text{Cr}_2\text{O}_7$  ion normally has symmetry lower than  $\text{C}_{2v}$ . In one possible conformation the anion loses the planes of symmetry but it retains the twofold axis (symmetry  $\text{C}_2$ ). Such a dichromate anion with crystallographic  $\text{C}_2$  symmetry and a conformation very close to that of A has been found in the type X  $\text{C}2/c$  structures of  $\text{Rb}_2\text{Cr}_2\text{O}_7$  and  $(\text{NH}_4)_2\text{Cr}_2\text{O}_7$ . In all the other known dichromate structures the anion has no crystallographic symmetry, though sometimes the deviations from the  $\text{C}_{2v}$  or  $\text{C}_2$  symmetry are rather small.

The conformation of the dichromate ion can be described by three angles: the bridging oxygen angle ( $\text{Cr-B-Cr}$ ),  $b$ , and the angles  $\alpha_1$  and  $\alpha_2$  which define the rotations of each of the two tetrahedra around the  $\text{Cr-B}$  (bridging atom) bond<sup>†</sup>.

#### 4.2 Analysis of the Temperature Factors

For the structures determined in this work the anisotropic temperature factors have been analysed to determine the

---

<sup>†</sup>An exact definition of  $\alpha_1$ ,  $\alpha_2$  is given in p 91.

magnitude and the directions of the principle axes of the thermal ellipsoids and are given in Tables 4.1, 4.2, 4.3, 4.4.

As can be seen from these tables, the thermal motion of the Cr atoms is nearly isotropic while that of the oxygen atoms is anisotropic with the minor axes of the ellipsoids lying within  $20^\circ$  of the direction of the Cr-O bonds and the major and intermediate axes approximately normal to it.

The information contained in the temperature factors is insufficient to account for the modes of vibration that are important in the thermal motion of the  $\text{Cr}_2\text{O}_7$  ion. Luu and Lafont (33) in a Raman study of  $\beta 1 \text{K}_2\text{Cr}_2\text{O}_7$  assign to the various modes the frequencies given in Table 4.5. From the 27 modes of the  $\text{Cr}_2\text{O}_7$  ion only the 8 lowest modes are likely to be important at room temperatures. The remaining one bending and two stretching modes of the Cr-B-Cr as well as the 16 internal bonding modes, while consistent with the observed temperature factors, can be discarded on the grounds of too high an energy.

The eight lowest modes are the three translational, the three librational around the principal axes of inertia of the ion and the two torsional. The normal coordinates for the torsion modes are the angles  $\alpha_1$  and  $\alpha_2$  defined in the previous section. These two modes are degenerate and therefore mix to give the  $A_2$  symmetric torsion mode  $\alpha_1 - \alpha_2$  and the  $B_2$  antisymmetric torsion mode  $\alpha_1 + \alpha_2$ .

Table 4.1  $\beta$ - $\text{Na}_2\text{Cr}_2\text{O}_7$ . Principal axes of anisotropic temperature factors

Atom	rms Displace- ments (Å)	Angles in degrees with respect to bond		Angles in degrees with respect to		
				a	b	c
Cr1	0.16			122	109	34
	0.15			45	159	103
	0.14			61	81	59
Cr2	0.17			128	118	72
	0.14			39	150	109
	0.14			97	81	153
O11		Cr1-O11				
	0.217	105		82	156	102
	0.171	98		92	73	156
O12		Cr1-O12				
	0.22	119		94	55	143
	0.17	84		151	91	83
O13		Cr1-O13				
	0.22	83		43	150	115
	0.18	128		111	81	138
O21		Cr2-O21				
	0.20	103		143	96	46
	0.18	126		66	167	103
O22		Cr2-O22				
	0.26	73		86	35	79
	0.20	59		24	123	94
O23		Cr2-O23				
	0.30	82		27	96	115
	0.20	69		88	108	148
OB12		Cr1-OB12 Cr2-OB12				
	0.24	89 104		129	105	39
	0.20	86 140		46	160	94
Cr3		5 127		71	77	51
	0.16			143	98	51
	0.14			125	17	96
	0.14			82	76	39

(continued next page)

Table 4.1  $\beta$ -Na<sub>2</sub>Cr<sub>2</sub>O<sub>7</sub> (continued)

Atom	rms Displace- ments (Å)	Angles in degrees with respect to bond		Angles in degrees with respect to		
				a	b	c
Cr3	0.16			143	98	51
	0.14			125	17	96
	0.14			82	76	39
Cr4	0.16			104	142	80
	0.15			19	126	121
	0.13			103	79	147
O31		Cr3-O31				
	0.26	84		64	77	59
	0.21	106		100	132	46
O32	0.14	17		28	135	120
		Cr3-O32				
	0.22	112		113	56	133
O33	0.21	99		23	99	129
	0.15	24		86	145	111
		Cr3-O33				
O41	0.23	72		75	42	87
	0.20	69		19	123	123
	0.14	152		101	67	147
O42		Cr4-O41				
	0.22	76		94	151	72
	0.19	81		16	117	103
O43	0.15	163		84	102	157
		Cr4-O42				
	0.26	86		109	22	111
OB34	0.19	63		60	78	72
	0.16	28		43	108	152
		Cr4-O43				
Na1	0.26	91		51	115	153
	0.20	137		46	77	85
	0.17	47		110	29	117
Na1		Cr3-OB34	Cr4-OB34			
	0.23	86	92	38	110	146
	0.16	102	127	97	20	105
Na1	0.13	12	143	127	88	119
	0.25			155	90	64
	0.17			77	131	133
	0.16			111	41	126

(continued next page)

Table 4.1  $\beta$ -Na<sub>2</sub>Cr<sub>2</sub>O<sub>7</sub> (continued)

Atom	rms Displace- ments ° (Å)	Angles in degrees with respect to bond	Angles in degrees with respect to		
			a	b	c
Na2	0.24		149	41	92
	0.19		68	49	90
	0.17		69	92	178
Na3	0.27		138	106	83
	0.18		112	40	124
	0.17		56	125	145
Na4	0.19		82	150	110
	0.18		138	61	112
	0.17		131	97	30



Table 4.2  $\alpha$ - $\text{Na}_2\text{Cr}_2\text{O}_7$ . Principal axes of anisotropic temperature factors

Atom	rms Displacements (Å)	Angles in degrees with respect to bond		Angles in degrees with respect to		
				a	b	c
Cr1	0.22			117	116	37
	0.20			51	154	115
	0.18			129	88	116
Cr2	0.23			134	109	53
	0.20			50	161	104
	0.18			107	88	140
O11		Cr1-O11				
	0.28	86		72	49	80
	0.27	88		104	56	139
O12		Cr1-O12				
	0.29	116		96	57	144
	0.25	27		82	103	113
O13		Cr1-O13				
	0.31	85		65	163	107
	0.29	97		143	83	103
O21		Cr2-O21				
	0.29	83		111	134	65
	0.26	76		21	134	102
O22		Cr2-O21				
	0.49	95		113	19	107
	0.27	89		72	73	52
O23		Cr2-O23				
	0.47	65		152	91	54
	0.27	76		80	82	37
OB12		Cr1-OB12 Cr2-OB12				
	0.40	90	84	41	99	151
	0.21	133	92	82	39	79
	0.19	137	7	130	52	116

(continued next page)

Table 4.2  $\alpha$ -Na<sub>2</sub>Cr<sub>2</sub>O<sub>7</sub> (continued)

Atom	rms Displace- ments (Å)	Angles in degrees with respect to bond	Angles in degrees with respect to		
			a	b	c
Na1	0.33		141	104	78
	0.25		55	141	129
	0.23		104	55	138
Na2	0.32		37	148	93
	0.25		81	70	45
	0.22		125	113	45

Table 4.3  $\beta$ - $\text{Rb}_2\text{Cr}_2\text{O}_7$ . Principal axes of anisotropic temperature factors

Atom	rms Displacements ( $\text{\AA}$ )	Angles in degrees with respect to bond		Angles in degrees with respect to		
				a	b	c
Cr1	0.17			132	45	99
	0.15			114	96	16
	0.11			51	45	78
CR2	0.16			132	85	129
	0.15			72	150	112
	0.14			133	120	47
O11		Cr1-O11				
	0.28	84		109	122	31
	0.15	61		74	148	115
O12		Cr1-O12				
	0.26	97		125	144	72
	0.19	81		134	69	122
O13		Cr1-O13				
	0.28	56		87	16	78
	0.20	47		138	78	122
O21		Cr2-O21				
	0.25	99		88	73	23
	0.15	79		143	126	69
O22		Cr2-O22				
	0.21	102		149	62	95
	0.15	52		80	93	173
O23		Cr2-O23				
	0.23	97		139	133	80
	0.18	85		122	55	125
OB12		Cr1-OB12 Cr2-OB12				
	0.21	56	141	178	93	83
	0.18	47	117	91	109	17
Cr3	0.13	62	64	88	161	105
	0.18			125	45	110
	0.16			78	53	46
	0.15			142	112	51

(continued next page)

Table 4.3  $\beta 1\text{-Rb}_2\text{Cr}_2\text{O}_7$  (continued)

Atom	rms Displace- ments (Å)	Angles in degrees with respect to bond		Angles in degrees with respect to		
				a	b	c
Cr4	0.18			128	47	108
	0.15			89	62	33
	0.13			142	124	64
O31		Cr3-O31				
	0.21	134		90	54	41
	0.20	56		120	46	118
	0.17	117		150	114	63
O32		Cr3-O32				
	0.22	94		98	159	66
	0.18	16		47	80	53
	0.13	106		44	108	134
O33		Cr3-O33				
	0.25	101		43	90	141
	0.21	109		100	16	104
	0.18	22		49	74	55
O41		Cr4-O41				
	0.27	92		32	85	67
	0.19	87		77	159	103
	0.11	4		119	110	27
O42		Cr4-O42				
	0.25	85		75	68	35
	0.19	64		115	143	57
	0.16	154		30	118	98
O43		Cr4-O43				
	0.22	69		143	85	119
	0.20	115		108	157	69
	0.13	34		59	113	143
OB34		Cr3-OB34	Cr4-OB34			
	0.23	81	99	48	134	105
	0.20	101	121	73	89	26
	0.09	15	147	133	136	69
Rb1	0.21			128	60	123
	0.16			142	109	48
	0.15			85	36	59
Rb2	0.20			65	152	101
	0.17			27	68	84
	0.14			100	106	13
Rb3	0.18			84	157	109
	0.16			98	69	155
	0.15			170	99	75
Rb4	0.20			115	27	94
	0.18			36	64	74
	0.15			114	97	16

Table 4.4  $P2_1/c$  NaRbCr<sub>2</sub>O<sub>7</sub>. Principal axes of anisotropic temperature factors

Atom	rms Displace- ments (Å)	Angles in degrees with respect to bond		Angles in degrees with respect to		
				a	b	c
Cr1	0.16			34	122	103
	0.15			101	123	35
	0.12			58	50	59
Cr2	0.17			95	7	94
	0.15			66	92	160
	0.12			24	83	70
O11		Cr1-O11				
	0.23	82		100	52	139
	0.21	83		168	102	83
O12		Cr1-O12				
	0.25	93		68	156	99
	0.19	78		26	71	77
O13		Cr1-O13				
	0.25	86		85	135	135
	0.21	116		164	104	80
O21		Cr2-O21				
	0.21	112		72	158	103
	0.20	82		92	78	167
O22		Cr2-O22				
	0.24	69		47	46	79
	0.20	88		59	104	148
O23		Cr2-O23				
	0.20	88		131	43	99
	0.19	53		75	63	33
OB12		Cr1-OB12 Cr2-OB12				
	0.31	95	72	114	31	106
	0.16	130	93	141	98	48
Cr3						
	0.13	139	18	61	61	46
	0.16			67	139	124
	0.15			123	131	56
	0.12			138	85	128

(continued next page)

Table 4.4  $P2_1/c$  NaRbCr<sub>2</sub>O<sub>7</sub>. (continued)

Atom	rms Displace- ments (Å)	Angles in degrees with respect to bond		Angles in degrees with respect to		
				a	b	c
Cr4	0.17			66	94	159
	0.16			110	24	101
	0.13			32	66	73
O31	0.25	Cr3-O31				
	0.22	103		76	55	40
	0.17	66		109	36	118
O32		28		156	98	64
	0.26	Cr3-O32				
	0.17	78		31	105	119
O33	0.13	53		112	73	150
		140		69	23	83
	0.26	Cr3-O33				
O41	0.23	95		57	34	86
	0.14	78		34	122	104
		167		96	79	166
O42		Cr4-O41				
	0.28	105		152	99	61
	0.23	84		116	52	130
O43	0.14	16		80	39	54
		Cr4-O42				
	0.26	84		44	75	54
OB34	0.23	67		96	17	106
	0.16	24		47	98	139
		Cr4-O43				
Na1	0.27	82		86	116	154
	0.21	109		173	87	92
	0.14	20		96	153	64
Na2		Cr3-OB34 Cr4-OB34				
	0.32	89	83	59	95	152
	0.17	132	86	96	173	88
Na2	0.14	137	8	148	85	118
	0.20			35	92	128
	0.17			70	34	65
Na2	0.15			117	56	132
	0.21			140	130	86
	0.19			88	95	175
	0.15			130	40	93

(continued next page)

Table 4.4  $P2_1/c$  NaRbCr<sub>2</sub>O<sub>7</sub> (continued)

Atom	rms Displace- ments ° (Å)	Angles in degrees with respect to bond	Angles in degrees with respect to		
			a	b	c
Rb1	0.19		169	100	82
	0.19		79	67	154
	0.16		83	155	115
Rb2	0.19		147	113	65
	0.18		72	77	25
	0.16		116	27	92

Table 4.5 Raman spectra of  $\beta 1$   $K_2Cr_2O_7$  according to Luu and Lafont (33).

		<u>Assignment</u>
41 $cm^{-1}$	34 $cm^{-1}$	libration
48	44	
60	55	
78	87	translation
83	71	
105	120	
133	127	
146	150	A <sub>2</sub>   torsion of Cr <sub>2</sub> O <sub>7</sub>
240	225	B <sub>2</sub>
		A <sub>1</sub> Cr-O-Cr bending
	280	A <sub>1</sub> +A <sub>2</sub> +B <sub>1</sub> + B <sub>2</sub> CrO <sub>3</sub> rocking
	290	
	300	
	320	
	335	
	340	
	367	A <sub>1</sub>   CrO <sub>3</sub> symmetric bend
	390	
	377	A <sub>2</sub>   CrO <sub>3</sub> antisymmetric bend
	380	
	390	
	394	
450-476-502-525		? Very weak
562	572	A <sub>1</sub> (O <sub>3</sub> Cr)-O symmetric stretch
605-650-694		? Very weak
755	743	B <sub>1</sub> (O <sub>3</sub> Cr)-O antisymmetric stretch
	826	?
917	916	A <sub>1</sub>   Cr-O symmetric stretch
	891	B <sub>1</sub>
962	962	A <sub>1</sub>   Cr-O antisymmetric stretch
926	930	
945	948	
954	956	



Estimates of the rms amplitudes for the libration around the minor (Cr-Cr) axis and for the two torsion, Table 4.6, have been calculated from the temperature factors after the subtraction of the translational motion. Usually it is assumed (34) that the translational and librational modes only are important. In this case the bridging oxygen atom should show librational amplitude around the Cr-Cr axis of the same size as the other oxygen atoms but the bridging oxygen atoms show systematically larger libration than the terminal oxygen atoms. Such an apparent libration can be explained if the antisymmetric torsion mode ( $\alpha_1 + \alpha_2$ ) is active. The bridging oxygen appears to have a larger vibration because of the coupling between the libration mode (around Cr-Cr) and the antisymmetric torsion mode which allows the terminal oxygens to remain relatively fixed in the crystal.

One consequence of the thermal motion is that the Cr-O bonds calculated from the atomic coordinates appear shorter than they really are (35). These bond lengths have been corrected using the method of Busing and Levy (36) and the corrected, together with the uncorrected bond lengths are given in Tables 4.7, 4.8, 4.9, 4.10. It is assumed that the oxygen atoms are riding on chromium atoms, an assumption that is in reasonable agreement with the proposed motion of the dichromate groups. As the Busing and Levy correction applies for small vibrations only bond lengths for some of the

Table 4.6 Estimates of libration and torsion amplitudes.  
Rms values in degrees

	$\alpha\text{-Na}_2\text{Cr}_2\text{O}_7$	$\beta\text{-Na}_2\text{Cr}_2\text{O}_7$		$\beta\text{I-K}_2\text{Cr}_2\text{O}_7$		$\beta\text{I-Rb}_2\text{Cr}_2\text{O}_7$		$\text{NaRbCr}_2\text{O}_7$	
*	1	2	3	4	5	6	7	10	11
	Cr1,Cr2	Cr1,Cr2	Cr3,Cr4	Cr1,Cr2	Cr3,Cr4	Cr1,Cr2	Cr3,Cr4	Cr1,Cr2	Cr3,Cr4
Libration of $\text{Cr}_2\text{O}_7$ around Cr-Cr	8	6	7	7	7	7	5	6	6
OB libration around Cr-Cr	27	13	14	9	12	8	14	21	25
† $B_2$ torsion	7	6	6	6	7	6	6	7	9
*† $A_2$ torsion	8	6	6	6	6	6	4	6	7

\*The numbers are used to identify the anions in Figure 4.3.  
The atoms in parentheses belong to the anion.

† Estimated from the apparent libration of  $\text{CrO}_4$  groups around an axis parallel to the line from the middle of the Cr-Cr distance to the bridging oxygen

\*† Estimated from the apparent libration of  $\text{CrO}_4$  around the Cr-OB axis.

Table 4.7  $\beta$ - $\text{Na}_2\text{Cr}_2\text{O}_7$ . Interatomic Distances

		Uncorrected	Corrected*	Angles (in degrees)		
		Distance	Distance	012	013	0B12
		(Å)	(Å)			
Cr1	O11	1.622	1.63	111	113	106
	O12	1.620	1.63		110	110
	O13	1.601	1.61			108
	OB12	1.782	1.79			
Cr2	O21	1.609	1.62	O22	O23	OB12
	O22	1.620	1.64	111	111	108
	O23	1.618	1.64		108	109
	OB12	1.778	1.79			110
		Cr1 - OB12 - Cr2	131.3°			
Cr3	O31	1.602	1.62	O32	O33	OB34
	O32	1.618	1.63	111	112	110
	O33	1.612	1.63		110	109
	OB34	1.790	1.80			104
Cr4	O41	1.602	1.61	O42	O43	OB34
	O42	1.624	1.64	109	111	110
	O43	1.612	1.63		107	109
	OB34	1.786	1.80			111
		Cr3 - OB34 - Cr4	131.3°			

\*Correction for thermal motion, see text.

Na-O distances less than 3.3 Å

Na1-O33	2.347	Na2-O23	2.375	Na3-O41	2.355	Na4-O42	2.386
O21	2.385	O32	2.391	O13	2.433	O12	2.411
O42	2.447	O22	2.432	O23	2.466	O43	2.414
O41	2.467	OB34	2.448	O32	2.580	O22	2.489
O12	2.476	O11	2.538	O11	2.634	O13	2.492
O31	2.545	O33	2.678	O21	2.673	O31	2.502
				O43	2.825		

Standard errors derived from least squares refinement:

$$\text{Cr-O} = 0.011\text{Å}; \text{Na-O} = 0.013\text{Å}; \text{O-Cr-O} = 1^\circ; \text{Cr-O-Cr} = 0.4^\circ$$

Table 4.8  $\alpha$ - $\text{Na}_2\text{Cr}_2\text{O}_7$ . Interatomic Distances

		Uncorrected	Corrected*	Angles (in degrees)		
		Distance ( $\text{\AA}$ )	Distance ( $\text{\AA}$ )	012	013	OB12
Cr1	O11	1.620	1.64	111	112	109
	O12	1.604	1.62		110	110
	O13	1.627	1.66			105
	OB12	1.785	1.82			
				O22	O23	OB12
Cr2	O21	1.604	1.62	109	111	110
	O22	1.618	1.69		109	107
	O23	1.583	1.64			110
	OB12	1.750	1.78			

Cr1 - OB12 - Cr2  $135.1^\circ$

Na-O Distances less than  $3.3 \text{\AA}$

		Distance ( $\text{\AA}$ )			Distance ( $\text{\AA}$ )
Na1	O13	2.367	Na2	O22	2.405
	O21	2.423		O23	2.425
	O12	2.561		O12	2.448
	O21	2.601		O11	2.526
	O11	2.654		O13	2.660
	O22	2.762		OB12	2.736
	O23	2.835		O22	2.939

Standard errors derived from least squares refinement:

Cr-O =  $0.010 \text{\AA}$ , Na-O =  $0.012 \text{\AA}$ , O-Cr-O =  $1^\circ$ , Cr-O-Cr =  $0.6^\circ$

\*Correction for thermal motion, see text.

Table 4.9  $\beta$ 1-Rb<sub>2</sub>Cr<sub>2</sub>O<sub>7</sub>. Interatomic Distances

		Uncorrected Distance (Å)	Corrected* Distance (Å)	Angles (in degrees)		
				012	013	OB12
Cr1	O11	1.600	1.61	110	112	108
	O12	1.604	1.62		109	110
	O13	1.602	1.62			109
	OB12	1.780	1.79			
				022	023	OB12
Cr2	O21	1.624	1.64	110	110	110
	O22	1.630	1.64		108	109
	O23	1.616	1.63			109
	OB12	1.772	1.78			
Cr1 - OB12 - Cr2 = 123.0°						
				032	033	OB34
Cr3	O31	1.600	1.61	110	110	106
	O32	1.615	1.62		111	109
	O33	1.609	1.62			111
	OB34	1.789	1.80			
				042	043	OB34
Cr4	O41	1.593	1.61	110	109	110
	O42	1.606	1.62		110	111
	O43	1.602	1.61			108
	OB34	1.759	1.77			
Cr3 - OB34 - Cr4 = 137.5°						

\*Correction for thermal motion, see text.

Rb-O Distances less than 3.31 Å

Rb1-O21	2.86	Rb2-O22	2.89	Rb3-O43	2.87	Rb4-OB34	2.90
O13	2.87	O23	2.91	O33	2.88	O33	2.90
O22	2.89	O31	2.99	O41	2.92	O32	2.94
O23	2.90	O12	3.04	O22	2.93	O12	2.96
O12	2.91	O13	3.04	O43	3.00	O43	2.96
O32	2.93	O42	3.06	O11	3.02	O42	3.11
O23	3.07	O11	3.07	O32	3.02	O31	3.23
O31	3.28	OB12	3.19	O21	3.09	O11	3.24
		O41	3.24			O41	3.31

Standard errors derived from least squares refinement:  
 Cr-O = 0.01 Å , Rb-O = 0.01 Å , O-Cr-O = 1°.

Table 4.10 NaRb Cr<sub>2</sub>O<sub>7</sub>. Interatomic Distances

		Uncorrected (Distance (Å))	Corrected* Distance (Å)	Angles (in degrees)		
				O12	O13	OB12
Cr1	O11	1.597	1.61	112	109	106
	O12	1.611	1.63			
	O13	1.593	1.61			
	OB12	1.769	1.79			
				O22	O23	OB12
Cr2	O21	1.615	1.62	112	110	107
	O22	1.618	1.64			
	O23	1.620	1.63			
	OB12	1.755	1.78			
				O32	O33	OB34
Cr3	O31	1.593	1.61	110	109	106
	O32	1.630	1.64			
	O33	1.630	1.65			
	OB34	1.746	1.77			
				O42	O43	OB34
Cr4	O41	1.607	1.63	111	111	106
	O42	1.608	1.63			
	O43	1.604	1.62			
	OB34	1.767	1.79			

$$\text{Cr1} - \text{OB12} - \text{Cr2} = 135.9^\circ$$

$$\text{Cr3} - \text{OB34} - \text{Cr4} = 141.4^\circ$$

\*Correction for thermal motion, see text.

Na-O Distances less than 3.0 Å				Rb-O Distances. less than 3.4 Å			
Na1-O11	2.332	Na2-O21	2.351	Rb1-O13	2.908	Rb2-O32	2.972
O42	2.362	O33	2.434	O23	2.994	O43	3.019
O23	2.442	O41	2.458	O42	3.004	O32	3.097
O12	2.452	O31	2.556	O22	3.008	O33	3.164
O21	2.568	O13	2.576	O22	3.065	O33	3.198
O31	2.608	O12	2.598	OB12	3.152	O13	3.208
O23	2.770	O32	2.874	O43	3.293	OB34	3.214
		O11	2.884	O41	3.316	O12	3.226
				O43	3.323	O41	3.316
				OB12	3.385	O31	3.337
						O42	3.338
						OB34	3.377

Standard errors indicated by the least squares refinement

Cr-O = 0.010 Å, Na-O = 0.010 Å, Rb-O = 0.010 Å, O-Cr-O = 1°

Cr-O-Cr = 0.6°.

$\alpha$ - $\text{Na}_2\text{Cr}_2\text{O}_7$  bonds which have large temperature factors are somewhat uncertain.

#### 4.3 Discussion on the Conformations of the Dichromate Ion

The main features of dichromate ions found in the various structures are summarised in Table 4.11. The mean bond lengths of the terminal oxygen atoms of the various conformations vary between 1.60 to 1.63 Å. The Cr-OB bond length varies between 1.76 to 1.80 Å. The mean O-Cr-O angle in all structures is very close to the tetrahedral value of 109.47°. What varies significantly from structure to structure is the bridging oxygen angle which ranges from 121° to 141° and the two torsion angles  $\alpha_1$  and  $\alpha_2$ . These angles are taken to be zero when a terminal oxygen atom lies in the Cr-B-Cr plane (A conformation), and are otherwise taken to be the smallest angle between this plane and the projection of one of the Cr-O (terminal) bonds on the plane perpendicular to Cr-B (bridging oxygen). The sense of the rotation is taken as positive if the terminal oxygen atom lies to the left of the Cr-B-Cr plane when viewed from the bridging oxygen.

The torsion angles found in a variety of dichromate ions are plotted against each other in Figure 4.3. Since the  $\text{CrO}_4$  tetrahedra of the anions have almost exact  $\text{C}_{3v}$  symmetry with the Cr-B bond as the threefold axis it is sufficient to consider values of  $\alpha_1$  and  $\alpha_2$  only in the -60 to +60 degrees. On the other hand in all of these structures two dichromate

Table 4.11 Geometry of the dichromate ion

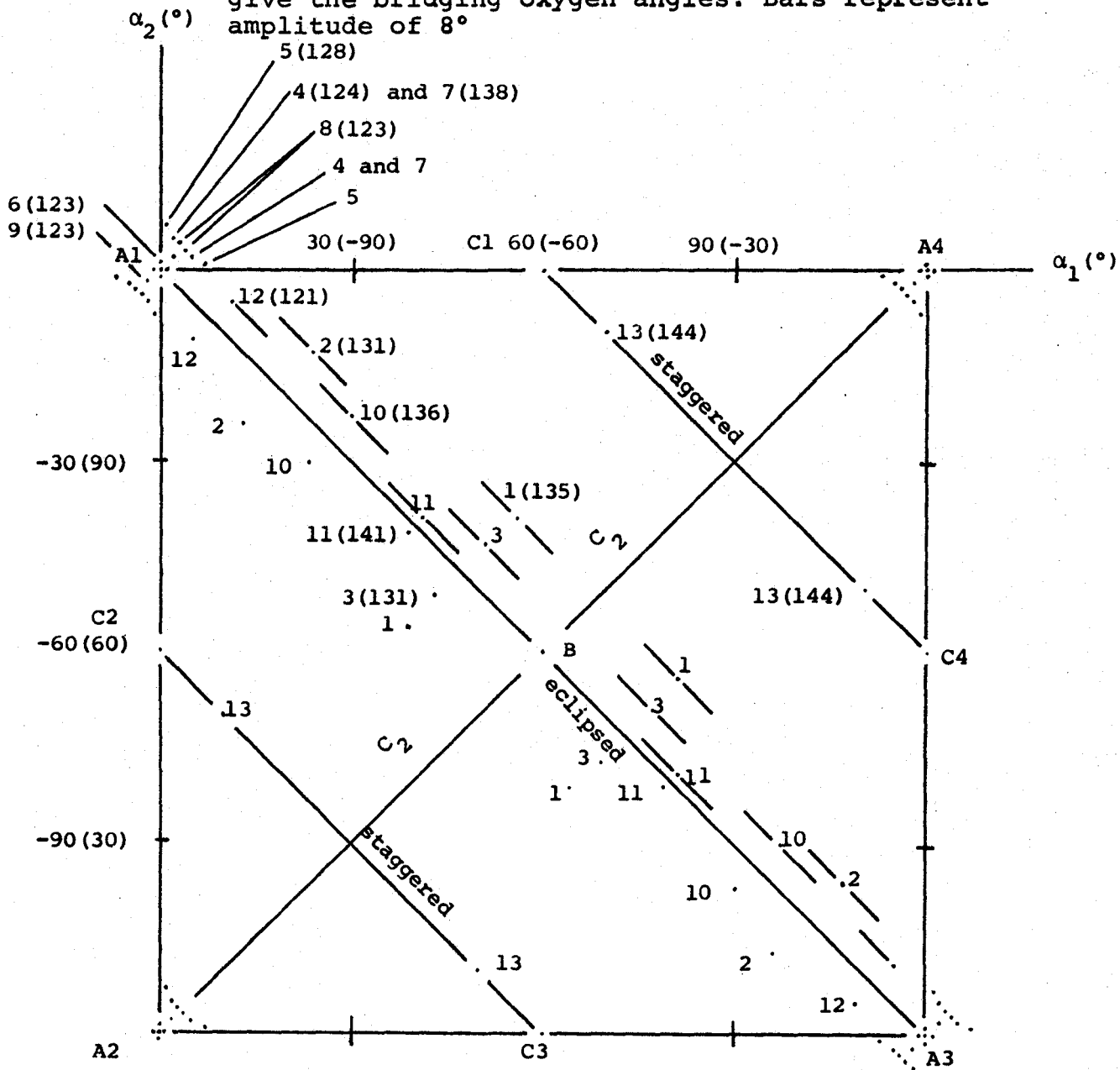
Phase	Na <sub>2</sub> Cr <sub>2</sub> O <sub>7</sub>			K <sub>2</sub> Cr <sub>2</sub> O <sub>7</sub>		Rb <sub>2</sub> Cr <sub>2</sub> O <sub>7</sub>				NaRbCr <sub>2</sub> O <sub>7</sub>		Ag <sub>2</sub> Cr <sub>2</sub> O <sub>7</sub>	Mg <sub>2</sub> P <sub>2</sub> O <sub>7</sub>
	α	β		β1		β1		VII	X	P2 <sub>1</sub> /c		P $\bar{1}$	α
Dichromate ion Number †	1	2	3	4	5	6	7	8	9	10	11	12	13
Symmetry	*	*	*	*	*	*	*	*	C <sub>2</sub>	*	*	*	
Mean Cr-OB (Å)	1.77	1.79	1.80	1.78	1.78	1.78	1.78	1.80	1.77	1.76	1.76	1.78	
Mean Cr-O (terminal) (Å)	1.61	1.63	1.63	1.63	1.60	1.63	1.62	1.60	1.62	1.61	1.61	1.62	
Cr-Cr (Å)	3.27	3.24	3.26	3.14	3.19	3.12	3.31	3.16	3.12	3.27	3.32		
Mean O-Cr-O (degrees)	109.4	109.5	109.4	109.6	109.4	109.6	109.7	109.4	109.3	109.5	109.5		
Cr-Ob-Cr (degrees)	135	131.3	131.3	124.0	127.6	123.0	137.5	122.9	122.9	135.9	141.4	121.0	144.
α <sub>1</sub> (degrees)	56	24	51	5	7	1	5	4	2	30	41	11	-50
α <sub>2</sub> (degrees)	-39	-13	-43	2	1	0	2	3	2	-23	-39	-5	-10

† The number given in Figure 4.3

\* Exact symmetry C<sub>1</sub>



Figure 4.3 Conformations of the dichromate ion. The anions are numbered as in Table 4.11. Numbers in parentheses give the bridging oxygen angles. Bars represent amplitude of  $8^\circ$



ions are related by centers of symmetry so each ion is accompanied by its enantiomorph, with  $\alpha_1 = -\alpha_1$  and  $\alpha_2 = \alpha_2$ . In addition the assignment of  $\alpha_1$  or  $\alpha_2$  to a particular end of the dichromate ion is arbitrary so  $\alpha_1$  and  $\alpha_2$  can be interchanged. These symmetries generate for each point on the graph a further three points.

The origin A1 (with  $\alpha_1 = 0$ ,  $\alpha_2 = 0$ ) corresponds to the conformation A with C<sub>2v</sub> symmetry, the points A2, A3, A4, each represent also the A conformation. The point B represents the B conformation with C<sub>2v</sub> symmetry and the points C1, C2, C3, C4 represent staggered conformations with C<sub>1</sub> symmetry. The line  $\alpha_1 = \alpha_2$  (A2A4) represents conformations with C<sub>2</sub> symmetry while the line  $\alpha_1 = -\alpha_2$  (A1A3) represents conformations where the terminal oxygens are eclipsed. The lines C1C2 and C3C4 represent conformations in which the terminal oxygens are in a staggered conformation.

All the conformations so far found in anhydrous dichromates<sup>†</sup> are concentrated around the  $\alpha_1 = -\alpha_2$  axis. Close to the origin the bridging angle lies between 121° to 128°<sup>††</sup>. For conformations with  $|\alpha| > 15^\circ$  the bridging angle is normally

<sup>†</sup>The anions in Na<sub>2</sub>Cr<sub>2</sub>O<sub>7</sub>·2H<sub>2</sub>O have conformations with bridge angle  $b=126^\circ$ ,  $\alpha_1=21^\circ$ ,  $\alpha_2=13^\circ$  and  $b = 122^\circ$ ,  $\alpha_1=12^\circ$ ,  $\alpha_2=3^\circ$ . We do not consider these anions because of the hydrogen bonding between the water molecules and the anions.

<sup>††</sup>The only exception is the angle 138° found in one of the ions in  $\beta$ 1(VIII) Rb<sub>2</sub>Cr<sub>2</sub>O<sub>7</sub>.

larger than 130 degrees. These larger values for conformations close to B can be understood in terms of the repulsion of the two terminal oxygen atoms which lie on the mirror plane. If the bridging angle were to be  $125^\circ$  the O-O distance would be around  $2.6 \text{ \AA}$ . With a bridging angle of  $130^\circ$  this distance increases to  $3.2 \text{ \AA}$  (Van der Waals O-O separation  $2.8(37)$ ).

The different conformations arising from different values of the torsion angles are related to the two torsion modes of vibration. The antisymmetric torsion mode corresponds to line segments parallel to the  $\alpha_1 = -\alpha_2$  line, the symmetric torsion mode to line segments parallel to the  $\alpha_1 = \alpha_2$  line.

The torsional motions can thus be displaced on the  $\alpha_1, \alpha_2$  graph by a line of  $6^\circ$  length corresponding to the rms torsional libration. If there is an appropriate change in the environment the dichromate ion can easily adopt a neighbouring conformation. All the conformations are connected by the antisymmetric torsion to form a continuous line. Thus the anion may readily undergo a continuous deformation from the configuration A1 to B and vice versa. As the terminal oxygen atoms are more or less fixed by adjacent atoms in the structure the antisymmetric torsion mode appears in the crystal as a libration of the bridging oxygen around the Cr-Cr axis. In the crystal frame of reference the transitions between conformations parallel to the  $\alpha_1 = -\alpha_2$  line appears as a

rotation of the bridging oxygen around the Cr-Cr axis .  
The position of the terminal oxygen atoms in this picture change by small amounts.

Since most dichromates have conformations lying close to the  $\alpha_1 = -\alpha_2$  line and that in the crystal a change of conformation along this line can be achieved by rotation of only the bridging oxygen atom, leaving the other atoms relatively unchanged, it can be seen that transformations involving such conformation changes might easily occur.

#### 4.4 The $\alpha$ to $\beta$ Phase Transition in $\text{Na}_2\text{Cr}_2\text{O}_7$

As the temperature of the  $\alpha$  phase of  $\text{Na}_2\text{Cr}_2\text{O}_7$  is lowered the torsional ( $\alpha_1 + \alpha_2$ ) and one of the librational oscillations around the mirror axis of the moment of inertia becomes large. The particular lattice mode is one in which  $\text{Cr}_2\text{O}_7$  ions in different layers<sup>†</sup> move in opposite directions. At the phase transitions these motions freeze out so that layers become different. As the temperature is decreased further the layers differ more and more from each other, an effect that continues to room temperature and probably below.

It is interesting to note that the same sort of torsional mode is invoked by Brown and Calvo (3) to explain

---

<sup>†</sup>Layers of dichromate ions parallel to the (010) plane, related above the transition temperature with the A face centering symmetry operation. A description of these layers is given in Chapter 5.

the  $\beta_1 \rightarrow \alpha$  phase transition in  $K_2Cr_2O_7$  but in this case there is a sudden flipping of half the bridging oxygen atoms through  $120^\circ$  with a corresponding transformation of half the sheets.

## CHAPTER 5

### LAYERS IN THORTVEITITE AND DICHROMATE LIKE STRUCTURES

#### 5.1 Introduction. Description of the Layers

Compounds with stoichiometry  $X_2Y_2O_7$  where the ionic radius of the Y atom is less than  $0.60 \text{ \AA}$  usually crystallize either in structures related to thortveitite if the ionic radius of X is less than  $0.97 \text{ \AA}$  or in one of a series of related structures typical of those found among the alkali metal dichromates if the ionic radius of X is greater than  $0.97 \text{ \AA}$ .

Thortveitite like structures are found for many pyrophosphates (38-40) and pyroarsenates (41). They usually have a high temperature  $\beta$  phase which is isomorphous with the mineral thortveitite ( $Sc_2Si_2O_7$ , (42)) and show a bridging angle Y-O-Y of  $180^\circ$  and a low temperature  $\alpha$  phase which have a bridging angle of less than  $180^\circ$ . The  $\alpha$  phases show great diversity in their structures although all similar to thortveitite.

Crystals which adopt one of dichromate structures include alkali dichromates,  $Ag_2Cr_2O_7$ ,  $\beta Ca_2P_2O_7$ ,  $\beta Sr_2V_2O_7$ ,  $Pb_2V_2O_7$ , Brown and Calvo (3) have developed a general scheme for classifying dichromate like structures by considering the various stacking arrangements of sheets of

dichromate ions. Their scheme does not extend to the thortveitite like structures nor does it include that of  $\text{NaRbCr}_2\text{O}_7$  or  $\alpha\text{-Ca}_2\text{P}_2\text{O}_7$ .

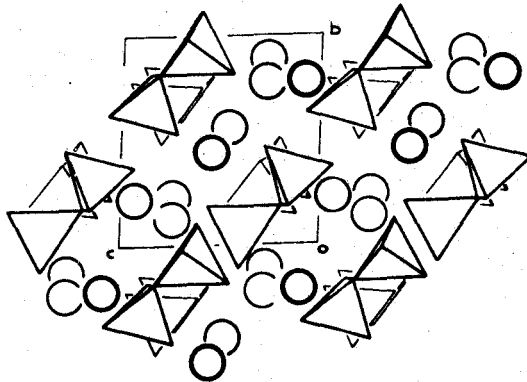
An alternative description can be used to describe both thortveitite and dichromate like structures. Both types of structures are built up from layers of  $\text{Y}_2\text{O}_7$  ions with the cations sandwiched between them, Figure 5.1a, b, the Y-Y vectors lie in the plane of the layer.

Orthogonal projections of the layers of a few structures are given in Figures 5.1c, 5.2, 5.3 and 5.4. The A and C axes lie in the plane of the layer and are chosen to give a B centered cell. The Y-Y vectors are roughly parallel to the A axis and perpendicular to C. We shall call the rows of anions parallel to the C axis C rows and the rows parallel to the A axis A rows.

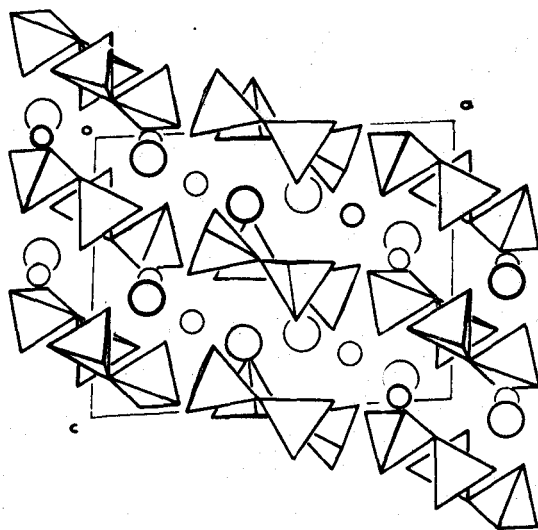
The  $\text{Y}_2\text{O}_7$  anions of the C rows are related in the thortveitite structures by a glide plane lying in the plane of the layer and in the dichromate structures by centers of symmetry. Both of these symmetry elements are present in thortveitite itself. With the exception of the  $\alpha\text{-Mg}_2\text{P}_2\text{O}_7$  (39) layer all the other layers of Figures 5.2 to 5.4 have the A row anions related by centers of symmetry, with the result that the unit cell defined by the A and C axes is B face centered, i.e. adjacent C rows are related to each other by a translation and there is only one crystallographically

Figure 5.1 Layers in  $\beta 1\text{-Rb}_2\text{Cr}_2\text{O}_7$ ,  $\text{NaRbCr}_2\text{O}_7$  and  $\text{Sc}_2\text{Si}_2\text{O}_7$

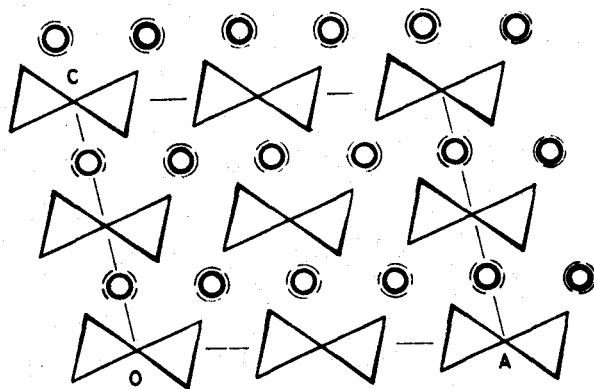
- a)  $\beta 1\text{-Rb}_2\text{Cr}_2\text{O}_7$  ( $P\bar{1}$ ). Viewed down the  $[101]$  axis, atoms around  $x=0$  and  $x=1/2$ .



- b)  $\text{NaRbCr}_2\text{O}_7$  ( $P2_1/c$ ). Viewed down the  $b$  axis, atoms around  $y = 0$  and  $y = \frac{1}{2}$ .



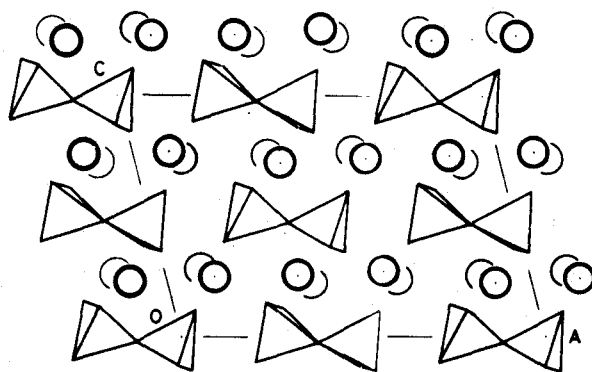
- c)  $\text{Sc}_2\text{Si}_2\text{O}_7$  ( $C2/m$ ) Plane  $(010)^*$ ;  $O = 0,0,0$ ;  $A = 2,0,0$ ;  $C = 0,0,2$ .





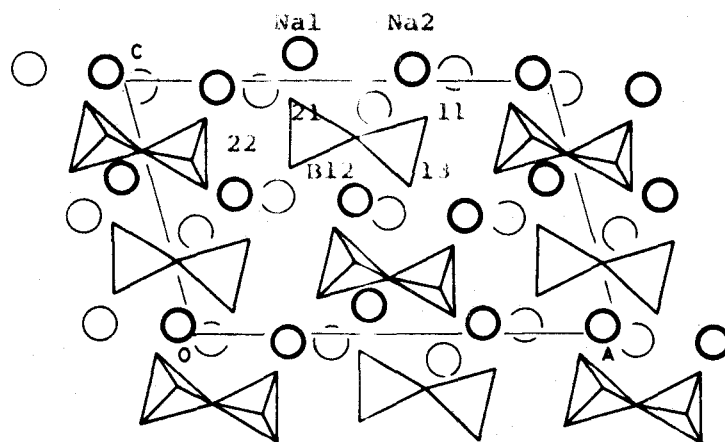
a)  $\alpha\text{-Mg}_2\text{P}_2\text{O}_7$  ( $B2_1/c$ ). Plane  $(0\bar{1}0)$ , viewed down the  $[0\bar{1}0]^*$ ;

$$O = 0, \frac{1}{4}, 0; A = 1, \frac{1}{4}, 0; C = 0, \frac{1}{4}, 1.$$



b)  $\alpha\text{-Na}_2\text{Cr}_2\text{O}_7$  ( $A\bar{1}$ ). Plane  $(010)$  viewed down the  $[010]^*$ ;

$$O = 1, 0, 0; A = \bar{1}, 0, \bar{1}; C = 1, 0, 1.$$



c)  $X\text{-Rb}_2\text{Cr}_2\text{O}_7$  ( $C2/c$ ) Plane  $(\bar{1}1\cdot)$  viewed down the  $[\bar{1}11]^*$

$$O = 0, 0, \frac{1}{2}; A = 1, 0, \frac{1}{2}; C = 0, 1, \frac{1}{2}.$$

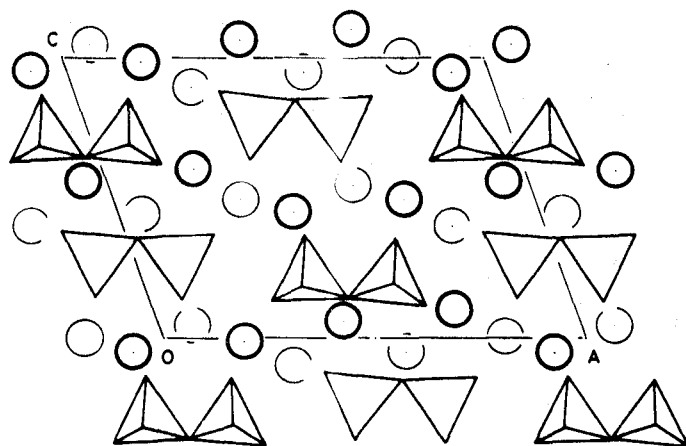
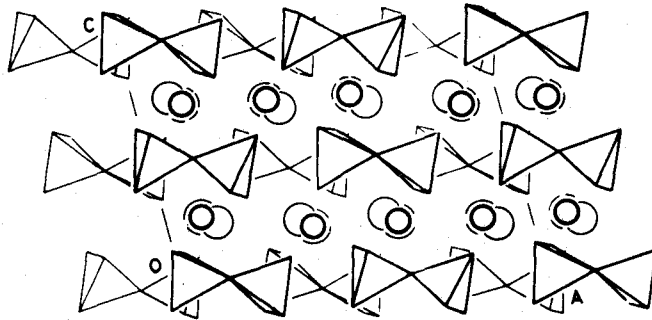


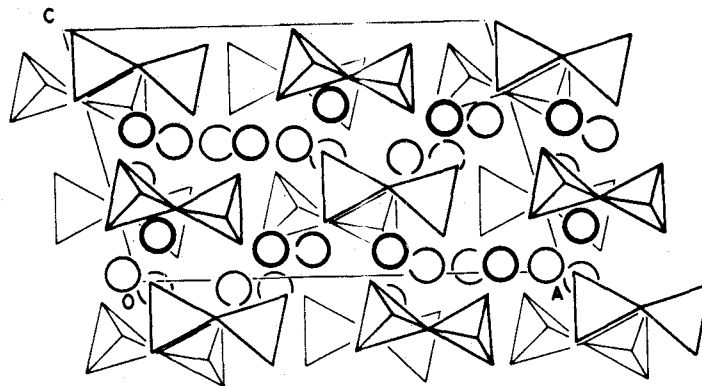
Figure 5.2 Layers of  $\alpha\text{-Mg}_2\text{P}_2\text{O}_7$ ,  $\alpha\text{-Na}_2\text{Cr}_2\text{O}_7$  and  $X\text{-Rb}_2\text{Cr}_2\text{O}_7$

Figure 5.3 Packing of the layers in  $\alpha\text{-Mg}_2\text{P}_2\text{O}_7$ ,  $\alpha\text{-Na}_2\text{Cr}_2\text{O}_7$  and  $X\text{-Rb}_2\text{Cr}_2\text{O}_7$ . The layers of Figure 5.2 and the next higher layer.

a)  $\alpha\text{-Mg}_2\text{P}_2\text{O}_7$



b)  $\alpha\text{-Na}_2\text{Cr}_2\text{O}_7$



c)  $X\text{-Rb}_2\text{Cr}_2\text{O}_7$

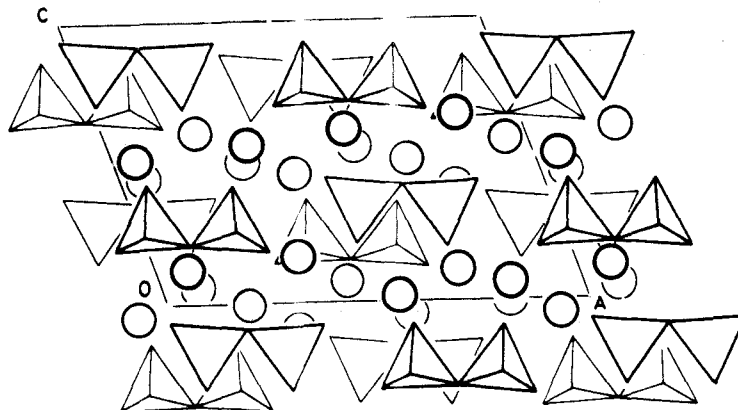
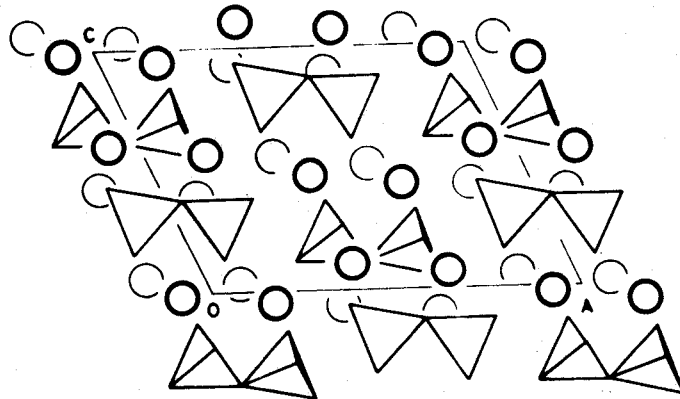
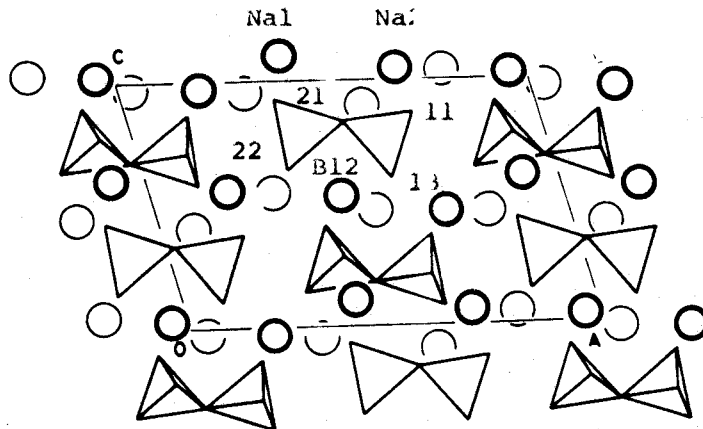


Figure 5.4 Layers of  $\text{Ag}_2\text{Cr}_2\text{O}_7$  and  $\beta\text{-Na}_2\text{Cr}_2\text{O}_7$ 

- a)  $\text{Ag}_2\text{Cr}_2\text{O}_7$  ( $\text{P}\bar{1}$ ). Plane (100) viewed down the  $[\bar{1}00]^*$ ;  
 $O = 1, 0, 0$ ;  $A = \bar{1}, 0, \bar{1}$ ;  $C = 1, 0, 1$



- b)  $\beta\text{-Na}_2\text{Cr}_2\text{O}_7$  ( $\text{P}\bar{1}$ ). Plane (010) viewed down the  $[010]^*$ ;  
 $O = 1, 0, 0$ ;  $A = \bar{1}, 0, \bar{1}$ ;  $C = 1, 0, 1$



- c)  $\beta\text{-Na}_2\text{Cr}_2\text{O}_7$  ( $\text{P}\bar{1}$ ). Plane (010) viewed down the  $[010]^*$ ;  
 $O = 1, \frac{1}{2}, \frac{1}{2}$ ;  $A = \bar{1}, \frac{1}{2}, \frac{1}{2}$ ;  $C = 1, \frac{1}{2}, 1\frac{1}{2}$

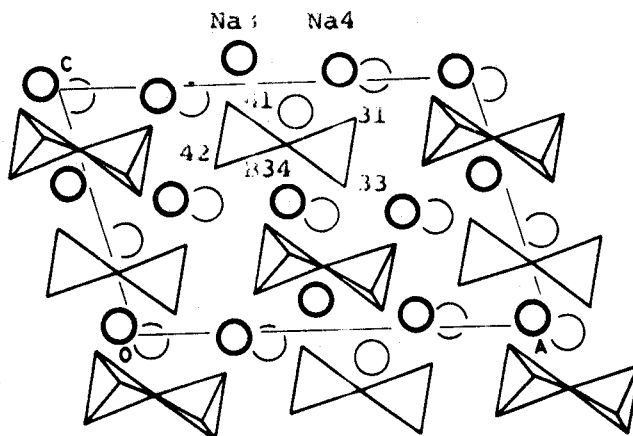
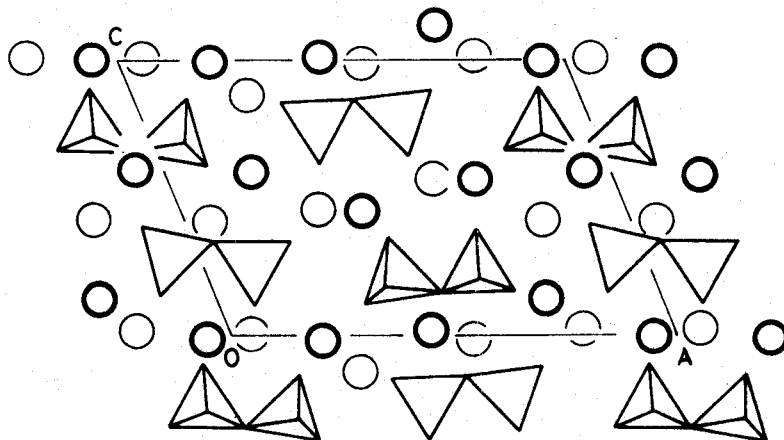
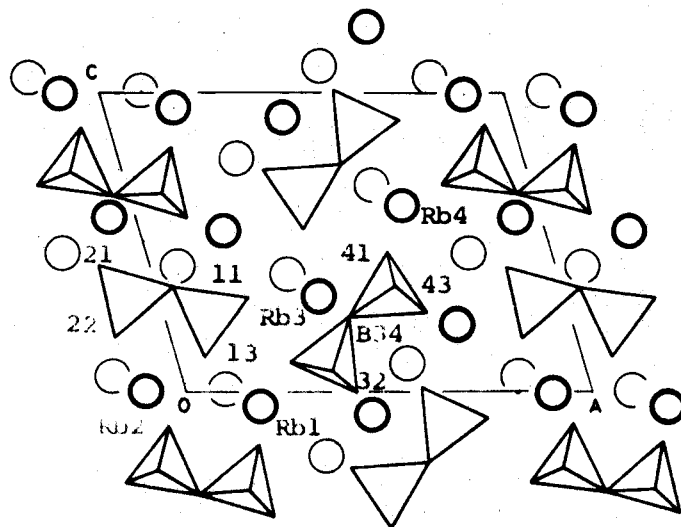


Figure 5.5 Layers of VII-Rb<sub>2</sub>Cr<sub>2</sub>O<sub>7</sub> and β1-Rb<sub>2</sub>Cr<sub>2</sub>O<sub>7</sub>

- a) VII-Rb<sub>2</sub>Cr<sub>2</sub>O<sub>7</sub> ( $2_1/n$ ). Plane (111) viewed down the  $[\bar{1}\bar{1}\bar{1}]^*$ ;  
 $O = 0, 1, 0$ ;  $A = 1, 1, \bar{1}$ ;  $C = 0, 0, 1$ .



- b) β1-Rb<sub>2</sub>Cr<sub>2</sub>O<sub>7</sub> ( $P\bar{1}$ ). Plane (111) viewed down the  $[\bar{1}\bar{1}\bar{1}]^*$ ;  
 $O = 0, 0, \frac{1}{2}$ ;  $A = 1, 0, \frac{1}{2}$ ;  $C = 0, 1, -\frac{1}{2}$ .



distinct anion.

In  $\text{Sc}_2\text{Si}_2\text{O}_7$  thortveitite the C glide becomes a mirror plane and there are additional centers of symmetry on the bridging oxygen, relating the two halves of the  $\text{Si}_2\text{O}_7$  anion and imposing a bridging oxygen angle of  $180^\circ$  and a staggered conformation to the anion.

In  $\alpha\text{-Mg}_2\text{P}_2\text{O}_7$  the A,C cell is B face centered but with the exception of the C glide there is no other symmetry element that relates anions of the A or C rows. With no restriction on its symmetry, the anion has a distorted staggered conformation similar to the anion in  $\text{Sc}_2\text{Si}_2\text{O}_7$  but with a bridging angle different from  $180^\circ$ . Though the centers of symmetry are lost, the differences from the  $\text{Sc}_2\text{Si}_2\text{O}_7$  layer are small and one can identify pseudocenters of symmetry that relate the A row anions.

## 5.2 The Structure and Packing of Typical Layers ( $\alpha\text{-Mg}_2\text{P}_2\text{O}_7$ , $\alpha\text{-Na}_2\text{Cr}_2\text{O}_7$ , X C2/c $\text{Rb}_2\text{Cr}_2\text{O}_7$ )

### The layers

We will examine the structure of the layers by concentrating on three typical structures only,  $\alpha\text{-Mg}_2\text{P}_2\text{O}_7$ ,  $\alpha\text{-Na}_2\text{Cr}_2\text{O}_7$  and type X C2/c  $\text{Rb}_2\text{Cr}_2\text{O}_7$ , Figures 5.2, 5.3, representing structures with small ( $r < 0.95 \text{ \AA}$ ), intermediate ( $0.95 < r < 1.05 \text{ \AA}$ ) and large ( $r > 1.05 \text{ \AA}$ ) cation respectively.

In both  $\text{Sc}_2\text{Si}_2\text{O}_7$  and  $\alpha\text{-Mg}_2\text{P}_2\text{O}_7$  the c glide has as a consequence that the bridging oxygens lie on the C axis

while in  $\alpha\text{-Na}_2\text{Cr}_2\text{O}_7$  and C2/c  $\text{Rb}_2\text{Cr}_2\text{O}_7$  the C glide is lost and the A rows are shifted in the A direction relative to each other by small amounts. In these layers the  $\text{Cr}_2\text{O}_7$  ions have eclipsed conformations for the terminal oxygens and the cations have moved from the positions they occupied in  $\alpha\text{-Mg}_2\text{P}_2\text{O}_7$ .

In  $\alpha\text{-Na}_2\text{Cr}_2\text{O}_7$  this shift is appreciable for the two cations which lie in the middle of the first C row, but the layer is still rather similar to that of  $\alpha\text{-Mg}_2\text{P}_2\text{O}_7$ . In going from  $\alpha\text{-Na}_2\text{Cr}_2\text{O}_7$  to X  $\text{Rb}_2\text{Cr}_2\text{O}_7$  the shifts become larger for all the cations and the layer differs more from that in  $\alpha\text{-Mg}_2\text{P}_2\text{O}_7$ . In X  $\text{Rb}_2\text{Cr}_2\text{O}_7$  there are crystallographic twofold axes running through the bridging oxygen atom at an angle of about  $45^\circ$  to the normal to the layers and a glide plane normal to this axis relating ions along the A rows.

#### Packing of the layers

In  $\alpha\text{-Mg}_2\text{P}_2\text{O}_7$  neighbouring layers, are related with a  $2_1$  axis perpendicular to the layer in a way that the layer above is not only rotated in relation to the layer below by  $180^\circ$  but also is shifted by  $1/4$  A. As a result the C rows of the layer above lie in the middle of two C rows of the layer below and are related by a pseudotranslation of  $\frac{1}{4}\text{A} + \frac{1}{2}\text{C}$ , Figure 5.3a.

In  $\alpha\text{-Na}_2\text{Cr}_2\text{O}_7$  where a simple translation relates neighbouring layers there is a shift of the centers of symmetry of the two layers by about  $1/6\text{A} + \frac{1}{2}\text{C}$ , Figure 5.3b.

In  $X\text{-Rb}_2\text{Cr}_2\text{O}_7$  neighbouring layers are related with a translation of  $1/5A + 1/2C$ , Figure 5.3c. Thus the relative shift between neighbouring layers decreases as the ionic radius of the cation increases.

In general in thortveitite like structures with a small cation radius there are symmetry elements such as two-fold axes or twofold screw axes normal to the layer. In structures with intermediate radii the layers are related only by translations and centers of symmetry while for cations of large ionic radius the symmetry elements lie at angles of  $45^\circ$  to the layer.

Because in most high symmetry dichromate like structures the layers are not parallel to the planes of symmetry the symmetry of the resulting structure is not apparent from the figures of the layers. For these structures the scheme proposed by Brown and Calvo (3) is more appropriate. In this classification the dichromate-like structures are described in terms of sheets corresponding to the C rows stacked in the A direction. These sheets are described in a system of axes in which a corresponds to the B centering translation described above and b and c lie on the plane of the sheet making angles of about  $45^\circ$  with the B and C axes described above. The symmetry elements in the larger cation alkali metal dichromate structures lie along the a, b and c axes of Brown and Calvo's classification.

### 5.3 Special Cases of Layers in Small Cation Structures (Thortveitite Like)

The layers described above are characterized by the fact that the Y-Y vectors are parallel to the A axis and the A, C cell is B centered. This type of layer can undergo certain transformations.

The low temperature pyrophosphate phases derived from the thortveitite structure, all differ from the parent structure in having a P-O-P angle of less than  $180^\circ$ . This is achieved by the bridging oxygen atom moving in a direction perpendicular to the layer either up or down. The variety of different structures that appear at low temperatures arise from different arrangements of bridging oxygen displacements.

In  $\alpha\text{-Cu}_2\text{P}_2\text{O}_7$  with C2/c symmetry (38), there are no centers of symmetry to relate neighbouring anions in the A rows. Instead they are related by twofold axes and translations while neighbouring A rows are related with a glide plane parallel to the layer.

In the I2/c  $\alpha\text{-Zn}_2\text{P}_2\text{O}_7$  (40) the structure is more complex. There are two anion conformations on each A row. Every third anion on the A row has a twofold axis passing through its bridging atom while the two anions in the middle are related to each other by a twofold axis.



## 5.4 Special Cases of Layers in Medium and Large Cation Structures

### 5.4.1 Ag<sub>2</sub>Cr<sub>2</sub>O<sub>7</sub>

The layers in  $P\bar{1}$  Ag<sub>2</sub>Cr<sub>2</sub>O<sub>7</sub>, Figure 5.4a, have structures intermediate to that of  $\alpha$ -Na<sub>2</sub>Cr<sub>2</sub>O<sub>7</sub> and X(C2/c) Rb<sub>2</sub>Cr<sub>2</sub>O<sub>7</sub>. The layer is B centered and the anion has conformation close to that of the anion in X-Rb<sub>2</sub>Cr<sub>2</sub>O<sub>7</sub>.

### 5.4.2 $\beta$ -Na<sub>2</sub>Cr<sub>2</sub>O<sub>7</sub>

$\beta$ -Na<sub>2</sub>Cr<sub>2</sub>O<sub>7</sub> is a superstructure derivative of  $\alpha$ -Na<sub>2</sub>Cr<sub>2</sub>O<sub>7</sub> and alternate layers differ from each other. The intermediate character of Na<sub>2</sub>Cr<sub>2</sub>O<sub>7</sub> in the series is rather strikingly illustrated by the fact that at low temperatures one of the two crystallographically distinct layers in  $\beta$ -Na<sub>2</sub>Cr<sub>2</sub>O<sub>7</sub> becomes similar to that in Ag<sub>2</sub>Cr<sub>2</sub>O<sub>7</sub>. The other layer becomes similar to that in the  $\alpha$ -Mg<sub>2</sub>P<sub>2</sub>O<sub>7</sub>. In each case the conformation of the dichromate ion is like that of the anion in the layer it resembles. Thus  $\beta$ -Na<sub>2</sub>Cr<sub>2</sub>O<sub>7</sub> is composed of alternating  $\alpha$ -Mg<sub>2</sub>P<sub>2</sub>O<sub>7</sub> like and Ag<sub>2</sub>Cr<sub>2</sub>O<sub>7</sub> layers.

### 5.4.3 P2<sub>1</sub>/n and $\beta 1 P\bar{1}$ Rb<sub>2</sub>Cr<sub>2</sub>O<sub>7</sub>

In P2<sub>1</sub>/n Rb<sub>2</sub>Cr<sub>2</sub>O<sub>7</sub> the centering of the A,C cell of X(C2/c) Rb<sub>2</sub>Cr<sub>2</sub>O<sub>7</sub> is lost but the n glide plane is retained, Figure 5.5a. However the differences between the P2<sub>1</sub>/n and the C2/c structure are small. The comparison of the P2<sub>1</sub>/n with the C2<sub>1</sub>/n have rotated around axes normal to the layer

in relation to their positions in C2/c.

In  $\beta 1 \text{ P}\bar{1} \text{ Rb}_2\text{Cr}_2\text{O}_7$  there is no symmetry element that relates adjacent C rows. One C row shows a small distortion the other a larger distortion from the C rows of C2/c  $\text{Rb}_2\text{Cr}_2\text{O}_7$ , Figures 5.2c and 5.5b. The relationship between them can best be understood in the scheme of Brown and Calvo where neighbouring C rows belong to different sheets and they are related by a non-crystallographic pseudoglide plane approximately perpendicular to C. As a result of the glide the role of  $\underline{b}$  and  $\underline{c}$  axes is interchanged between one sheet and the next. The slight inequalities in the lengths of  $\underline{b}$  and  $\underline{c}$  necessarily result in a distortion of the second sheet compared to the first. The small differences in environment of the dichromate ions result in differences of the angle at the bridging oxygen atom and the torsion angles  $\alpha_1$  and  $\alpha_2$ .

#### 5.4.4 $\beta 1(\text{V}) \text{ P}\bar{1} \text{ K}_2\text{Cr}_2\text{O}_7$

The layers of  $\beta 1 \text{ K}_2\text{Cr}_2\text{O}_7$  are parallel to the (111) plane and show rather striking similarities with the  $\beta 1(\text{VIII}) \text{ P}\bar{1} \text{ Rb}_2\text{Cr}_2\text{O}_7$  layer. The packing of the layers is similar in these two structures. The similarities between the layers of the  $\beta 1$  structures of K and Rb pose some interesting questions as to what extent the  $\beta 1 \rightarrow \alpha \rightarrow \beta 2$  phase transitions in K and Rb are similar or different. These questions can not be answered at present. Information on the symmetry of the  $\alpha \text{ Rb}_2\text{Cr}_2\text{O}_7$  phase is needed.

#### 5.4.5 $P2_1/c$ NaRbCr<sub>2</sub>O<sub>7</sub>

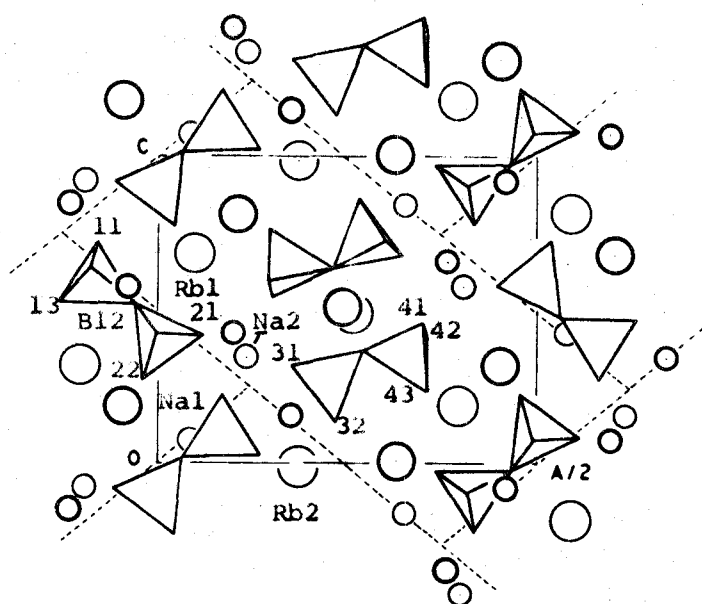
The structure of the  $P2_1/c$  NaRbCr<sub>2</sub>O<sub>7</sub> layer which is parallel to the (20 $\bar{1}$ ) plane is appreciably different from that of the other dichromate layer, Figure 5.6. The A axis, parallel to the [201], has twice the length found in the other dichromates. The C axis is parallel to [010]. Parallel to the C axis there are twofold screw axes which alternate with rows of centers of symmetry. The Na atoms form bonds mainly with the oxygen atoms of the anion that contains Cr1 and Cr2 while the Rb atoms form bonds mainly with the anion that contains Cr3 and Cr4. The arrangement of the cations in the layer is such that rectangular regions of the layer, containing four dichromate ions and 8 rubidium atoms can be identified. Sodium atoms define the bounds of these rectangles. Each rectangle has a structure similar to that of a segment of a C row with a center of symmetry at its center. The rectangles are related by a twofold screw axis parallel to C resulting in a layer that resembles a parquet floor, Figure 5.6b. Neighbouring layers are related by glide planes, normal to the C axis at  $C = 1/4$  and  $C = 3/4$ , Figure 5.6c.

#### 5.4.6 $\alpha$ -Ca<sub>2</sub>P<sub>2</sub>O<sub>7</sub>

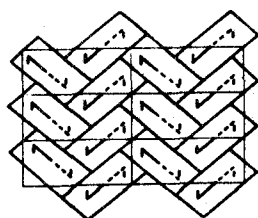
An extreme use of transformation of the layers is found in  $\alpha$ -Ca<sub>2</sub>P<sub>2</sub>O<sub>7</sub> (43) in which the cations instead of lying above and below the Y<sub>2</sub>O<sub>7</sub> layer nearly lie on the same plane that the Y-Y vectors lie, Figure 5.7. The Y-Y vectors have

Figure 5.6 The  $\text{NaRbCr}_2\text{O}_7$  layer

- a)  $\text{NaRbCr}_2\text{O}_7$ , ( $P2_1/c$ ). Plane  $(20\bar{1})$  viewed down the  $[\bar{2}01]^*$ ;  
 $O = 0, 0, \frac{1}{4}$ ;  $A/2 = 1, 0, \frac{3}{4}$ ;  $C = 0, 1, \frac{1}{4}$ .



- b) The rectangles of the layer



- c) Packing of layers

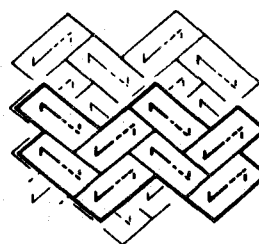
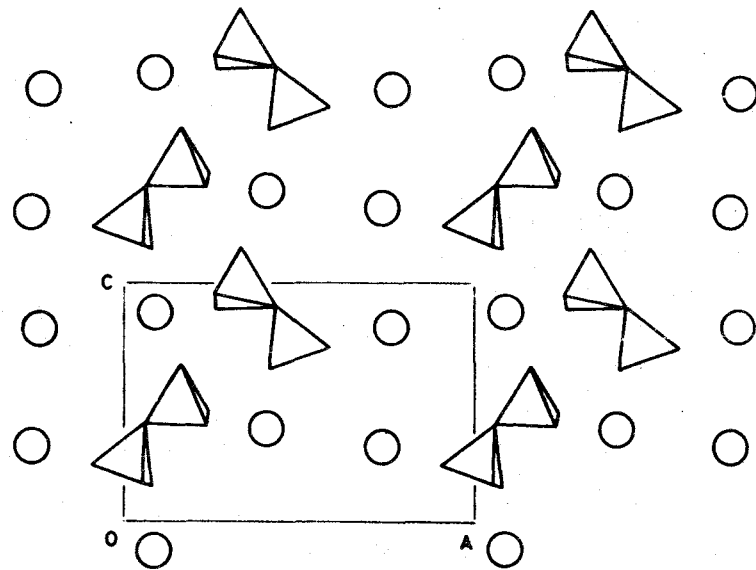


Figure 5.7 Layer of  $\alpha\text{-Ca}_2\text{P}_2\text{O}_7$

$\alpha\text{-Ca}_2\text{P}_2\text{O}_7$  ( $P2_1/n$ ) Plane (001) down the c axis;

O =  $0, 0, \frac{1}{4}$ ; A =  $1, 0, \frac{1}{4}$ ; C =  $0, 1, \frac{1}{4}$ .



an angle of  $45^\circ$  with the A and C axes and there are twofold screw axes on the plane of the layer which relate neighbouring rows.  $\alpha\text{-Sr}_2\text{P}_2\text{O}_7$  (44) has a similar layer but the plane of the layer is a mirror plane so the cations lie onto the plane and the anion has an m symmetry.

### 5.6 The Structure of $\beta 2 \text{Rb}_2\text{Cr}_2\text{O}_7$

The unit cell of  $\beta 2 \text{Rb}_2\text{Cr}_2\text{O}_7$ , Table 3.10, corresponds to that expected for a type I structure.

Unfortunately since all the axes are of roughly the same length it is not immediately obvious what orientation a type I structure would have in the crystal.

The thickness of the sheets described by Brown and Calvo for the three known  $\text{Rb}_2\text{Cr}_2\text{O}_7$  structures varies between 6.7 to 6.9 Å while the thickness of the layers described in the previous sections is around 5.0 Å.

The interplanar distances in the  $\beta 2\text{-Rb}_2\text{Cr}_2\text{O}_7$  lattice that are close to these values are:

$$\begin{array}{ll} d_{100} = 7.32 & d_{10\bar{1}} = 5.4 \\ d_{001} = 6.90 \text{ (Å)} & d_{110} = 4.7 \text{ (Å)} \\ d_{010} = 6.67 & d_{111} = 5.2 \end{array}$$

From these it is apparent that the sheets are either parallel to the b,c, plane or parallel to the a,c, plane. Since the angle between the axes which lie in the sheets always is close to  $90^\circ$  the sheets are likely to be parallel to the b,c, plane.

The interplanar distances which are close to  $5.0 \text{ \AA}$  are the  $d_{110} = 4.7 \text{ \AA}$  and the  $d_{111} = 5.2 \text{ \AA}$  both cut the  $b,c$  plane in the  $[01\bar{1}]$  direction which is the expected orientation between the sheets and the layers but it is not possible to decide which of these planes is in fact parallel to the layers.

The twin plane being parallel to the  $b,c$  plane cuts both the sheets and the layers.

In conclusion the  $\beta 2(P\bar{1}) \text{ Rb}_2\text{Cr}_2\text{O}_7$  structure is probably a type I structure in the classification scheme of Brown and Calvo with the sheets parallel to the  $b,c$  plane. The axes have been chosen to conform with the convention of Brown and Calvo.

## CHAPTER 6

### SUMMARY

The alkali metal dichromates show extensive polymorphism. The structures of the polymorphs which have been determined so far belong to a large series of structures of the  $X_2Y_2O_7$  compounds. This series includes dichromate like structures with medium and large cation radii and thortveitite like structures with small cation radii. All these structures are built from layers of  $Y_2O_7$  ions with the cations sandwiched between them.

From the alkali metal dichromates  $Na_2Cr_2O_7$  has four phases. We have determined the structure of the room temperature  $\beta$  and the next higher temperature  $\alpha$  phase. These structures illustrate rather strikingly the intermediate character of the  $Na_2Cr_2O_7$  in the series.  $\alpha$ - $Na_2Cr_2O_7$  is built up from identical layers intermediate in structure between the large and small cation layers.  $\beta$ - $Na_2Cr_2O_7$  is built up from two crystallographically nonequivalent layers. One of them resembles the layers of the larger cation and the other the layers of the smaller cation structures. The phase transition  $\alpha \rightarrow \beta$  is very close to a second order phase transition and probably it is triggered by a torsional mode of vibration of the dichromate ion. There is no information



on the higher temperature phases c and d. Probably the  $a \rightarrow c$  transition is a first order transition as we have observed an abrupt change in the diffraction pattern at around  $300^\circ\text{C}$ .

$\text{Rb}_2\text{Cr}_2\text{O}_7$  has three phases growing from aqueous solutions  $\beta 1$ , VII and X. On heating the  $\beta 1$  phase an irreversible transition occurs  $318^\circ\text{C}$  to an  $\alpha$  phase of unknown symmetry and on further heating a transition to the c phase at  $337^\circ\text{C}$ . On cooling the  $\alpha$  phase a reversible transition takes place at  $260^\circ\text{C}$  to a  $\beta 2$  phase whose cell constant we have determined and for which we have suggested a possible structure. We have determined the structure of the  $\beta 1$  phase, Löfgren and Walterson (10,11) the structures VII and X. The X- $\text{Rb}_2\text{Cr}_2\text{O}_7$  layer has a typical structure of a large cation layer. The VII- $\text{Rb}_2\text{Cr}_2\text{O}_7$  has layers which are a slightly distorted form of the X layer structures, while the layer of  $\beta 1$   $\text{Rb}_2\text{Cr}_2\text{O}_7$  is a further, very much distorted, form of the VII layer.

$\text{Cr}_2\text{O}_7$  has two phases grown from aqueous solutions  $\beta 1$  ( $P\bar{1}$ ) and an unstable C2/c phase probably of type X structure. On heating  $\beta 1$  an irreversible transition takes place rapidly at  $270^\circ\text{C}$  to an  $\alpha$  phase of P2/n symmetry and probably type VII structure. On further heating two transitions take place at  $345^\circ\text{C}$  and  $380^\circ\text{C}$  to phases c and d both of unknown symmetry.

On cooling the  $\alpha$  phase a reversible transition takes

place to a  $\beta 2$  phase. The existence of  $\beta 2$  phase is disputed. The only structure which has been determined is that of  $\beta 1$  whose layers look similar to those of  $\beta 1$   $\text{Rb}_2\text{Cr}_2\text{O}_7$ .

The  $\text{Cs}_2\text{Cr}_2\text{O}_7$  two phase transitions take place at  $347^\circ$  and  $362^\circ\text{C}$ . The only crystallographic information on this system is our work on the room temperature phase which shows that it belongs to the triclinic systems but is both disordered and twinned.

From the binary systems of dichromates the only compounds formed are those of  $\text{NaRbCr}_2\text{O}_7$  and  $\text{P}2_1/\text{c}$   $\text{NaCsCr}_2\text{O}_7$ . In view of the large polymorphism of the dichromates it is rather surprising that all the other binary systems form solid solutions. We have determined the structure of  $\text{NaRbCr}_2\text{O}_7$ . The layer in this structure shows blocks of four dichromate ions similar in structure to regions found in the other  $\text{Rb}_2\text{Cr}_2\text{O}_7$  layers.

$\text{NaCsCr}_2\text{O}_7$  is probably isostructural with  $\text{NaRbCr}_2\text{O}_7$ . No phase transitions have been determined for these two phases. It would be interesting to look for such transitions at lower temperatures. The fact that the bridging oxygen atoms show large librations around the Cr-Cr axis might indicate the existence of a lower temperature transition similar to the  $\alpha$ - $\beta$  transition in  $\text{Na}_2\text{Cr}_2\text{O}_7$ .

Although we have studied a few polymorphs and one phase transition in somewhat more detail there is a large number of questions which remain unanswered.

## BIBLIOGRAPHY

1. A. Bystrom and K. Wilhelmi. Acta Chem. Scand. 5, 1003 (1951).
2. J. K. Brandon and I. D. Brown, Can. J. Chem. 46, 933 (1968)
3. I. D. Brown and C. Calvo. J. Solid State Chem. 1, 183 (1970).
4. Yu. I. Vesnin and L. A. Khripin. Zh. Neorg. Khim. 11, 2216 (1966) [English translation: Russ. J. Inorg. Chem. 11, 1188 (1966)].
5. R. G. Samuseva, I. F. Poletaev and V. F. Plyushchev. Zh. Neorg. Khim. 7, 1146 (1962) [English translation: Russ. J. Inorg. Chem. 7, 589 (1962)].
6. U. Klement and G. Schwab. Z. Krist. 114, 170 (1960).
7. J. Jaffray and A. Labavy, Compt. Rend. 242, 1421 (1956).
8. K. A. Wilhelmi. Arkiv. Kemi 26, 149 (1967).
9. N. Ch. Panagiotopoulos and I. D. Brown. Canad. J. Chem. 48, 537 (1970).
10. P. Löfgren and K. Waltersson. Acta Chem. Scand. 25, 35 (1971).
11. P. Löfgren. Acta Chem. Scand. 25, 44 (1971).
12. J. Jaffray. J. de Phys. 12, 565 (1951).
13. J. Jaffray. J. de Phys. 13, 430 (1952).
14. A. Lehrman. H. Selditsch and P. Skell. J. Am. Soc. 58, 1612 (1936).
15. R. G. Samuseva, Yu. A. Okanev and V. E. Plyushev. Russ. J. Inorg. Chem. 12, 1489 (1967).

16. R. G. Hazell. *Acta Cryst.* A25, S116 (1969) and private communication.
17. Yu. A. Kharitonov, E. A. Kuzmin and N. V. Belov. *Kristallografiya* 15, 942 (1970). [English translation: *Soviet Physics Crystallography* 15, 820 (1971)].
18. I. D. Datt, N. V. Rannev, T. G. Balicheva and R. P. Ozerov. *Kristallografiya* 15, 949 (1970). [English translation: *Soviet Physics Crystallography* 15, 821 (1971)].
19. R. W. James. *The Optical Principles of the Diffraction of X-rays*. G. Bell and Sons Ltd., London. 1962.
20. H. Lipson and W. Cochran. *The Determination of Crystal Structures*. G. Bell and Sons Ltd., London 1962.
21. J. Karle and I. L. Karle. *Acta Cryst.* 21, 849 (1966).
22. D.W.J. Cruickshank, D.E. Pilling, A. Bujosa, F. M. Lovell and M. R. Truter: *Computing Methods in the Phase Problem*, Oxford: Pergamon Press (1961).
23. ASTM (American Society for Testing and Materials) *Powder Diffraction File*, Philadelphia, Pa. (1968).
24. K. Sakurai. *Acta Cryst.* 11, 840 (1958).
25. *International Tables for X-ray Crystallography*, Vol. III, Tables 3.3.1A, 3.3.2B, 3.3.2C, Birmingham: Kynoch Press (1962).
26. W. C. Hamilton. *Acta Cryst.*, 18, 502 (1965).
27. J. Le Bel. *Compt. Rend.* 153, 1081 (1911).
28. W. Storhtenbekker. *Rec. Trav. Chim.* 26, 240 (1907).

29. G. N. Vyrubov. Bull. Soc. Chim. (France) [4], 3, 7 (1908).
30. M. E. Straumanis, T. Ejima and W. J. James. Acta Cryst. 14, 493 (1961).
31. Handbook of Chemistry and Physics 48th ed. The Chemical Rubber Co. p. B-215 (1967).
32. ABSORP a program from Cornell University.
33. D. V. Luu and R. Lafont. Journal de Phys. 31, 85 (1970).
34. H. Lynton and M. R. Truter. J. Chem. Soc. 5112 (1960).
35. D.W.J. Cruickshank. Acta Cryst. 9, 757 (1956).
36. W.R. Busing and H.A. Levy. Acta Cryst. 17, 142 (1964).
37. L. Pauling. The Nature of the Chemical Bond, p. 260, Cornell University Press, Ithaca, N. Y. (1960).
38. B.E. Robertson and C. Calvo. Acta Cryst. 22, 665 (1967).
39. C. Calvo. Acta Cryst. 23, 289 (1967).
40. B.E. Robertson and C. Calvo. J. of Solid State Chem. 1, 120 (1970).
41. C. Calvo and K. Neelakantan. Can. J. Chem. 48, 890, (1970).
42. D.W.J. Cruickshank, H. Lynton and G. A. Barclay. Acta Cryst. 15, 491 (1962).
43. C. Calvo. Inorg. Chem. 7, 1345 (1968).
44. L.H. Hagman, I. Jansson and C. Magneli. Acta Chem. Scand. 22, 1419 (1968).